SORLA regulates processing of amyloid precursor protein via interaction with adaptors GGA1 and PACS1

Dissertation

zur Erlangung des akademischen Grades des
Doktors der Naturwissenschaften

doctor rerum naturalium
(Dr. rer. nat.)

eingereicht im Fachbereich Biologie, Chemie, Pharmazie

der Freien Universität Berlin

vorgelegt von

VANESSA SCHMIDT

aus Berlin

August, 2008

Die Arbeit wurde von 03/2004 bis 08/2008 unter der Leitung von Prof. Dr. Thomas E. Willnow am Max-Delbrück Centrum für Molekulare Medizin in Berlin durchgeführt.

1. Gutachter: Herr Prof. Dr. Wolfgang Schuster,

                  Freie Universität Berlin

2. Gutachter: Herr Prof. Dr. Thomas E. Willnow

                  Max-Delbrück Centrum Berlin-Buch

Tag der Disputation: 11.11.2008

Summary

Alzheimer disease (AD) is the most common form of neurodegenerative diseases. Only little is known about the control mechanisms which affect APP metabolism and that cause Alzheimer´s Disease. Gene expression profiling studies revealed reduced levels of *Sorla* mRNA in brain autopsies from patients suffering from AD compared with healthy individuals. Based on this observation, reduced SORLA activity may be considered a causal event in AD development.

The mammalian receptor SORLA is a type-1 membrane protein that shares structural similarity to members of the group of VPS10P domain-containing receptors. In my studies, I have been able to uncover the molecular mechanisms how this receptor impacts on APP metabolism and progression.

I showed that SORLA binds directly to APP and that both proteins co-immunoprecipitate from cell lysats, suggesting a direct interaction between SORLA and APP. Overexpression of SORLA in CHO and SH-SY5Y cell lines caused sequestration of APP in the Golgi compartment and protection from proteolytic processing as deduced from intracellular accumulation of mature APP. In addition, SORLA overexpression decreased the activity of both amyloidogenic and non-amyloidogenic processing pathway for APP. This inhibitory effect may either be attributed to an inhibition of the interaction of APP with the respective proteases or by controlling the transport of APP to the distinct subcellular compartments less favorable for proteolytic breakdown.

Furthermore, the crucial role of SORLA in APP trafficking and processing fates has been established by site-directed mutagenesis of *Sorla* cDNA sequence to generate trafficking deficient receptor variants. Using these mutants, I was able to elucidate two trafficking routes for SORLA, and their dependence on interaction of the cytoplasmic domain of the receptor with the adaptor proteins GGA1 and PACS1. Finally, I identified the functional relevance of these sorting pathways for regulation of APP trafficking and metabolism. SORLA$^{\Delta cd}$ and SORLA^{acidic} variants were predominantly localized to the cell surface and showed defects in endocytosis leading to accelerated Aβ production. In contrast, the SORLA^{GGA} variant failed to undergo

shuttling between TGN and endosomal compartments. Cells overexpressing this receptor mutant displayed increased sAPPα and decreased Aβ secretion, suggesting a shift from the amyloidogenic to the non-amyloidogenic pathway.

As well as in cell culture experiments, I investigated the influence of SORLA on murine and human APP metabolism *in vivo*. I was able to demonstrate that ablation of *Sorla* gene expression in gene-targeted mice caused an elevated level of Aβ peptides and, consequently, enhanced plaque burden in the mouse brain, substantiating a central role for this receptor in amyloidogenic processing of APP *in vivo*.

Zusammenfassung

Die Alzheimer-Krankheit ist eine der häufigsten neurodegenerativen Erkrankungen beim Menschen. Über die Kontrollmechanismen des APP Stoffwechsels, welche die Alzheimer-Krankheit verursachen, ist nur wenig bekannt. Mittels Genexpressionsanalysen konnte eine reduzierte Menge an *Sorla* mRNA im Gehirn von Alzheimer-Patienten nachgewiesen werden. Dementsprechend könnte eine reduzierte SORLA-Aktivität die Ursache für die Entwicklung der Alzheimer Krankheit bedeuten.

Der Rezeptor SORLA ist ein Typ-1 Membranprotein, welches charakteristische Eigenschaften zu einer Gruppe der Transportrezeptoren aufweist. In meiner Arbeit konnte ich den molekularen Mechanismus aufklären, wie SORLA auf den APP Stoffwechsel und Entwicklung einwirkt. Mittels Koimmunopräzipitation konnte eine direkte Interaktion zwischen SORLA und APP gezeigt werden. Eine Überexpression von SORLA in CHO und SH-SY5Y Zellen verursachte ein Zurückhalten von APP-Molekülen im Golgi-Kompartiment und eine Inhibierung der APP-Prozessierung, welche ich anhand der erhöhten Menge von glycosylierten APP-Molekülen im Golgi-Kompartiment nachweisen konnte. Des weiteren führt eine SORLA Überexpression zu einer Reduzierung des amyloidogenen und nicht-amyloidogenen Prozessierungsweges von APP.

Weiterhin wurde der Einfluss von SORLA im APP-Transport und der APP-Prozessierung untersucht. Durch den Austausch von spezifischen Aminosäuren im Bereich der zytoplasmatischen Domaine des *Sorla*-Gens wurden transportdefiziente Rezeptorvarianten generiert. Mittels dieser Mutanten konnte ich zwei Transportwege für SORLA identifizieren, sowie die Abhängigkeit dieser Transportwege von der Interaktion von SORLA mit den Adaptorproteinen GGA1 und PACS1. Auf diesem Wege konnte ich die funktionelle Relevanz beider Transportwege für die Regulation von APP-Transport und Metabolismus beweisen. Die SORLA-Mutanten SORLA[Δcd] and SORLA[acidic] wurden überwiegend an der Zelloberfläche lokalisiert. Der Defekt der Endozytose dieser SORLA-Mutanten führte zur erhöhter Aβ-Produktion in den Zellen. Im Gegensatz dazu wies die SORLA[GGA]-Variante Mängel im Transportweg zwischen Trans-Golgi-Network und Endosomen auf, wodurch es zu einem Anstieg von sAPPα-Molekülen und zu einer Reduzierung der Aβ-Sekretion kam.

Analog zu den Experimenten in Zellen habe ich auch den Einfluss von SORLA auf den murinen und humanen APP-Metabolismus in Mäusen untersucht. *Sorla*-gen-defiziente Mäuse wiesen eine erhöhte Menge an Aβ-Molekülen und dementsprech-end erhöhte amyloidogene Plaqueablagerungen im Mausgehirn auf.

Aus meinen Studien kann ich schliessen, dass SORLA eine zentrale Rolle in der amyloidogenen APP-Prozessierung *in vivo* und *in vitro* darstellt.

Contents

List of Figures

x

List of Tables

Abbreviations

α2M	alpha-2-macroglobulin
AD	Alzheimer disease
ADP	adenosindiphosphat
AICD	APP intracellular domain
APP	amyloid precursor protein
APOE	apolipoprotein E
ARF	ATP-ribosylation factor
ATP	adenosine triphosphate
BACE	β-site APP cleaving enzyme
bp	basepairs
CHO	Chinese hamster ovarey
CK2	casein kinase 2
COP	coat protein
CTF	C-terminal fragment
dNTP	deoxynucleotide triphosphate
DNA	desoxyribonucleic acid
EDTA	ethylenediaminetetraacetic acid
EEA	early endosomal antigen
ELISA	Enzyme-linked immunosorbent assay
ER	endoplasmic reticulum
ERC	endosomal recycling compartment
ERGIC	ER-Golgi intermediate compartment
FACS	Fluorescence activated cell sorting
g	gram
GTP	guanosintriphosphat
HCl	hydrogen chloride
HEPES	hydroxyethylpiperazineethanesulfonic acid
ICD	intracellular domain
K	potassium
KCl	potassium chloride
kDa	kilodalton

l	liter
LB	lysogeny broth
LDL	low-density lipoprotein
mg	miligram
MgCl2	magnesium chloride
min	minute
ml	milliliter
mM	millimole
mRNA	messenger ribonucleic acid
M	mole
MVB	multivesicular body
NaCl	sodium chloride
NaOH	sodiumhydroxide
ng	nanogram
PAGE	Polyacrylamide gel electrophoresis
pH	potential of hydrogen
RAP	receptor associated protein
PM	plasma membrane
sec	second
SDS	sodium dodecyl sulfate
SMC	smooth muscle cells
SOC	super optimal broth with catabolite repression
Taq	thermus aquaticus
TGN	trans-Golgi network
Tris	trishydroxymethylaminomethane
U	unit
UV	ultraviolett
V	volt
VPS	vacuolar protein sorting
wt	wildtype
μ	micro

1. Introduction

Receptor-mediated endocytosis is the main mechanism that enables selective transport of macromolecules across the plasma membrane into cells. It is initiated by binding of ligands to endocytic receptors on the cell surface, followed by internalization through clathrin-coated vesicles. Most ligands are delivered to lysosomal compartments for catabolism while the unliganded receptors recycle back to the plasma membrane. So far, significant progress has been made in elucidating the various steps of endocytosis at the cellular level. However, the physiological relevance of many endocytic pathways for organ function remained elusive. The main class of endocytic receptors is a group of proteins known as the LDL receptor gene family. In addition, a novel group of orphan endocytic receptors designated VPS10P-domain receptor has recently been uncovered. Both receptor gene families will be introduced in the first part of the introductory section.

1.1 SORLA

1.1.1 The low-density lipoprotein receptor gene family

The low-density lipoprotein receptor (LDLR) gene family comprises 9 members of structurally related type I transmembrane proteins in mammals which are termed low-density lipoprotein receptor (LDLR), the LDLR related proteins 1, 1B, 5, and 6 (LRP1, LRP1B, LRP5, LRP6), the very low-density lipoprotein receptor (VLDLR), the apolipoprotein E receptor-2 (APOER2), megalin, the multiple epidermal growth factor repeat containing protein-7 (MEGF7), as well as the chimeric sortilin-related receptor containing LDLR class A repeats (SORLA) (figure 1). Members of this family can be found in a variety of organisms including annelids, vertebrates, and insects, suggesting an evolutionary conserved roles in many different species. All act as endocytic receptors that bind lipoproteins from the extracellular space, internalize them via clathrin-coated pits and release them in early endosomal compartments. However, recent findings have shown that these receptors can have also additional cellular roles. For instance, some members act as signal transducers in neuronal mi-

gration processes, some regulate vitamin homeostasis, while others control synaptic plasticity. An overview of functions, expression patterns and possible ligands of each receptor species is summarized in table 1. Although each receptor has a distinct ligand profile, two proteins are known that can interact with all family members. One universal binding partner is the receptor associated protein (RAP) which binds to the nascent amino acid chain of the receptors in the endoplasmic reticulum assisting receptor folding. The second ligand is apolipoprotein E (APOE) which transports lipoproteins, fat-soluble vitamins, and cholesterol (Mahley, 1988). All receptors of the LDL receptor gene family share common structural motifs which are required for interaction with ligands and for releasing them again. The amino-terminal part consists of two distinct structural motifs which alternate in order and quantity. The complement-type repeats are involved in ligand binding and the epidermal growth factor precursor homology domains are necessary for the pH-dependent release of ligands in endosomes (Brown et al., 1997; Rudenko et al., 2002). In addition, some members possess an *O*-linked sugar domain, which follows the transmembrane domain. Attached carbohydrate chains prevent proteolytic cleavage of the extracellular part of these receptors (Kozarsky et al., 1988). The cytoplasmic tails show less homology between receptors. They exhibit sequences elements responsible for adaptor protein binding (Goretzki and Müller, 1998; Gotthardt et al., 2000) and for receptor internalization. The consensus sequence which is involved in receptor clustering and internalization of the receptors into coated pits consists of the four amino acid motiv NP*x*Y (Asn-Pro-*x*-Tyr, where *x* is any amino acid) (Chen et al., 1990; Owen et al., 1998; Li et al., 2001).

1.1.2 The VPS10p receptor gene family

The vacuolar protein sorting 10p (VPS10p) receptor gene family comprises 5 members in mammals (sortilin, SORCS1, SORCS2, SORCS3, SORLA) which display a structural related extracellular VPS10p-domain (figure 1). In addition, they all have a transmembrane region and a short cytoplasmic tail. In contrast to SORLA and sortilin, the three SorCS receptors contain small imperfect leucine-rich repeats N-terminal to the transmembrane region which might serve as interaction or adhesion

domain. The VPS10p-domain was firstly described in the VPS10p receptor in *Saccharomyces cerevisiae* where it binds the soluble vacuolar hydrolase carboxypeptidase Y in the Golgi compartment and delivers it to the vacuole via clathrin coated vesicles (Marcusson et al., 1994; Cooper et al., 1996).

Sortilin was shown to interact with neurotensin, a small neuropeptid which is produced in the brain and in the small intestine (Mazella et al., 1998; Nielsen et al., 1999). It can also interact with other polypeptides such as sphingolipid activator protein (SAP), brain-derived neurotrophic factor (BDNF), and lipoprotein lipase (LpL). It has been suggested that sortilin is involved in intracellular trafficking of these ligands to and from the Golgi compartment. This hypothesis is supported by
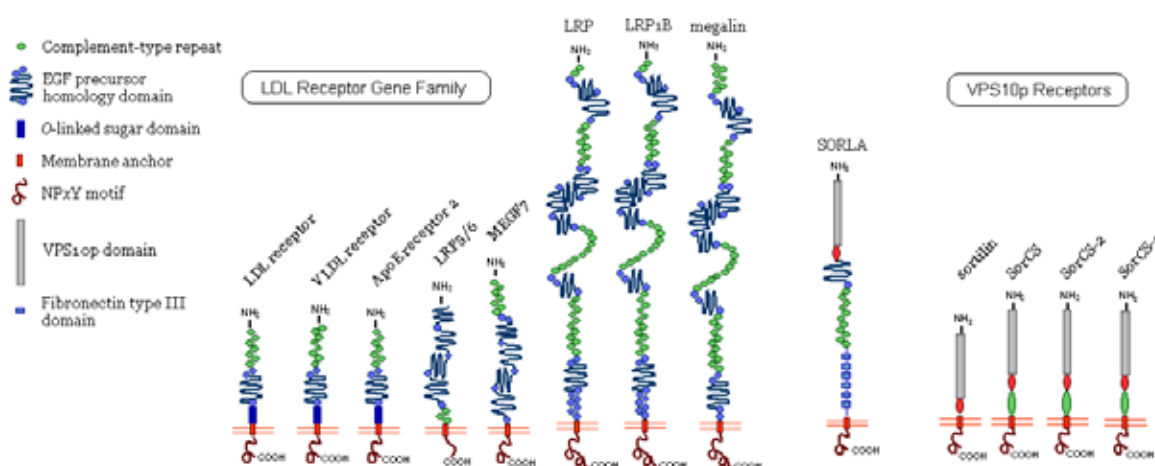
Figure 1: The structural organization of the mammalian receptors of the low-density lipoprotein (LDL) receptor family and the VPS10p receptor family.
The LDL receptor family shares common motifs, including a single membrane anchor, complement-type repeats and epidermal growth factor (EGF) precursor homology domains. NP*x*Y designates the four amino acid motif Asp-Pro-*x*-Tyr, which mediates endocytosis. The VPS10p receptor family consists of only one principle domain, the VPS10p-domain, which is essential for ligand binding. Abbreviations: VLDL, very low density lipoprotein; ApoE, apolipoprotein E; LRP, LDL receptor related protein; MEGF7, multiple EGF repeat containing protein; SorCS, sortilin-related VPS10 domain containing receptor; SORLA, sortilin-related receptor containing LDLR class A repeats; VPS10p, vacuolar protein sorting 10 protein.

the fact that sortilin resides mainly intracellularly (~90%), in particular, the Golgi apparatus (Nielsen et al., 1999; Lefrancois et al., 2003; Chen et al, 2005). Formation of a trimeric protein complex of sortilin, the neurotrophine receptor p75, and the common ligand pro nerve growth factor (proNGF) induces pro-NGF-mediated apoptosis (Nykjaer et al., 2004). Furthermore, sortilin is an essential constituent of muscle specific glucose transporter-4 (GLUT4) containing vesicles which are responsible for regulation of the blood glucose level in mammals (Lin et al., 1997).

Only little is known about SORCS1, -2 and -3. These receptors could be involved in the development of the central nervous system since the expression level are tightly regulated during embryogenesis (Hermey et al., 2004). Despite their extensive structural homology, SORCS1, -2, and -3 are expressed in a non-overlapping pattern suggesting distinct functions for each receptor.

1.1.3 Structural organization of SORLA

The mammalian receptor SORLA is a type-1 membrane protein that shares structural similarities to members of the VPS10p sorting receptors in yeast as well as to the low-density lipoprotein (LDL) receptor family (figure 1). Hence, the luminal part of SORLA starts with a VPS10p-domain, the structural hallmark of yeast sorting protein VPS10p and the mammalian VPS10p receptors (figure 2). However, the middle portion of the extracellular receptor domain possesses characteristic features of the LDL receptor gene family including a cluster of five F/YWTD/β-propeller modules, an epidermal growth factor precursor-like module, and a cluster of 11 LDLR class A (LA) repeats. Finally, six fibronectin type III repeats are also included in this receptor domain, a structural element not found in either LRPs or other VPS10p domain receptors (Jacobsen et al., 2001). The C-terminal part of SORLA exhibits a transmembrane domain and a 54-residue cytoplasmic tail comprising features typical of endocytosis receptors (NP*x*Y) and sorting receptors (Yamazaki H. et al., 1996; Jacobsen et al., 1996).
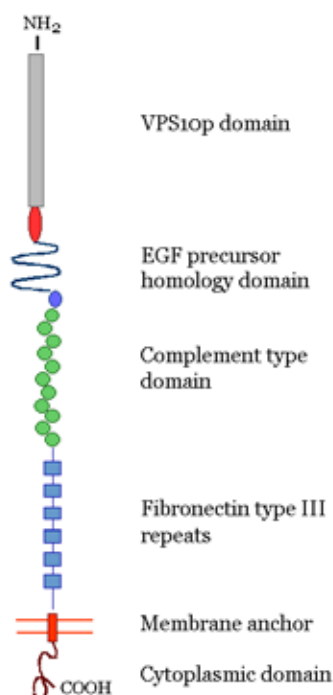
Figure 2: Structural organization of SORLA.

Table 1: The mammalian LDL receptor and VPS10p receptor gene family members. The table highlights some biological features including cellular activities, expression patterns, ligands, and relevance for diseases of the listed receptors.

LDLR	
Expression	ubiquitous
Biological function	cholesterol homeostasis (endocytosis of LDL particles)
Ligands	APOE, APOB
Disease	familial hypercholesterolemia

VLDLR	
Expression	heart, skeletal muscle, ovary, kidney
Biological function	metabolism of APOE-containing triacylglycerol-rich lipoproteins, regulation of neuronal migration and synaptic plasticity
Ligands	APOE, Reelin, lipoprotein lipase
Disease	VLDLR-associated cerebellar hypoplasia (VLDLRCH)

APOER2	
Expression	brain, placenta, platelets, megakaryocytic cells
Biological function	regulation of neuronal migration, synaptic transmission, male fertility
Ligands	APOE, reelin
Disease	susceptibility to premature myocardial infarction

megalin	
Expression	Absorptive epithelia, including renal proximal tubules, yolk sac, neuroectoderm
Biological function	vitamin/nutrient supply, calcium homeostasis, recovery of filtered low molecular weight proteins
Ligands	APOB, APOE, APOJ, APOH, retinol binding protein, vitamin D binding protein, sonic hedgehog, bone morphogenic protein 4
Disease	Donnai-Barrow syndrome, murine holoprosencephaly

LRP1	
Expression	almost all cell types but most abundant in liver, brain and lung
Biological function	phagocytosis of apoptotic cells, cellular lipid homeostasis, plasma clearance of chylomicron remnants and activated LRPAP1 (alpha 2-macroglobulin), metabolism of complexes between plasminogen activators and their inhibitors, regulation of amyloid precursor protein (metabolism, kinase-dependent intracellular signaling, neuronal calcium signaling)
Ligands	APOE, APP, lipoprotein lipase, alpha2-macroglobulin, protease/protease inhibitor complexes, platelet derived growth factor
Disease	unknown

LRP1B	
Expression	thyroid gland, salivary gland, adult and fetal brain
Biological function	unknown
Ligands	synaptotagmin, laminin receptor precursors, APOE
Disease	tumor supressor associated with non-small cell lung cancer

LRP5	
Expression	widely expressed, highest level in the liver
Biological function	Wnt/beta catenin signaling pathway, regulation of bone formation
Ligands	different Wnt/Frizzled complexes, axin
Disease	familial exudative vitreoretinopathy, osteoporosis pseudoglioma syndrome, high bone mass trait, van Buchem disease type 2

LRP6	
Expression	widely co-expressed with LRP5 during embryogenesis and in adult
Biological function	Wnt/beta catenin signaling pathway, limb development, mid- and hindbrain development
Ligands	Wnt proteins, DKK1, DKK2
Disease	autosomal dominant coronary artery disease type 2

MEGF7	
Expression	brain, lung, sceletal muscle
Biological function	limb development, body growth
Ligands	APOE
Disease	unknown

SORLA	
Expression	brain, spinal cord, testis, liver, kidney, pancreas
Biological function	uptake of lipoproteins and of proteases, role in cell-cell interaction
Ligands	LDL, APOE, APP, lipoprotein lipase, head activator protein, neurotensin
Disease	late onset Alzheimer Disease

sortilin	
Expression	high levels in brain, spinal cord, heart, skeletal muscle, thyroid, placenta and testis
Biological function	Promotes neuronal apoptosis, formation of storage vesicles containing the glucose transporter SLC2A4/GLUT4
Ligands	GM2A, PSAP, (pro) NGF and (pro) BDNF, neurotensin
Disease	unknown

SorCS1-3	
Expression	fetal and infant brain
Biological function	unknown
Ligands	unknown
Disease	unknown

1.1.4 Modification and processing of SORLA

SORLA is proteolytically processed in several steps (figure 3). During translation at the rough endoplasmic reticulum membrane the immature protein becomes glycosylated and the signal peptid is removed. Further on the way through the Golgi, SORLA aquires additional *O*- and *N*-linked oligosaccharides (Fiete et al., 2007) while the N-terminus is cleaved by furin, a mammalian subtilisin/Kex2p-like proprotein convertase (Hampe et al., 2000). The released propeptid can interact with the VPS10p domain to prevent binding of other ligands to SORLA. Similar to mem-
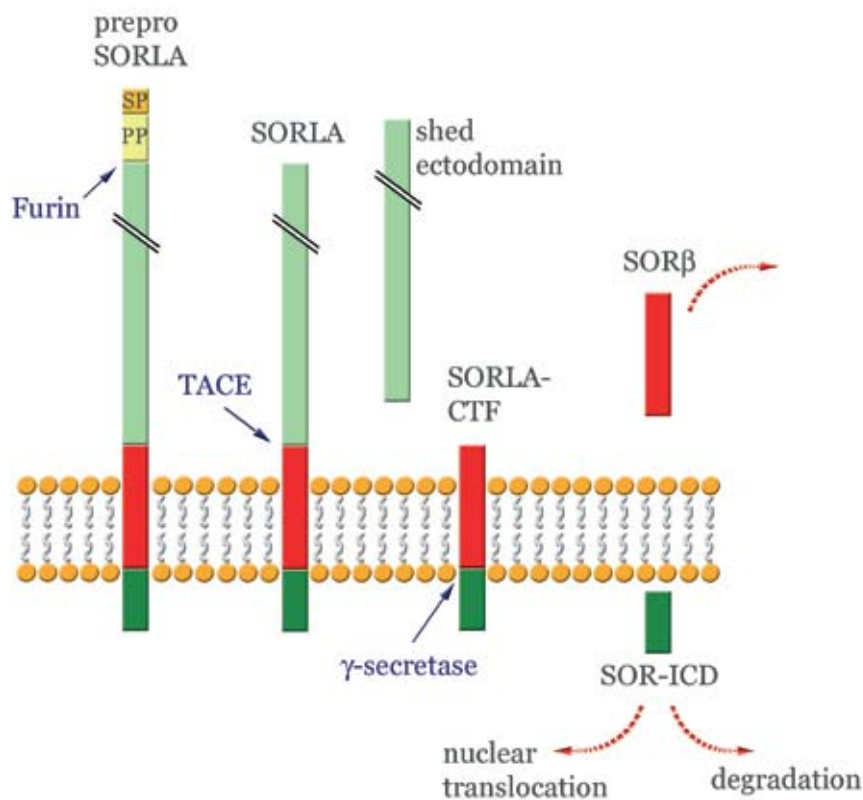
Figure 3: Model for regulated intramembrane proteolysis of SORLA.
Prepro-SORLA is cleaved by furin in late-Golgi compartments. The metalloprotease TACE can shed the large ectodomain of mature SORLA in a ligand-induced manner. The remaining SORLA CTF is then proteolytic cleaved by the γ-secretase complex producing the SORLA intracellular domain (SOR-ICD) and an β-peptide (SORβ). SOR-ICD can subsequently enter the nucleus and might regulate the transcription or the mRNA stability of target genes.

bers of the LDL receptor family, RAP, the receptor-associated protein, is also able to bind the VPS10p domain as well as the complement type / class A repeats of SORLA. Both RAP and propeptide are believed to assist protein folding and to inhibit protein aggregation through premature association of the receptor with its ligands in the endoplasmic reticulum and the early Golgi compartments (Bu et al., 1995). As well as in the biosynthetic pathway, SORLA is also subject to processing during mature receptor function on the cell surface. Thus, the large luminal domain of SORLA can be released by the metalloprotease tumor necrose factor α-converting enzyme TACE (Hampe et al., 2000). The remaining C-terminal fragment (CTF) can be further cleaved by a gamma secretase into a β-peptide (SORβ) and a SORLA intracellular domain (SOR-ICD) (Böhm et al., 2006). Guided by a nuclear localization signal KHRR in the cytoplasmic domain, SORLA-ICD can translocate into the nucleus where it might regulate transcription of so far unknown target genes (Böhm et al., 2006).

1.1.5 The function of SORLA

SORLA is mainly expressed in the nervous system (Motoi et al., 1999) but it is also found in non-neuronal tissues such as smooth muscle cells of arterial walls (Kanaki et al., 1999), testis, ovary, kidney, and lymph nodes (Jacobsen et al., 1996). Little is known about the molecular function of SORLA. There are indications that SORLA expression is upregulated during periods of morphogenesis and proliferation (Kanaki et al., 1998; Hermans-Borgmeyer et al., 1998; Hirayama et al., 2000) but downregulated during differentiation of neuroblastoma cells (Hirayama et al., 2000). In non-neuronal cell types, induced SORLA espression can be found in the intimal smooth muscle cells (SMC) of arterial walls during atherogenesis, especially after arteriosclerotic lesions (Kanaki et al., 1999). It was further reported that SORLA and urokinase-type plasminogen activator receptor (uPAR) are elevated in intimal SMC and that both receptors cooperate with uPA to mediate SMC migration in atheromata (Zhu et al., 2002, 2004).

Based on the different structural domains in SORLA one may speculate about additional roles for this receptor. For instance, SORLA shows structural homology to the head activator binding protein HAB of *Hydra vulgaris* (Hampe et al., 1996; Lintzel et al., 2002). HAB is a type I transmembrane receptor with a short cytoplasmic

domain, that interacts with the head activator peptide (HA) via its VPS10p domain, much like mammalian SORLA also binds HA. In *Hydra vulgaris,* binding of HA to its receptor causes head-specific growth and differentiation processes (Hampe et al,.1999). In mammals, HA stimulates entry into mitosis and proliferation of neural and endocrine precursor cells (Kayser et al., 1998; Boels et al.,2001). Binding of HA to SORLA inhibits the HA-stimulated mitosis and proliferation supporting a funtion for SORLA in HA signaling (Hampe et al., 2000).

Also, it was shown that the fibronectin type III repeats of the neuron-glia cell adhesion molecule promotes neurite outgrowth (Burgoon et al., 1995). Accordingly, the fibronectin type III repeats in SORLA may suggest a potential role for this receptor in cell-cell interaction which, however, still needs to be elucidated. Furthermore, the presence of a putative internalization signal in the cytoplasmic tail suggests the ability of SORLA to act as endocytic receptor, possibly in the uptake of lipoproteins and proteases. The VPS10p domain of SORLA can bind neurotensin (Mazella et al., 1998; Petersen et al., 1999), and is therefore, like sortilin, a neuropeptide receptor. Other proteins like apolipoprotein E (APOE) and APOE-rich β-very low density lipoprotein (β-VLDL) can also interact with SORLA. Cells expressing this receptor are able to internalize and degrade the bound β-VLDL which leads to excessive amounts of intracellular lipid accumulation (Taira et al., 2001). Last but not least, SORLA possess a domain which is not found in classical endocytic receptors, the VPS10p domain. This domain was first identified in the vacuolar protein-sorting 10 protein (VPS10p) in yeast that directs carboxypeptidase Y from Golgi into the vacuole (ortholog of mammalian lysosomes) (Marcusson et al., 1994; Cooper et al., 1996). Accordingly, SORLA is not only classified into the LDL receptor gene family but also the group of VPS10p domain receptors (figure 1). The fact that SORLA shuttles between the plasma membrane, endosomes and Golgi compartments, and that it predominantly resides intracellularly (Jacobsen et al., 2001) further lends support to the notion that this receptor may have a prominent function in protein sorting.

Taken together, all the features discussed above suggest that SORLA is a multifunctional receptor possibly be involved in several functions including ligand transport and sorting, but also in ligand-induced signal transduction.

1.1.6 SORLA as trafficking receptor

The fact that SORLA is rather a sorting receptor than an endocytic receptor was clarified by dissecting the specific sorting motives in the cytoplasmic domain. The 54-residue intracellular domain comprises a putative internalization motif (F_{12}AN-SHY$_{17}$), an acidic cluster (D_{30}DLGEDDED$_{38}$) and a C-terminal part of hydrophobic residues (D_{47}DVPM$_{51}$) (Jacobsen et al., 1996). It has been shown that similar motifs in other transmembrane proteins have an essential role in protein trafficking via the sorting machinery of a cell. Such pathways seem particularly relevant for sorting processed involving trans-Golgi network (TGN) and the endosomal recycling compartment (ERC) that are central pathways for directing proteins to various intracellular destinations (figure 4). Typically, a protein which is synthesized in the endoplasmatic reticulum (ER) and which passes the early secretory compartment has two options when arriving at the trans-Golgi/trans-Golgi network (TGN): In the constitutive secretory pathway, proteins are delivered to the cell surface. In the alternative pathway, proteins are sorted at the Golgi and transported to other intracellular compartments including endosomes or lysosomes. Sorting at the TGN is mediated by specific recognition signals in the cytoplasmic tail of cargo proteins. Such signal represents D_{47}DVPM$_{51}$ in the intracellular domain of SORLA which interacts with GGA-1 and GGA-2 (Golgi membranes localizing-adaptin ear homologous ADP-ribosylating factor binding adaptor protein) (Jacobsen et al., 2002). Since the cytoplasmic tail of SORLA exhibits also other signal motifs which are assumed to interact also with other adaptor proteins like PACS1 or the retromer complex I want to explain those trafficking proteins in more detail in the next chapters.

1.2 Adaptor proteins

1.2.1 GGA proteins

The three mammalian proteins GGA-1, -2 and -3 are ubiquitously expressed. Their predominant localization is the trans-Golgi/TGN and to, a weeker extent, also the endosomal compartment (Boman et al., 2000; Hirst et al., 2001; Puertollano et al.,
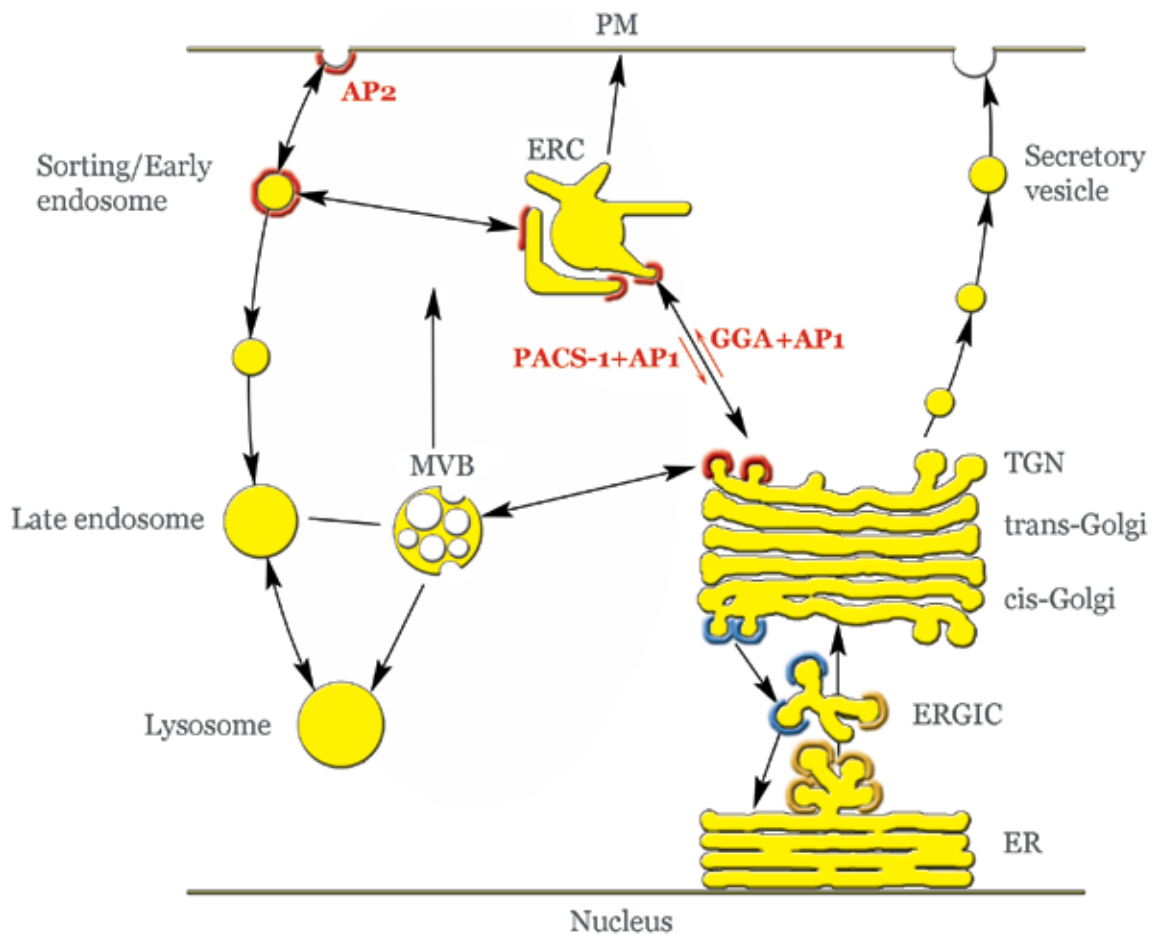
Figure 4: The secretory, lysosomal and endocytic compartments in a mammalian cell. Model depicts the secretory, lysosomal and endocytic system and various trafficking pathways. The transport steps are indicated by arrows. The localization of coat protein II (COPII) (orange), COPI (blue) and clathrin (red) are shown in color. Proteins synthesized in the ER are transported via COPII proteins to the Golgi compartment where they are sorted to other destinations. The GGA proteins transport their cargo anterograde from the TGN to the endocytic recycling compartment (ERC) whereas PACS-1 proteins sort cargo molecules retrograde back to the TGN. Internalization of proteins occurs in clathrin-coated vesicles which form sorting/early endosomes. Those proteins rapidly exit the sorting endosomes and are either returned directly to the plasma membrane or retained in the sorting endosomes which fuse with the endocytic recycling compartment. Here they can recycle to the cell surface or undergo retrograde transport to the TGN by either PACS-1 containing vesicles or related pathways. Proteins destined for degradation remain in the early endosomes which mature to late endosomes/lysosomes. Abbreviations: MVB, multivesicular body; ERC, endocytic recycling compartment; ERGIC, ER-Golgi intermediate compartment; TGN, trans-Golgi network; ER, endoplasmic reticulum; PM, plasma membrane.

2003). The GGA proteins consist of three folded domains (figure 5): The N-terminal VHS (VPS27, Hrs and STAM) domain interacts with the cytosolic tail of cargo receptors such as sortilin (Nielsen et al., 2001), the cation-independent mannose-6-phosphat receptor (CI-MPR) (Puertollano et al., 2001; Zhu et al. 2001), and the cation-dependent mannose-6-phosphat receptor (CD-MPR) as well as β-site APP cleaving enzyme (BACE). Binding to the cargo is dependent on a specific sorting signal in the cytoplasmic tail, DxxLL, that includes a cluster of acidic residues around the aspartate and a serine residue whose phosphorylation enhances sorting efficiency. C-terminal to the VHS domain follows the GAT domain (GGA and TOM1) which binds to the guanosintriphosphat (GTP)-bound form of the adenosindiphosphat (ADP)
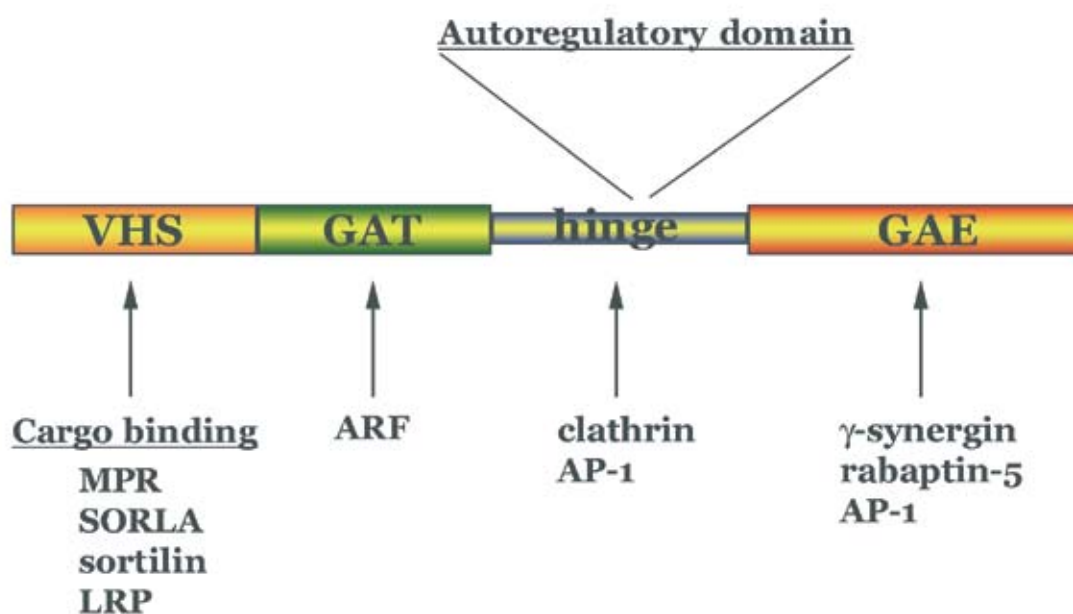
Figure 5: Schematic presentation of GGA.
All GGA proteins consist of four functional domains: an N-terminal VHS domain for cargo binding, a GAT domain for interacting with ARF, a variable hinge domain and a GAE domain at the C-terminus for binding to clathrin and other accessory proteins. Abbreviations: MPR, mannose-6-phosphat receptor; LRP, low-density lipoprotein receptor; ARF, ADP-ribosylation factor; AP-1, adaptor protein-1.

ribosylation factor (ARF) family of proteins (Puertollano et al., 2001; Zhu et al., 2003) that recruit GGAs from the cytosol to the Golgi membrane. The GAT domain can also interact with rabaptin-5 (Mattera et al., 2003) and ubiquitin (Bilodeau et al., 2004; Puertollano, 2004; Shiba et al., 2004) and is connected with the next GAE domain via a hinge linker. The hinge linker is responsible for recruitment of adaptor protein-1 (AP-1), clathrin and/or clathrin-box motives. It contains an autoinhibitory acidic cluster motif (Doray et al., 2002; Shiba et al., 2002; Ghosh et al., 2003) similar to the binding sequence of the cargo proteins. The last domain, gamma adaptin ear (GAE), interacts with additional accessory adaptor proteins such as γ-synergin, rabaptin-5, adaptor protein-1 (AP-1) and also clathrin. Rabaptin-5 binds to rabex-5 at the membrane of endosomes to mediate fusion of the cargo containing clathrin coated vesicle with the endosomal membrane (Zhai et al., 2003). The involvment of rabaptin-5 in this process is the essential and rate limiting step. Binding and release of cargo molecules by the GGAs is regulated by several phosphorylation events. Phosphorylation of the cytoplasmic domain of the cargo protein enhances binding (Wan et al., 1998) whereas phosphorylation of the GGA-1 and GGA-3 autoinhibitory domain by AP-1 associated casein kinase-2 (CK2) inhibit cargo binding. Hence, a complex formation is only possible when the GGAs are dephosphorylated. The cytosolic phosphatase PP2A is one of the enzyme which was shown to dephosphorylate GGAs and other proteins of the sorting machinery like PACS-1 (Molloy et al., 1998; Dorey et al., 2002; Ghosh, 2003).

Proteins that originate from the plasma membrane or from the TGN enter early sorting endosomes where they are seperated into either endosomal tubular membrane extensions or remain within the central endosomes which mature into late endosomes or multivesiclular bodies. The tubular membrane extensions further form recycling or trafficking vesicles. Some of them fuse with the plasma membrane while others translocates to the TGN for further rounds of transport (Schmid et al., 1988). Retrograde transport to the TGN is mediated by signal sequences directing TGN localization for cargo proteins whose predominant steady-state localization is at the TGN. One of the proteins which direct cargo molecules back to the Golgi is phosphofurin acidic cluster sorting-1 protein (PACS-1).

1.2.2 Phosphofurin acidic cluster sorting-1 protein (PACS-1)

PACS-1 is a cytosolic connector protein which consists of four different domains: An atropin-1-related region (ARR), a cargo-binding region (FBR), a middel region (MR) and a C-terminal region (CTR) (figure 6). The FBR domain is the only fully characterized region so far. It comprises several recognition sequences for binding to cytosolic proteins like AP-1 and AP-3, GGA-3, casein kinase-2 (CK2) and cargo proteins (Wan et al., 1998; Crump et al., 2001; Scott et al., 2006). PACS-1 has been shown to direct the TGN localization by binding to an acidic cluster motif on several cellular proteins, including proprotein convertase 6B (Xiang et al, 2000), polycystin-2 (Köttgen et al, 2005) and VAMP4 (Hinners et al, 2003), as well as the viral
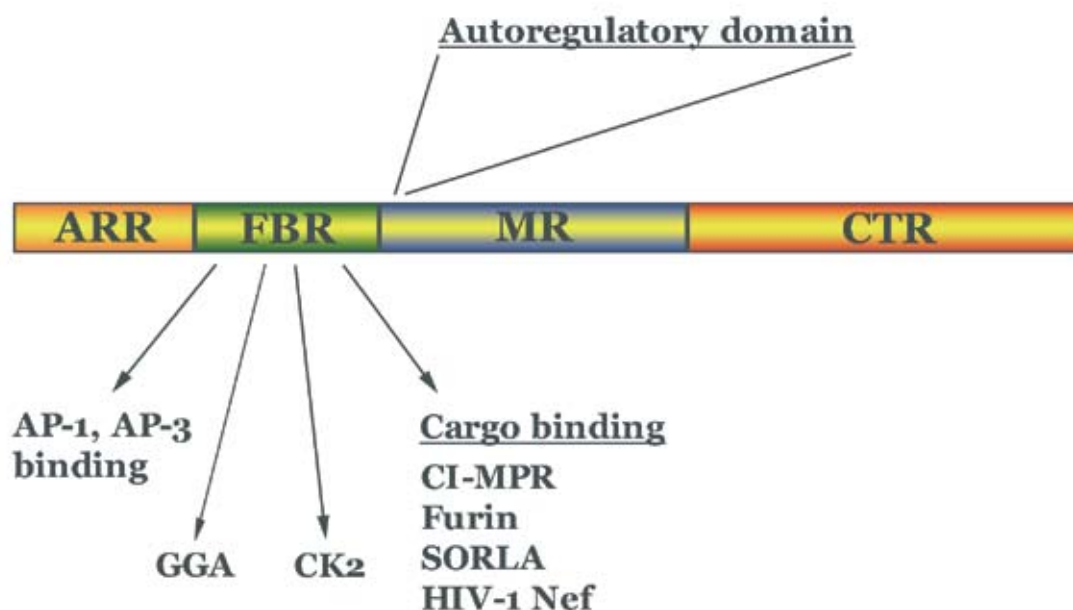
Figure 6: Schematic presentation of PACS-1.
PACS-1 showing the atropin-1-related region (ARR), cargo-binding region (FBR), which interacts with cargo, Golgi membranes localizing-adaptin ear homologous ADP-ribosylating factor binding adaptor protein (GGA), casein kinase II (CK2), and adaptor protein-1 and -3 (AP-1/AP-3), the middle region (MR), which contains the autoregulatory acidic cluster, and the C-terminal region (CTR).

proteins HCMV gB (Crump et al, 2003) and HIV-1 Nef (Piguet et al, 2000). It is also published that PACS-1 is involved in endosomal retrieval of the cation-independent mannose-6-phosphat receptor (CI-MPR) which sort cathepsin D to lysosomes (Wan et al, 1998; Puertollano et al, 2001; Crump et al, 2001; Ghosh et al, 2003). Dissecting the cytoplasmic tail of SORLA one can find an acidic cluster (D_{30}DLGED-DED$_{38}$) which was shown to interact with PACS-1 (Schmidt et al., 2007) and therefore might be involved in PACS-1 dependent retrograde trafficking of SORLA to the TGN supporting a function for SORLA as sorting receptor. PACS-1 binding to its cargo is regulated by a casein kinase-2 (CK2) which phosphorylates the autoregulatory domain and the FBR domain of PACS-1 leading to an activation of cargo binding and execution of endosome-to-Golgi retrieval of furin, CIMPR and HIV-1 Nef (Scott et al., 2003 and 2006). In parallel, CK2 also phosphorylates the autoregulatory domain of GGA-1 and -3 within the hinge domain (Doray et al., 2002; Ghosh, 2003), thereby inactivating the GGA proteins and inhibiting binding to CI-MPR causing a release of cargo proteins from the VHS domain of GGA in endosomes.

1.2.3 The retromer complex

In addition, other molecules including TIP47 and retromer also function in the endosome-to-TGN transport of proteins. For example, the CI-MPR can interact with the retromer complex mediating the retrieval from early endosomes to TGN (Arighi et al., 2004; Seaman, 2004). The retromer complex was first identified in yeast when investigating the trafficking of the VPS10p receptor. The VPS10p receptor has a function similar to that of the CI-MPR in mammalian cell types, namely, to deliver hydrolases to the vacuole, the equivalent of the lysosomes. Following cargo delivery, retromer complex recycles back to the TGN for additional rounds of enzyme transport (Bankaitis et al., 1986; Rothman, 1986; Cooper, 1996). This recycling step is a Vps5p-dependent process (Westphal et al., 1996). Further studies identified four more proteins which form the retromer complex together with Vps10p and Vps5p (Seaman et al., 1998) (figure 7). Mutation or inactivation of any of these genes (Vps10p, Vps5p, Vps17p, Vps26p, Vps29p, Vps35p) results in defects in protein recycling from endosomes to the trans-Golgi network (Horazdovsky et al., 1997; Seaman et al., 1997; Nothwehr et al., 1999). The hallmark of the retromer

is the presence of a PX domain that has been shown to bind phosphatidylinositol phosphates thereby recruiting cargo-bound retromer complex to specific endosomal membranes enriched in these phospholipids (Worby, 2002). Sorting nexin-1 and -2 (SNX-1, SNX-2) are the human orthologs of yeast Vps5p (Horazdovsky et al., 1997; Haft et al., 1998) which interact with many receptors, including sortilin (Canuel et al., 2008), CI-MPR (Arighi et al., 2004), or receptors for platelet-derived growth factor, insulin (Chien et al., 2001), and epidermal growth factor (Kurten et al., 1996). In terms of CI-MPR Bonifacino and colleagues (2004) identified at least two regions in the cytoplasmic tail that might interact with the retromer complex. One of the signals is a short tyrosine-containing peptide sequence YXXΦ (where Φ is any hydrophobic amino acid) (Ohno et al., 1996) which is also recognized by the
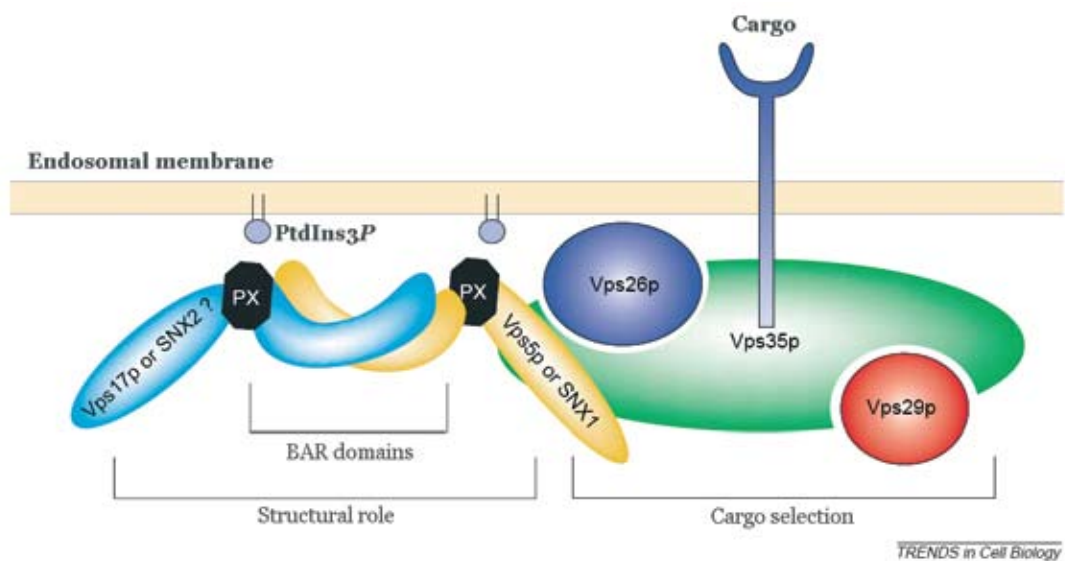
Figure 7: The retromer complex and its interactions.
The retromer complex comprises different subunits. Vps35p interacts with Vps26p through its N-terminus and with Vps29p through its C-terminus. Vps35p also interacts with cargo such as Vps10p or the CI-MPR. Vps5p and Vps17p dimerize through their C-terminal (BAR) domains. Both Vps5p and Vps17p and their mammalian homologues, SNX1 and SNX2, have PX domains that can bind to PtdIns3P (phosphatidylinositol 3-phosphate). Vps5p or SNX1 alone interacts with the Vps35p–Vps29p–Vps26p subcomplex through the N-terminal regions of both Vps35p and Vps5p (Seaman, 2005).

clathrin adaptor complexes, and Trp-Leu-Met (Seaman, 2007). Two similar motives YSVL (Canuel et al., 2008) and Phe-Leu-Val (Seaman, 2007) were found in the tail of sortilin and one motif, YLVI, was found in the cytoplasmic domain of the EGF-receptor both of which interact with the retromer complex. Surprisingly, the putative internalization motif in the cytoplasmic tail of SORLA (F_{12}ANSHY$_{17}$) has no influence on the endocytosis rate of this receptor (Nielsen et al., 2007) although it has strong similarity to the common internalization motif NPxY of other receptors including the endocytic receptors of the LDL receptor gene family. However, there are hints that a part of this motif belongs to a putative retromer binding motif, $_{17}$YS-SRL$_{21}$ (YXXXΦ), and may interact with SNX1. Studies indicate that SNX1 is needed for the retraction of SORLA from the endosomes to escape lysosomal degradation (Nielsen et al., 2007) because deficiency of one of the retromer components, Vps35 or SNX1, was accompanied by a reduction of cellular SORLA protein level.

In summary, SORLA fulfills all requirements of a multifunctional trafficking receptor comprising multiple cytoplasmic sorting motives which allow direct interaction with components of the cellular sorting machinery.

1.3 Alzheimer´s Disease

The close connection between SORLA and Alzheimer´s disease (AD) came from Scherzer and colleagues (Scherzer et al. 2004). They performed gene expression profiling studies to find new candidate genes associated with AD. These studies revealed reduced levels of SORLA in lymphoblasts of patients suffering from AD compared with healthy individuals. Moreover, they could observe a dramatic and consistent loss of immunocytochemical staining for SORLA in neurons in AD brains. Based on this observation, reduced SORLA activity may be considered a primary cause of increased Aβ production and AD development.

1.3.1 Histopathology of Alzheimer's disease

Today, Alzheimer´s disease (AD) is the most common type of dementia. It was first characterized by Alois Alzheimer in the early 20th centrury as a disease with "a clotting of fibrils...in addition an extraordinary number of peculiar patches disseminated throughout the entire cortex." After the advent of electron microscopy, the pathologists described the fibrils as neurofilaments and the central core of the patches as amyloid. To date, Alzheimer´s Disease is characterized as a disease with loss of neurons and synapses in the cerebral cortex and certain subcortical areas leading to atrophy of the affected regions, including degeneration in the temporal lobe and parietal lobe, and parts of the frontal cortex and cingulate gyrus (Wenk, 2003). There is still an ongoing debate about the molecular mechanisms underlying neuronal cell death in Alzheimer disease. One theory is the amyloid hypothesis, which was first postulated in 1992. According to this hypothesis, the amyloid plaques consist of insoluble deposits of cellular material outside and around the neurons. The principal component of the amyloid plaques is the amyloid beta protein (Aβ), which is produced and secreted by neurons. Aβ aggregates as amyloid deposits in the brain. This process is a consequence of either Aβ overproduction or reduced clearance. The amyloid plaque formation and the toxic soluble Aβ oligomers lead to a cascade of pathological events including impaired cell-to-cell communication, neuronal loss, and ultimately, to cognitive and behavioral dysfunction of the diseased patient. Initially,

it was thought that the amyloid plaques mediate this toxic cascade but now more and more data suggest that already mono- and oligomeric Aβ peptides initiate this process by disrupting synaptic function. This process sets in even long before the first plaques appear (Hardy, 2002; Kawasumi et al., 2002; Walsh et al., 2002). The second theory of pathogenesis concerns the protein tau. Tau is a neuronal microtubule-associated protein which promotes together with tubulin the formation of microtubules in the neuronal axons (Mandelkow et al., 1996). In a diseased brain, tau appears as a hyperphosphoryated protein which causes dissociation of tubulin and, subsequently, disintegration of the microtubules. The microtubules in turn form insoluble twisted fibers (neurofibrillary tangles) which fall apart. As a consequence, the movement of micronutrients, neurotransmitters and organelles that requires a proper microtubular network is severely impaired (Iqbal et al., 1989 ; Bouras et al., 1994). In the end, this fatal events result in a loss of the biological activity and communication between neurons and, ultimately, cell death (Iqbal et al., 1998).

1.3.2 Characteristics of Alzheimer´s Disease

Patients which suffer from Alzeimer´s Disease have an average life expectancy of 8 years after diagnosis but it can increases up to 20 years depending on health conditions. Since the world population gets older and the age is a known risk factor for developing AD, the numbers of Alzheimer patients double every 4 years of life after age 65. Today, there are 24 million people worldwide which are diagnosed of Alzheimer´s Disease (Ferry et al., 2005). In its most common form (95%), it occurs in people at the age of 65 or later (LOAD, late onset Alzheimer´s Disease) but in some cases also younger people develop AD, in particular, when they exhibit specific gene mutations leading to an accelerated onset (EOAD, early onset Alzheimer´s Disease) (Jellinger, 2005).

The progression of Alzheimer´s disease can be classified in several stages. In its early stage, plaques and tangles begin to form long before symptomes can be detected. The first affected regions are the entorhinal cortex and the hippocampus of the brain, both involved in learning and short-term memory. In the following mild and moderate Alzheimer disease stages, the plaques and tangles become more evident in

these brain areas and also extend to other regions important for speach, long-term memory, and in body-to-object-relations. Individuals in this stage are confused and have problems to cope with their work and social life. Some may even change in personality and behavior and have problems recognizing friends and family members. This is the stage when most patients are diagnosed with Alzheimer´s Disease (Tabert et al., 2005; Waldemar et al., 2007). In the last, most severe stage of the disease, the patients lose their ability to communicate, to recognize their family and objects and they are unable to care for themselves. In the end they will lose bodily functions until death occurs.

1.3.3 Genetics of Alzheimer´s Disease

Inheritance of known genes that predispose to familial AD (FAD) accounts for only 5–10% of all patients. The genes implicated in FAD are the APP gene and the two presenilins PSEN1/2 (Schellenberg, 1995; Nishimura et al., 1999; Hardy, 2001). Mutations within the APP occur around the processing sites of the APP molecule resulting in increased production of the Aβ peptide (Suzuki et al., 1994) or in a decreased ratio of Aβ40 to Aβ42 (Ancolio et al., 1999; Makrarova et al., 2004). The Aβ42 variant is more prone to aggregate and to form plaques. Those patients exhibit an early age of onset (EOAD, early onset Alzheimer´s disease) usually younger than 60 years which is only modified by the presence of the APOE genotype (Hardy, 2001). The PSEN1 gene mutations account for 18–50% of the early-onset autosomal dominant forms of AD (Theuns et al., 2000) resulting in an aggressive form of the disease having an age of onset between 30 and 50 years, which is not influenced by the APOE genotype (Hardy, 2001). All presenilin mutations leads to an increase of the production and accumulation of the Aβ42 peptide.

The late-onset form of sporadic AD (LOAD) (>65 years) is influenced by genetic risk factors like the APOE gene (Roses, 1997). APOE is a protein component of lipoproteins and is important for receptor-mediated uptake and metabolism of cholesterol. There are three APOE isoforms (APOE2, APOE3, APOE4). Thus, six genotypes were possible: three homozygous genotypes (E4/4, E3/3, and E2/2) and three heterozygous genotypes (E4/3, E3/2, and E4/2). The APOE4 allel occurs in 74% of the popu-

lation. The *Apoe* genes do not cause AD but increase the risk for an earlier onset in patients exhibiting the allelic combination E4/E4 (Corder et al., 1993) by stronger binding to Aβ and enhancing the formation of amyloid plaques (Strittmatter et al., 1993). APOE2, however, reduces the risk for AD (Corder et al., 1993). The cause therefor is not clear but it is assumed that APOE2 protects cells for oxidative stress (Miyata, 1996).

Further genes which are implicated as genetic risk factor in sporadic AD are alpha-2 macroglobulin, a protease inhibitor found in neuritic plaques (Blacker et al., 1998; Dodel et al., 2000), the monoamine oxidase A gene which assists into regulation of metabolism of neuroactive and vasoactive amines in the central nervous system (Takehashi et al., 2002), and myeloperoxidase (MPO), an enzyme which catalyses the production of the oxidant hypochlorous acid and is thought to contribute to Alzheimer´s pathology through oxidation of either Aβ or APOE (Combarros et al., 2002). Further suceptibility for AD are mutations in the *tau* gene. Patients with a tau mutation show cognitive impairment similar to AD but lack senile plaque formation. The latter observation support the hypothesis that dementia can arise directly from abnormal processing and accumulation of tau independently of any influence of Aβ metabolism (Hutton et al., 1998; Tanahashi et al., 2004).

1.3.4 The molecular biology of Alzheimer´s Disease

1.3.4.1 The APP-like protein family

Amyloid plaque formation begins with the amyloid precursor protein (APP), a transmembrane protein that is ubiquitously expressed in all tissues (Kang et al., 1987). The *App* gene was detected on human chromosome 21. It is encoded by 18 exons, of which exons 7, 8, and 15 are alternatively spliced in a development fashion (Sandbrink et al., 1997). APP is found in mammals, but homologous proteins have also been identified in other species like *Drosophila melanogaster* (Rosen et al., 1989) and *Caenorhabditis elegans* (Daigle et al., 1993). The three major isoforms of APP are APP_{695}, APP_{751}, and APP_{770}. The APP_{751} and APP_{770} variant exhibit a Kunitz-type inhibitor sequence (Kitaguchi et al., 1988; Ponte et al., 1988; Tanzi et al., 1988)

and are widely expressed throughout the body. In contrast, the APP$_{695}$ isoform is predominantly expressed in neurons (Sandbrink et al., 1994; Selkoe, 2001). APP belongs to an evolutionarily conserved family of proteins which also includes the APP-like proteins 1 (APLP1) and 2 (APLP2) (Wasco et al., 1992; Wasco et al., 1993; Slunt et al., 1994). Compared with APP, the APLPs show a high degree of sequence conservation at the N-terminal and cytoplasmic regions but divergence in the Aβ and transmembrane domains (Wasco et al., 1992). APP knockout mice are viable and display only a mild phenotype, including reduced forelimb grip strength and locomotor activity (Müller et al., 1994; Zheng et al., 1995). However, combined knockouts APLP2/ALPL1 and APLP2/APP or triple knockout result in lethality after birth (Heber et al., 2000). Interestingly, APP and APLP1 double knockout mice are viable with no obvious phenotype (Heber et al., 2000) suggesting an essential function of APLP2 during development. This finding indicates that APP, APLP1 and APLP2 have unique but also overlapping roles.

1.3.4.2 The structure of APP

The APP polypeptid sequence comprises a number of distinct, independently-folding structural domains (figure 8). The extracellular region is divided into the E1 and E2 domains. E1 contains several subdomains including a growth factor-like domain (GFLD) and a copper-binding domain (CuBD) (Sisodia et al., 1993; Rossjohn et al, 1999). The GFLD domain is cysteine rich and possesses disulfide bridges that stabilize a β-hairpin loop and seems to be critical for neurite outgrowth (Small et al, 1994) and MAP kinase activation (Greenberg et al, 1995). This domain may represent one of the putative heparin-binding sites and be involved in protein-protein interaction as well as APP-APP dimerization. The E1 domain is connected via a flexible acidic region to the carbohydrate domain, which can be divided into the E2 domain (central APP domain (CAPPD)) and the linker region. In two of the three isoforms (APP$_{751}$ and APP$_{770}$) the APP holoproteins contain a Kunitz-type protease inhibitor domain (KPI) which is located between the acidic region and the E2 domain. In the APP$_{695}$ isoform this KPI domain is absent (Small et al., 1994). The E2 region might provide interaction sites for binding partners. It contains a highly conserved heparan sulfate proteoglycan (HSPG)-binding site and a pentapeptide sequence

(RERMS) (Ninomiya et al., 1993; Jin et al., 1994; Wang et al., 2004). The latter is implicated in the growth-promoting properties of APP (Ninomiya et al., 1993; Li et al, 1997). The E2 domain is followed by a transmembrane region and a APP intracellular domain (AICD).
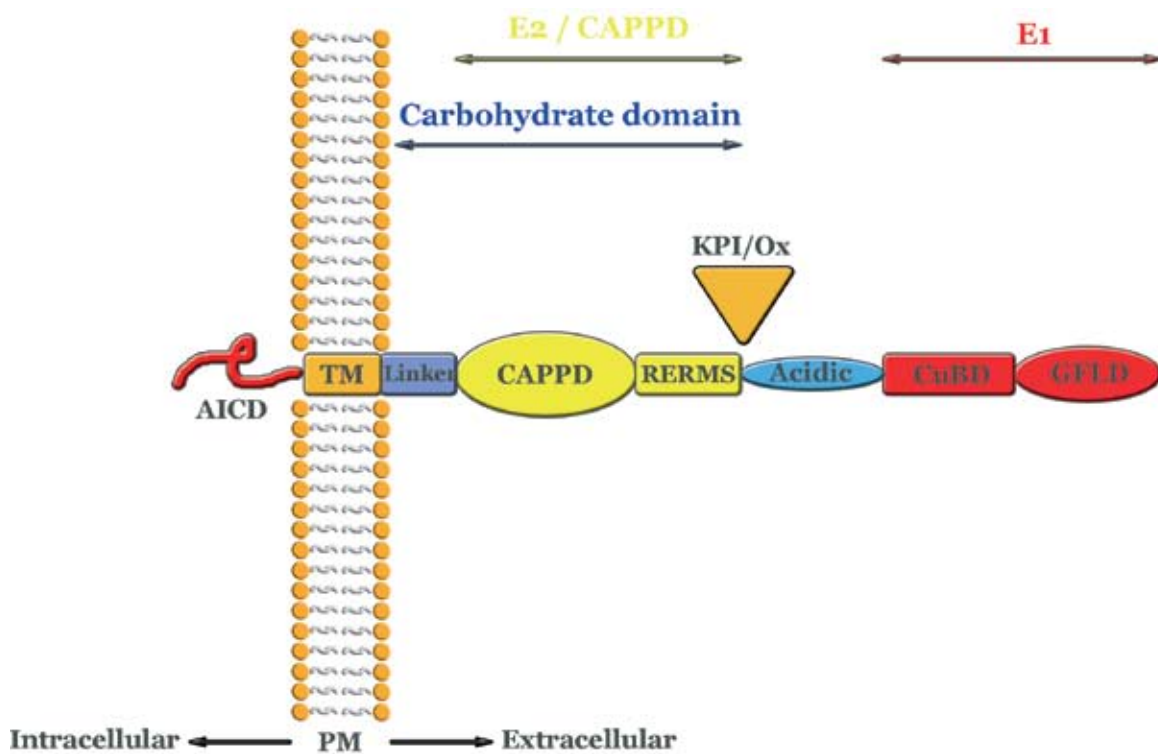
Figure 8: Schematic representation of the human APP$_{695}$ protein.
The E1 region consists of a growth factor-like domain (GFLD) and the copper-binding domain (CuBD). The E1 region is linked via the acidic region to the carbohydrate domain. The carbohydrate domain can be subdivided into the E2 domain, also called central APP domain (CAPPD), the RERMS sequence, and a linker. The carbohydrate domain is followed at the C-terminus by the transmembrane (TM) and the APP intracellular domain (AICD). The Kunitz-type protease inhibitor domain (KPI), which is present in APP$_{751}$ and APP$_{770}$, and the Ox2 sequence, which is present in APP$_{770}$ exclusively, are shown above their insertion site.

1.3.4.3 Modification and processing of APP

APP can be modified and processed by multiple pathways. During and after translation, APP is *N*- and *O*-linked glycosylated at the rough endoplasmic reticulum mem-
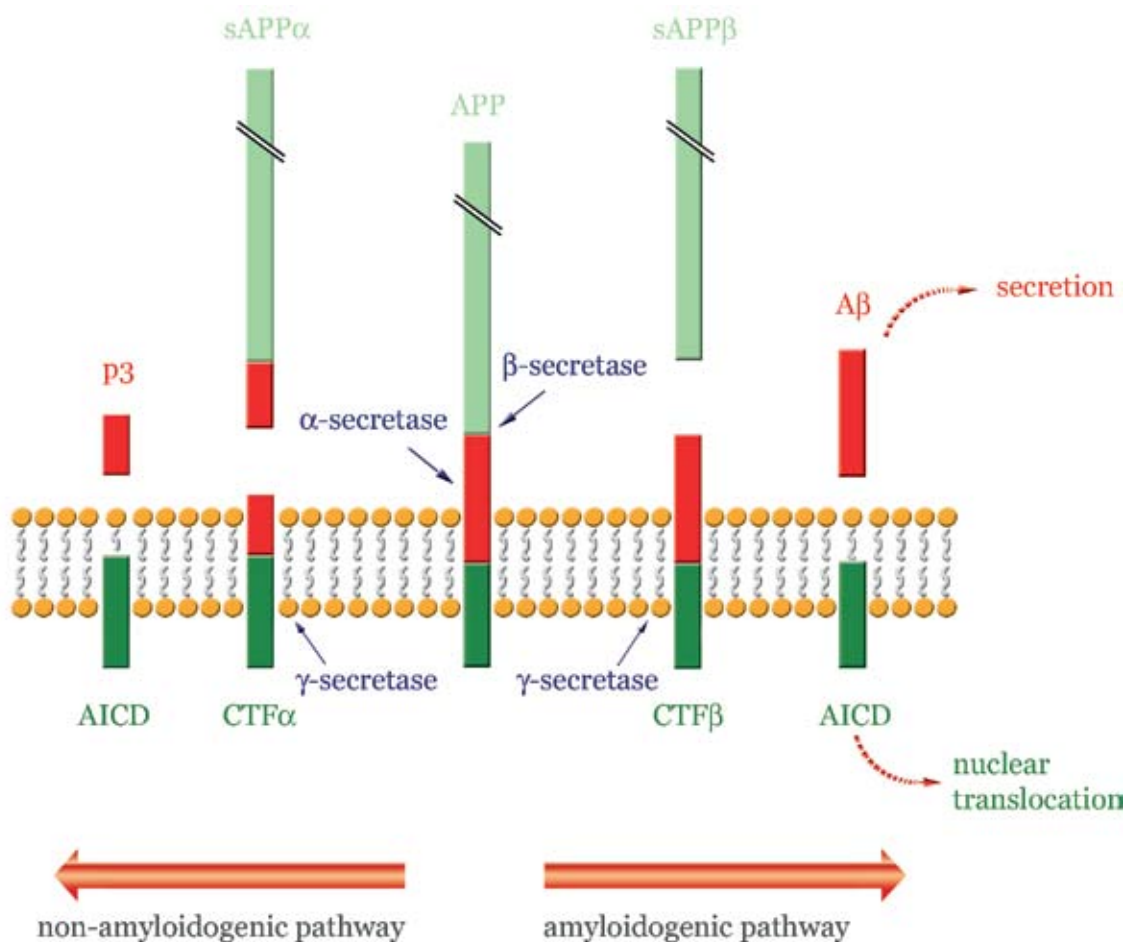
Figure 9: The non-amyloidogenic and amyloidogenic pathway of APP processing. APP is cleaved either at the α- or β-site releasing the large ectodomain (sAPPα or sAPPβ) and a membrane retained C-terminal fragment (CTFα or CTFβ). The CTFs are further processed by the γ-secretase complex, generating Aβ from CTFβ in the amyloidogenic pathway or p3 from CTFα in the non-amyloidogenic pathway. Cleavage at the γ-site releases the APP intracellular domain (AICD) which translocates to the nucleus.

brane and the Golgi compartment. Later, APP becomes posttranslational phosphorylated (Oltersdorf et al., 1990) and sulfated (Weidemann et al., 1989; Oltersdorf et al., 1990), as well as modified by the addition of glycosaminoglycans side chains to yield a chondroitin sulfate proteoglycan (Shioi et al., 1992).

There are several possibilities how the APP holoprotein can be proteolytically processed. The two main pathways are: the non-amyloidogenic pathway and the amyloidogenic pathway (figure 9). The non-amyloidogenic pathway is thought to be the physiologically relevant one. Thereby, newly synthesized APP molecules move to the plasma membrane where they are cleaved by the α-secretase TACE (tumor necrosis factor-α-converting enzyme) or ADAM17, two metalloproteinases (figure 9). This cleavage releases a large soluble ectodomain (sAPPα) into the extracellular space and a shorter membrane ancored C-terminal fragment (CTFα) (Weidemann et al., 1989; Selkoe et al., 1989) (figure 10). The processing precludes the formation of the pathological form Aβ, since α-secretase cleavage occurs within the Aβ sequence (Esch et al., 1990). Alternatively, uncleaved APP molecules may internalize via clathrin-coated vesicles and can either be processed by β- and γ-secretases or become degraded in lysosomes (Golde et al., 1992) (figure 10). Processing by the aspartyl proteinase β- secretase BACE1 (β-APP cleaving enzyme) in the endocytic compartments produces the soluble sAPPβ molecule (Vassar et al., 1999). Further cleavage by γ-secretase complex generates the toxic Aβ peptid. Both processing products are secreted into the extracellular fluid. The γ-secretase multiprotein complex consists of presenilin 1 and 2, two catalytic active multi-transmembrane phosphoproteins. They are associated with nicastrin, APH1, and PEN-2 (De Strooper, 2003; Baulac et al., 2003), additional components of the secretase complex. The combined action of β- and γ-secretases on APP is called the amyloidogenic pathway (figure 9) and it is thought to be enhanced in Alzheimer´s Disease (Vassar et al., 1999; Edbauer et al., 2004). Aβ , in contrast, can be degraded by the insulin-degrading enzyme (IDE) (Farris et al., 2003) and the neutral endopeptidase neprilysin (Iwata et al., 2001). Cleavage at either the α- or β-secretase site produces a truncated APP molecule (CTFα and CTFβ) that is now a substrate for the γ-secretase, which can cleave APP within its transmembrane domain. The released CTFγ (or APP intracellular domain, AICD) translocates into the nucleus where it might regulate gene transcription (Cao et al., 2001; von Rotz et al., 2004).
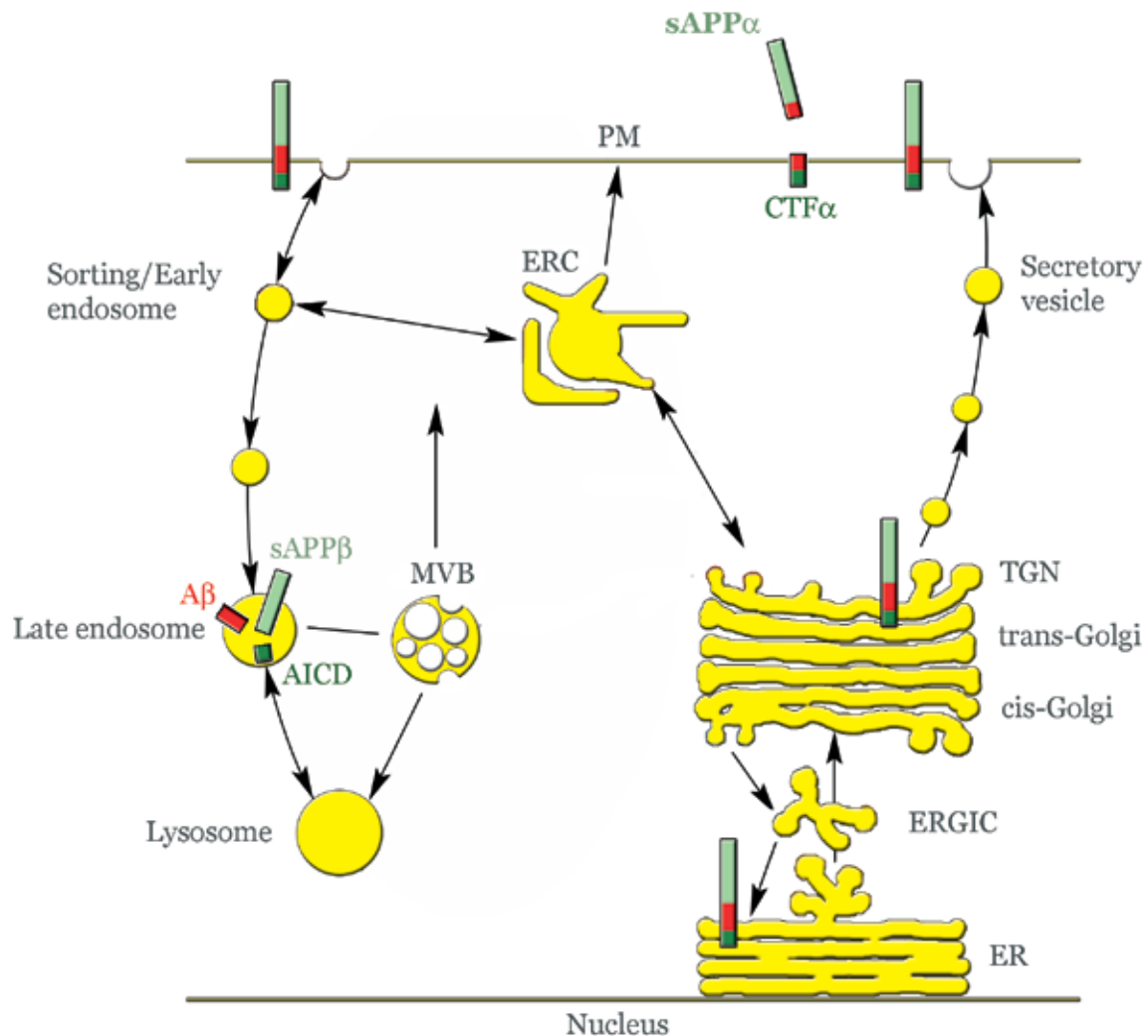
Figure 10: Subcellular localization and processing of APP.
After synthesis of APP at the membrane of the rough endoplasmic reticulum (rER), and further glycosylations and maturations in the Golgi, APP holoprotein is transported to the plasma membrane (PM) where it can be cleaved by α-secretases. This process, also called the non-amyloidogenic pathway, releases a large soluble domain (sAPPα) and a cytoplasmic terminal fragment (CTFα). In the amyloidogenic pathway, cleavage by β- and γ-secretases occurs mainly after internalization of the APP holoprotein from the cell surface. Neurotoxic Aβ peptides, as well as sAPPβ and CTFβ are generated in endocytic compartments. Alternatively, APP holoproteins can be rescued by retrograde transport to the Golgi, recycle back via recycling endosomes to the plasma membrane, or it may be degraded via the lysosomal pathway.

1.3.5 The physiological role of APP

The amyloid precursor protein (APP) is ubiquitiously expressed in many tissues and homologues are found in different species. Together with the fact that combined gene defects of members of the APLP family leads to lethality and neurological deficits, assume an important physiological function of APP.

1.3.5.1 APP deficient and transgenic animals

App-transgenic animals do provide clues as to the potential physiological roles of the protein. For example, overexpression of members of the APP family in *Drosophila melanogaster* affects the peripheral nervous system by transformation of cell fates during development. Genetic analysis showed that APP induces Notch gain-of-function phenotypes by interacting with Numb, a negative regulator of Notch signaling (Merdes et al., 2004; Loewer et al., 2004) as well as axonal transport deficits (Gunawardena et al., 2001) and induction of neurite outgrowth and arborization after traumatic brain injury (Leyssen et al., 2005). Indeed, APP can directly interact with Notch receptor through their transmembrane domains (Fassa et al., 2005; Oh et al., 2005). APP null mutant flies are viable and fertile but display neuronal defects such as reduced number of synapsis (Ashley et al., 2005; Torroja et al.; 1999).

As already mentioned before, APP deficient mice display hypersensitivity to seizures (Steinbach et al., 1998) and combined gene deficiency of APLP2/ALPL1 and APLP2/ APP or all three genes result in lethality after birth (Heber et al., 2000). Mice which are deficient in all three genes display characteristics of cobblestone (type II) lissencephaly (Herms et al., 2004). They exhibit cortical dysplasia by fragmented basal lamina and enhanced migration of neurons suggesting a putative function for APP in neuronal cell adhesion and migration.

1.3.5.2 APP and its interaction partners

Another possibility to get more insights into the physiological role of APP is the indentification of interaction partners. So far, APP has been shown to a number of proteins whose proposed functions can be grouped into distinct biological catagories including neurite outgrowth, dendritic arborization and synaptogenesis. For instance, one of the APP ligands is F-spondin, a secreted neuronal extracellular matrix protein that promotes the attachment of spinal cord and sensory neuron cells and the outgrowth of neurites. Expression of F-spondin prevents cleavage of APP by β-secretases and reduces Aβ production (Ho et al., 2004).

A further interacting partner is the Nogo-66 receptor that regulates the axonal regeneration and plasticity in the adult central nervous system. It can also interact with APP and thereby prevent Aβ generation (Park et al., 2006).

Finally, the receptors BRI2, LRP, and SORLA also bind to APP and alter Aβ production (Kang et al., 2000; Fotinopoulou et al., 2005; Andersen et al., 2005). For example, LRP1 influences both the generation and clearance of Aβ (Ulery et al., 2000). LRP1 can directly interact with full length APP on the cell surface and facilitates its internalization which, in turn, leads to enhanced production of amyloidogenic C-terminal β-fragments and increased Aβ secretion (Kounnas et al., 1995). In contrary, LRP1 can clear Aβ from the extracellular space by forming complexes with ligands such as APOE, lactoferrin, and α2M, which can bind Aβ. This pathway may contribute to the cellular catabolism of the peptid.

1.3.5.3 A putative role for APP in signal transduction

There are also some indications for an influence of APP on signal transduction. When APP is cleaved by γ-secretases the APP intracellular domain (AICD) is released into the cytosol where it interacts with the adaptor protein Fe65. This complex translocate to the nucleus and acts as transcription factor by influencing the expression of genes involved in cell motility, developmental and injury-related cytoskeletal dynamics (Sabo et al., 2001; Sabo et al., 2003; Guenette et al., 2006; Müller et al., 2007). The transcriptional activity of AICD is still strongly debated. However, such as mecha-

nism is plausible as it resembles the role of presenilins, the principal component of the γ-secretase complex, in the cleavage of other signal transducers including Notch-1, ErbB4, LRP and catherin (Kopan et al., 1996; Schroeter et al., 1998). Furthermore, the cytoplasmic domain of APP can interact with proteins involved in cell-cycle regulation such as APP-binding protein 1 (APP-BP1) and the serine/threonine kinase p21-activated kinase (PAK3) which is implicated in DNA synthesis and neuronal apoptosis (Chow et al., 1996; McPhie et al., 2003). The cytoplasmic tail of APP harbors a YENPTY motif which serves as internalization signal but can also interact with several adaptor proteins like X11 (Mint1) (Borg et al., 1996), Fe65 (Fiore et al., 1995; Borg et al., 1996), mDab (Howell et al., 1999), c-Abl (Zambrano et al., 2001), JIP-1 (Scheinfeld et al., 2002), and Numb (Roncarati et al., 2002). Interaction of APP with Fe65 or X11 influences APP processing and consequently Aβ formation.

There are indications that AICD may also be involved in phosphoinositide-mediated Ca^{2+} signaling. Cells deficient in APP display defects in Ca^{2+} signaling which can be rescued by overexpressing AICD (Leissring et al., 2002). It was also shown that the γ-secretase needs the release of Ca^{2+} from the endoplasmic reticulum Ca^{2+} stores to carry out its activity.

1.3.5.4 APP can influence cell adhesion and cell migration

APP homodimerization or heterodimerization with heparin and collagen of the extracellular matrix mediates cell-cell adhesion and neurite outgrowth (Breen et al., 1991; Soba et al., 2005). It was also reported that APP is involved in cell migration (Sabo et al., 2001). APP together with Fe65 colocalize with actin and Mena. The latter factor is known to regulate actin dynamics. Increased APP expression leads to accelerated cell movement which is regulated by Fe65. On the cell surface of neurons it was shown that APP colocalizes with the adhesion protein integrin (Yamazaki et al., 1997). Integrins are involved in cell proliferation, differentiation, and cell migration by connecting cells with proteins of the matrix.

1.3.5.5 APP is involved in axonal transport processes

APP can undergo axonal transport by binding to kinesin-I. This interaction occurs either directly or indirectly via adaptor protein Jip-1 (Jun N-terminal kinase (JNK) interacting protein) (Kamal et al. 2000; Scheinfeld et al., 2002). Both BACE-1 and presenilin-1 are also members of the anterograde axonal vesicles which transport is mediated by APP and kinesin-1 (Kamal et al., 2001). Therefore, one function of APP might be to act as kinesin-I membrane receptor which carries proteins along the axons of neurons.

1.3.5.6 APP may influence the cell metabolisms

It was shown that mice deficient in APP$^{-/-}$ or APLP2$^{-/-}$ or both display reduced plasma glucose levels compared to wild-type mice (Needham et al., 2008). Plasma insulin, calcium, magnesium, and phosphate levels were also significantly lower in the double deficient mouse compared to control animals. Furthermore, they displayed growth restriction and, moreover, the double deficient mice died before birth.These results suggest APP and APLP2 as key regulators of glucose metabolism and growth by some yet unclear mechanism.

The APP extracellular domain strongly binds copper (Cu II) and reduces it to Cu I (Hesse et al., 1994). Since APP deficient mice display an enhanced copper level in the brain, APP is thought to act as a key regulator of neuronal copper homeostasis (White et al., 1999). Increasing the copper concentration reduces Aβ production while the concentrations of cell-bound and secreted forms of APP are enhanced (Borchardt et al., 1999).

1.3.5.7 The role of sAPPα

Besides the function of full length APP, also the APP cleavage products were shown to affect the biological functions of a cell. APP can be cleaved by α-secretases to gen-

erate soluble APPα. This process is triggered by activation of protein kinase C (Buxbaum et al., 1993). The APP ectodomain might serve as a signaling molecule and as a neuroprotective factor for primary neurons (Mattson et al., 1993). In fact, soluble APPα has been implicated in various cellular processes including regulation of neuronal excitability and synaptic plasticity, neuroprotection, and enhancing memory (Roch et al., 1994; Furukawa et al., 1996; Meziane et al., 1998; Mattson et al.,1998; Turner et al.,2003). Furthermore, sAPPα can modulate axonal and dendritic growth (Perez et al., 1997). In contrast, binding of fibulin-1 to the N-terminal head of sAPPα inhibits sAPP-mediated proliferation of neural stem cells (Ohsawa et al., 2001).

1.3.5.8 The role of intracellular Aβ-peptid

Soluble Aβ aggregates are possibly the most important mediator of neuronal toxicity in AD (Klein et al., 2001;Walsh et al., 2002). Aβ accumulation within neurons disrupts synaptic activity by accumulation in axons and axon termini, leads to proteasome dysfunction, causes imbalance in calcium homeostasis, and even facilitates hyperphosphorylation of tau. It was shown that Aβ oligomers inhibit long-term potentiation (LTP) *in vivo* and lead to neuronal dysfunction (Walsh et al., 2002). Concentrated soluble Aβ oligomers impair Erk/MAPK, CaMKII and Akt/PKB activation which are responsible for the signal transduction cascades that mediate LTP (Townsend et al., 2007). Another and early key feature of Alzheimer´s disease is the loss of cholinergic neurons (Yan et al., 2004) which express high levels of the p75 neurotrophin receptor (p75NTR). p75 mediates cell death after ligand binding (Kenchappa et al., 2006). Aβ can interact with the extracellular domain of p75 and may activate p75-mediated cell death in AD (Yaar et al., 1997).

Besides the pathological function of Aβ, this peptid might also have an essential physiological role in lipid homeostasis. Changes in lipid homeostasis are known to be one reason for neurodegenerative diseases since it affects neuronal function. There are also indications that hypercholesterolemia is a risk factor to develop amyloid pathology, and more and more evidences points towards an involvement of lipids in AD by effecting APP processing and Aβ generation. Hence, Aβ production is increased by cholesterol and conversely an increase of Aβ-peptids cause a decrease in cholesterol biosynthesis (Bodovitz et al., 1996; Simons et al., 1998).

2. Aim of the Study

Alzheimer disease (AD) is the most common form of neurodegenerative diseases. Previously, major attention has been focused on understanding the pathways leading to proteolytic cleavage of APP and Aβ deposition, and the characterization of the enzymes involved. In contrast, little is known about the control mechanisms which affect APP metabolism and how this receptor is transported to the various compartments where this processing occurs. Gene expression profiling studies revealed reduced levels of SORLA in patients suffering from AD compared with healthy individuals (Scherzer et al., 2004). Based on this observation, reduced SORLA activity may be considered a primary cause of increased Aβ production and AD development. Conceivably, SORLA could have an important impact on APP metabolism by either inhibiting the interaction of APP with the respective proteases thereby influencing the processing and degradation of APP molecules, or by controlling the transport of APP to the distinct subcellular compartments less favorable for amyloid formation.

The aim of my work was to exactly elucidate the role of SORLA in APP metabolism. Ultimately, I wanted to validate the *Sorla* gene as a genetic cause of the progression of Alzheimer´s disease and uncover the mechanism whereby this gene product affect neurodegenerative processes.

In particular, I tested the hypothesis that SORLA acts as an intracellular receptor which influences the transport and processing of APP. Accordingly, SORLA may function as a sorting receptor that protects APP from processing into Aβ and reduces the burden of amyloidogenic peptide formation. Consequently, a lack or a reduced SORLA level in human brain of AD patients or SORLA knockout mice should lead to enhanced Aβ production and thus promote spontanous AD.

3. Material and Methods

3.1 Animal Experiments

3.1.1 *Sorla*-deficient mice

Sorla-deficient mice were generated by gene targeting in embryonic stem cells with mouse lines generated from three independently targeted cell clones (M. Gotthardt, Max-Delbrueck Center, Germany). Animals were analyzed on hybrid (129SvEmcTer x C57BL6N) or (129SvEmcTer x Balbc) genetic backgrounds with identical results in all strains compared with age- and sex-matched control mice.

3.1.2. Immunohistology

For immunohistology, PBS perfused and formalin-fixed mouse brains were sagitally cut into halves and kept in formalin for 72 hours. After two hours washing with water the brains were adapted to ethanol (2 hours 70% ethanol; 2 hours 90% ethanol; over night 96% ethanol; 2 hours 100% ethanol; 2 hours 100% ethanol; 2 hours 100% ethanol). Subsequently, the brain halves were incubated in roti-histol 2 x 20 min, and transfered for 2 x 2 hours in paraffin at 60°C, and finally embedded in paraffin. The tissues were cut in 4 µm sections on a rotary microtome (Rm2155, Leica microsystems GmbH, Germany) and blocked for 1 hour with M.O.M. (Vector Lab., USA) at room temperature. Thereafter, the slides were stained with primary antibodies for APP (CT695, 1:500, Zymed, Germany; CT15, 1:1000, C. Pietrzik, University of Mainz, Germany), SORLA (solSORLA, 1:1000, J. Gliemann, University of Aarhus, Denmark), or Aβ (4G8, 1:400, Signet Lab., USA), followed by peroxidase-conjugated secondary antibodies (1:500 in TBST, 1% BSA, Sigma-Aldrich Co., Germany). Detection was done by diaminobenzidine (DAB peroxidase substrate, Vector Lab., USA). The slides were mounted with Canada balsam. Amyloid plaques were visualized with 1% thiovlavin-S/water (8 min in the dark) and, subsequently, mounted with cytomation fluorescent mounting medium (Dako).

3.1.3 Tissue homogenization for Aβ measurements

Brains were homogenized in cold guanidine solution (5 M guanidine HCl, 50 mM Tris HCl) using a homogenizer (3 x 30 sec, Ultra-Turrax, IKA Werke, Germany). The homogenates were incubated for 4 hours at room temperature and thereafter diluted with cold reaction buffer (5% BSA, 0,03% tween-20, 1 x protease inhibitor cocktail in PBS) to a final concentration of 0,1 M guanidine. Thereafter, the samples were centrifuged (16000 x rpm, 20 min, 4°C) and the supernatents containing murine or human Aβ40 and Aβ42 were analysed and quantified by ELISA using specific antibodies (BioSource International, CA).

3.1.4 Tissue homogenization for Western blotting

Brains were homogenized in cold TEE lysis buffer (25 mM Tris, 1 mM EDTA, 1 mM EGTA, 1 x protease inhibitor cocktail, pH 7,4) by a mortar (30 strokes, Braun, Germany) and then diluted with sodium deoxycholate (5 % in TEE) to a final concentration of 1 % sodium deoxycholate. The mixtures were 4 x 20 sec sonificated and centrifuged (15 min at 17000 g). The supernatents were collected and the proteins were detected by Western blot analysis.

3.2 Cell culture experiments

3.2.1 Freezing of cells

Cells were harvested and washed once with complete medium. The cells were centrifuged (3 min 800 x rpm) and resuspended in ice-cold freezing medium (20 ml FCS, 20 ml complete medium, 10 ml DMSO). The mixtures were aliquoted, transfered to freezer vials and placed in freezing boxes that contained isopropanol. After freezing the cells over night at -80°C the vials were transferred to liquid nitrogen storage containers.

3.2.2 Thawing of cells

The frozen cells were warmed up by adding 1 ml of warm complete medium to the vial. The cells were then centrifuged (3 min 800 x rpm) and resuspended in fresh growth medium before plating onto the culture dish.

3.2.3 Cell growth and splitting

CHO cells were grown in Dulbecco's modified Eagle medium (DMEM, Cambrex Corp., USA) with 10 % fetal calf serum (FCS, PAA Lab., Austria) and penicillin/ streptomycin (Cambrex Corp., USA). SH-SY5Y cells were grown in Ham's F12/ DMEM (1:1, PAA Lab., Austria) with 10 % FCS, 0,1 mM non-essential amino ac- ids (NEAA, Gibco/Invitrogen, UK), 2 mM L-glutamine (Gibco, UK), and penicillin/ streptomycin. For selection of the various stably transfected cell lines the following selection reagents were used: hygromycin-B (Invitrogen, UK, 500 µg/ml for APP positive CHO cells and 100 µg/ml for APP positive SH-SY5Y cells) and zeocin (In- vitrogen, UK, 333 µg/ml for SORLA positive CHO cells and 25 µg/ml for SORLA positive SH-SY5Y cells). All cells were incubated at 37°C and 5 % CO_2 atmosphere, and expanded every 2-3 day when the cells were semi-confluent. For splitting the medium was removed from culture dish and the cells were washed in PBS. Trypsin- EDTA solution was added to the cells to cover the bottom of the culture dish and the cells were transfered to an incubator for 2 min at 37°C. The detached cells were resuspended in growth medium and an aliquot was plated onto a new culture dish.

3.2.4 Transfektion and selection

Semi-confluent cells were kept in antibiotic free medium and transfected with multi-component lipid-based transfection reagents (FuGENE6, Roche, Germany; lipofectamine 2000, Invitrogen, UK; HiFect, Amaxxa biosystems, Germany; PEI, Polyethylenimine, Polyscience, USA) based on manufacturers´recommendations. After 24 hours, the medium was removed from the transfected cells and substituted by fresh growth medium. For generating stable cell lines, the medium was replaced

by hygromycin B and/or zeocin containing medium after 48 hours and refreshed each second day. Positive colonies were picked and transferred into new culture dishes until they were analysed for protein expression.

3.3 Microbiological methods

3.3.1 Culture media and culture plates

DH5α bacteria cells were cultured in LB medium (1 % Bacto-Tryptone, 0,5 % Bacto-Yeast extract, 0,5 % NaCl) with the appropriate selective agent (ampicillin, Sigma-Aldrich Co., Germany; kanamycin, Sigma-Aldrich Co., Germany). For culture plates 7,5 g agar were resolved in 500 ml LB medium by heating. After the agar was resolved the medium was chilled to 50°C before the antibotic was added (ampicillin to a final concentration of 100 μg/ml; kanamycin to a final concentration of 15 μg/ml) and the medium was portioned to petri dishes. The plates were stored at 4°C.

3.3.2 Preparation of electrocompetent bacteria

E. coli DH5α cells were grown overnight at 37°C with shaking. The next day 10 ml of the cell suspension was diluted into 1 l of LB medium and grown at 37°C until the OD600 reached 0.5. The bacteria cells were cooled for 20 min on ice and then harvested by centrifugation (15 min, 4000 x g, 4°C). The pellet was resuspended in 1 l of icecold sterile 10 % glycerol. Cells were again collected by the same centrifugation step. The resulted cell pellet was again resuspended in 500 ml of icecold sterile 10 % glycerol and pelleted again by centrifugation. Thereafter, the cells were resuspended in 20 ml icecold sterile 10 % glycerol and collected again (4000 x g, 15 min, 4°C). Finally, the bacteria cells were resuspended in 2 ml of 10 % icecold sterile glycerol once more and portioned in 100 μl aliquots. The aliquots were stored at -80°C.

3.3.3 Transformation of bacteria with DNA

Electrocompetent *E. coli* DH5α cells were transformed with ligation reaction or directly with purified DNA: 40 µl of DH5α cells were mixed with 2 µl ligation reaction or 10 ng of plasmid DNA and placed in a electroporation cuvette. After electroporation at 1.8 kV the cell suspension was transferred to a 2.0 ml tube and mixed with 1 ml of SOC medium (LB medium with 10 mM MgCl2, 10 mM MgSO4, 20 mM glucose). The cells were incubated at 37°C for 60 min with shaking and plated on LB agar plates containing the appropriate selective antibiotic.

3.3.4 Cryopreservation of bacteria

An overnight culture of E. coli was mixed 1:1 with glycerol and immediately frozen at -80°C.

3.4 Molecular biology methods

3.4.1 Isolation of plasmid DNA from bacteria

One single colony from a selective culture plate was picked and the bacteria cells were grown in LB medium containing the appropriate selection marker over night at 37°C with shaking. The next day, cells were harvested by centrifugation (5 min, 14000 x g, RT). The pellet was resuspended in resuspension buffer (50 mM Tris-HCl, 10 mM EDTA, 100 µg/ml RNase A, pH 8.0) and subsequently lysed by lysisbuffer (200 mM NaOH, 1% SDS). The solution was gently mixed with chilled neutralization buffer (3.0 M K-acetate, pH 5.5) and incubated on ice for 15 min to precipitate material containing genomic DNA, proteins, cell debris and SDS. After centrifugation (14000 x g, 20 min, 4°C) the plasmid DNA containing supernatent was transferred to a new reaction tube and the DNA collected by adding 10 % volume of 3 M LiCl and 2.5 volume of 100% isopropanol followed by centrifugation (14000 x g, 30 min, 4°C). The pellet was washed once with 70 % ethanol and resuspended in 30 µl of steril water. The purified plasmid DNA was stored at -20°C.

3.4.2 Isolation of genomic DNA from tissue samples

Genomic DNA from mice was obtained by digesting the tissue in tail buffer (10 mM Tris-HCl, 0.3 M Na-Acetate, 0.1 mM EDTA, 1% SDS, pH 7.0) with Protease K (final concentration: 0.5 mg/ml) at 52°C over night. Proteins were removed by adding phenol/chloroform/isoamylalcohol (25:24:1) followed by centrifugation (14000 x g, 5 min, RT) to separate the phases. The upper, aqueous DNA containing phase was mixed with 2.5 volumes of 100% ethanol. The DNA was collected by centrifugation (14000 x g, 10 min, 4°C) washed once with 70% ethanol and dissolved in TE-buffer (10 mM Tris-HCl, 1 mM EDTA, pH 8.0). Isolated genomic DNA was stored at 4°C.

3.4.3 DNA concentration determination

The concentration of DNA samples was determined by spectrophotometry at a wavelength of 260 nm. For DNA, 98 µl steril water and 2 µl of DNA solution were mixed and the DNA concentration was measured at 260 nm wavelength. DNA quality measurement was done by measuring at 280 nm wavelength. The ratio between 260 nm : 280 nm should be 1.8 or higher to ensure proper DNA quality. A lower ratio indicates protein contamination of the sample.

3.4.4 Enzymatic digest of DNA

The amount of 2 µg DNA was incubated with the selected restriction enzymes (0.5 U emzyme/µg DNA), the corresponding buffer, BSA and water. The digest was incubated at 37°C for 2 hours with shaking. After incubation, the digested DNA was subjected to gel electrophoresis to isolate the required DNA fragments. All restriction enzymes, buffers and BSA were obtained from New England Biolabs, USA.

3.4.5 Agarose gel electrophoresis of DNA

DNA fragments were separated according to their molecular weight on 0.8-2.0% agarose gels in TAE buffer (40 mM Tris, 1 mM EDTA, 20 mM glacial acetic acid, pH 8.0). To visualize the DNA, ethidium bromide was added to the gel prior to electrophoresis (final concentration: 0.5 µg/ml).

3.4.6 Isolation of DNA from agarose gels

To recover DNA from agarose gels the gel was exposed to UV-light, and bands of interest were cut from the gel. The DNA was extracted using the High Pure PCR Product Purification Kit (Roche, Switzerland). Briefly, the gel slice was incubated with binding buffer (3 M guanidine-thiocyanate, 10 mM Tris-HCl, 5 % ethanol, pH 6.6) at a ratio of 300 µl buffer/100 mg agarose at 52°C until the gel slice was completely dissolved. The sample was transferred to a filter column and subjected to centrifugation (14000 x g, 1 min, RT). The filter column was washed twice with 500 µl washing buffer (2 mM Tris-HCl, 20 mM NaCl, 80 % ethanol, pH 7.5) and the DNA was eluted with 30 µl sterile water and stored at -20°C.

3.4.7 Ligation of PCR-products using the pGEM-T Easy Vector System

The purified DNA was ligated into the pGEM-T Easy Vector (Promega, USA) according to the manufacturer´s instructions. Briefly, 4 µl of DNA solution were incubated with 5 µl Rapid Ligation Buffer (60 mM Tris-HCl, 20 mM MgCl2, 20 mM DTT, 2mM ATP, 10 % polyethylenglycole, pH 7.8), 30 ng of pGEM-T Easy Vector and 3 U of T4 DNA ligase. The ligation reaction was incubated at 16°C overnight. The next day, 2 µl of the ligation reaction was used to transform electrocompetent E. coli DH5α.

3.4.8 Ligation of a DNA-fragment in a target vector

100 ng of vector DNA were mixed with the appropriate amount of insert DNA according to the equation:

$$\text{mass}_{\text{insert}} \text{ (ng)} = \frac{5 \text{ x mass}_{\text{vector}} \text{ (ng) x length}_{\text{insert}} \text{ (bp)}}{\text{length}_{\text{vector}} \text{ (bp)}}$$

After addition of 2 µl ligation buffer (400 mM Tris-HCl, 100mM MgCl2, 100 mM DTT, 5 mM ATP, pH 7.8), 1 U of T4 DNA ligase (Fermentas, Germany) and water to a final volume of 20 µl, the mixture was incubated at 16°C over night. The next day, 2 µl of the ligation reaction was used to transform electrocompetent E. coli DH5α.

3.4.9 Polymerase chain reaction

The following components were added to a 0.5-ml microcentrifuge tube on ice:

DNA	100 ng
dNTP	0.2 mM
forward primer	0.2 µM
reverse primer	0.2 µM
PCR buffer (200 mM Tris-HCl, 500 mM KCl, pH 8.4)	1/10 volume
MgCl2	1.5 mM
water	not applicable
Taq DNA polymerase (Invitrogen, UK)	2.5 U

The tube was placed into a thermocycler (MJ Reasearch, USA) and the reaction was started by the first cycle of denaturation at 95°C for 10 min. The primers were allowed to anneal at 60°C for 30 sec and DNA synthesis was carried out at 72°C for 1-2 min. For the following 25 cycles the reaction mix was denatured at 95°C for 45 sec, annealed at 60°C for 30 sec and elongated at 72°C for 1-2 min. This was followed by a final elongation step at 72°C for 10 min. The reaction mix was then chilled to

10°C. The amplification products were analysed by agarose gel electrophoresis.

3.4.10 Generation of SORLA variants

SORLA variants were generated by site-directed mutagenesis of the human cDNA using a PCR based cloning strategy (table 2). The amino acid changes introduced into the SORLA polypeptide sequence were SORLA$^{\Delta cd}$ (stop at F2141), SORLA^{GGA} (D2180A, M2183A), and SORLA^{acidic} (D2162A, D2163A, E2166A, D2167A, D2168A, E2169A, D2170A), and SORLA^{KKLN} (in addition after stop codon K2188KLN).

Table 2: Human specific primer for site-directed mutagenesis	
Primer identifier	Sequence (5´-> 3´)
SORLA sfuI fw.	CTT GCA AAC GTC ACT GCT GCC TCC
SORLA GGA mut rev.	CCG CTC GAG TCA GGC TAT CAC CGC GGG GAC GGC ATC TGA AAA TCC AGT TAT CAT AGG GGC
SORLA acidic mut rev.	CAG CTG CCC CCA GGG CAG CCC CAG AGG AGA AGA TTG CGG ACC
SORLA acidic mut fw.	CAA TCT TCT CCT CTG GGG CTG CCC TGG GGG CAG CTG CTG CAG CTG CCC CTA TGA TAA CTG GAT TTT C
SORLA stop xhoI rev.	CTC GAG TCA GCT GCT CTG CAG CCT CCG GTG C

3.4.11 Sequencing of DNA

DNA sequencing was performed by using BigDye Terminator v3.1 Cycle Sequencing Kit (Applied Biosystems, USA) according to manual instructions:

purified DNA	3 µl
sequencing primer (10 µM)	0,25 µl
5 x BigDye buffer	2 µl
water	4 µl
BigDye reaction mix	1 µl

43

The tubes were placed in a thermal cycler and the following program was started:

Initial denaturation	96°C	1 min	
Denaturation	96 °C	10 sec	
Primer Anealing	55 °C	5 sec	25 x
Elongation	60 °C	4 min	
stop reaction	10°C	ever	

After amplification, the DNA was purified with Sephadex G-50 (Amersham Pharmacia, UK), sequenced (ABI PRISM 377 DNA Sequencer), and, subsequently, analysed by Lasergene DNA Star SeqMan Version 7.0.0 (table 3).

Table 3: Human specific primer for sequencing.	
Primer identifier	Sequence (5´-> 3´)
SORLA seq 1 fw.	GGG CTC CTC CCA TCC ACA CCC ATG GCC
SORLA seq 2 fw.	CCC GGA CAG CAG GCT TCC ACC CCG
SORLA seq 3 fw.	GCG ACG GGA TGG ATG ATT GCG GCG
SORLA seq 4 fw.	GGA TGT GAC TTT GAC CTG GAT GAG GCC C
SORLA seq 5 fw.	GCC AAG ACT GAC TTG GGG GAT AGC CC
SORLA seq 6 fw.	GCA ACC AGA TCT GTG GGG AGC TGC C
SORLA nsiI fw.	GGT CTG GTG CAG ATG CAT CTG CAA CGC
pcDNA BGH rev	GGC AAC TAG AAG GCA CAG TCG AGG
pBS seq 1 fw.	GGT GCG GGC CTC TTC GCT ATT ACG CC

3.4.12 Isolation of proteins from eukaryotic cells

CHO or SH-SY5Y cells were lysed in lysis buffer (50 mM Tris-HCl, 150 mM NaCl, 1 % NP40, 1 % Triton-X, pH 8.0) with 1 x protease inhibitor cocktail (Roche, Germany) for 30 min on ice. Cell debris was removed by centrifugation (14000 x rpm, 10 min, 4°C) and the protein concentration of the supernatent were determined.

3.4.13 Protein concentration determination

The procedure is based on the formation of a complex between the dye Brilliant Blue G, and the basic and aromatic amino acids of the proteins in solution. The protein-dye complex causes a shift in the absorption maximum of the dye from 465 nm to 595 nm. The assay was prepared by diluting 1 ml Bradford reagent (Bio-Rad, CA) with 2 µl protein solution. The absorbance spectrum of the sample was record at 595 nm. The protein concentration was calculated as follows:

$$OD_{959} \text{ nm} / 0{,}042 = x \text{ µg/µl}$$

3.4.14 SDS polyacrylamide gel electrophoresis

Proteins are separated by continuous or gradient SDS polyacrylamide gel electrophoresis depending on their molecular weigth. If not stated otherwise, 50 µg of protein were mixed with sample buffer (62.5 mM Tris-HCl, 10% glycerol, 2% SDS, 0.01 mg/ml bromphenol blue, pH 6.8), incubated for 5 min at 95 °C, and resolved at 110 V in 6% SDS-gels using running buffer (960 mM glycine, 1% SDS, 125 mM Tris-HCl). After electrophoresis the gels were subjected to western blotting.

3.4.15 Western blotting

After gel electrophoresis, proteins were transfered to a nitrocellulose membrane (Hybond-C, Amersham, UK). The membrane was probed with antibodies specific to

the target protein. The setup in one gel holder cassette was as follows: one fiber pad (Bio-Rad, CA), two Whatman paper, gel, nitrocellulose membrane , two Whatman paper, one fiber pad. The assembled case was inserted in the case holder (Bio-Rad, CA) and put into the transfer chamber (Bio-Rad, CA) which was filled with transfer buffer (25 mM Tris-HCl, 192 mM glycine, pH 8.4). The transfer took 2 hours at 80 V. After transfer, proteins were blocked with blocking solution (133 mM NaCl, 2.7 mM KCl, 25 mM Tris, 5% dry milk, pH 7.4) for 1 hour at RT with shaking. The primary antibody was applied in blocking buffer and the memrbane was incubated with the primary antibody solution at 4°C overnight on a rocking platform (table 4). The next day, the primary antibody was removed and the membrane was washed 3 times 10 min in wash buffer (133 mM NaCl, 2.7 mM KCl, 25 mM Tris, pH 7.4) prior to 1 hour exposure to peroxidase-conjugated secondary antibody (dilution: 1:2000 in blocking buffer). After washing (2 x 10 min with wash buffer and 1 x 10 min with wash buffer-T (133 mM NaCl, 2.7 mM KCl, 25 mM Tris, 1% NP40, 1% triton-X, pH 7.4)), the membrane was incubated with detection solution (Super Signal West Pico Sta-

antibody	epitope	dilution	Provided by
Table 4: Antibodies for Western blotting.			
1227	C-terminal of APP	1:1000	J. Gliemann (University of Aarhus, Denmark
WO2	C-terminal of sAPPα	1:2000	K. Beyreuther (Center for mol. biology, Germany),
JP18957	C-terminal of sAPPβ	1:1000	IBL, USA
SORLAgt	N-terminal of SORLA	1:1000	J. Gliemann (University of Aarhus, Denmark
SORLAhale	C-terminal of SORLA	1:1000	J. Gliemann (University of Aarhus, Denmark
β-integrin 1	C-terminal of β-integrin 1	1:1000	Chemicon, USA
EEA1	N-terminal of EEA1	1:1000	Calbiochem, USA
golgin-97	not specified	1:1000	Molecular Probes, USA
Grp78	N-terminal of Grp78	1:1000	Stressgene, Canada
GS28	not specified	1:1000	Stressgene, Canada

ble Peroxide/Luminol Enhancer solution, Pierce, USA). Bands were detected using a CCD-camera (Fujifilm LAS-1000/ Intelligent Dark Box, Fujifilm, Japan).

3.5 Cell biology methods

3.5.1 Subcellular fractionation

CHO cells were grown on 5 x 15 cm culture dishes, harvested and resuspended in 3 ml homogenizaton buffer (10 mM HEPES, 1 mM EDTA, 250 mM sucrose, 1 x protease inhibitor cocktail, pH 7.4). The sample was sonicated 3 x 10 sec and pressed 5 x up and down through a canule (26 g, Braun, Germany). Cellular debris was removed by centrifugation of the homogenate (1500 x rpm, 10 min, 4°C). The supernatent was ultracentrifuged (45000 x rpm, 1 hour, 4°C). The resulting pellet was resuspended in 800 µl homogenization buffer and loaded on the top of a discontinuous sucrose and iodixanol density gradient (300 µl of 30% sucrose, 500 µl of 20% sucrose, 500 µl of 17.5% sucrose, 2 ml of 15% sucrose, 500 µl of 12.5% sucrose, 2 ml of 10% sucrose, 2 ml of 7.5% sucrose, 2 ml of 5% sucrose, 1 ml of 2.5% sucrose) and, finally, ultracentrifuged at a high g-force (45000 x rpm, 150 min, 4°C) to seperate cellular organelles. Fractions of 500 µl were collected and stored at -20°C.

3.5.2 Co-immunoprecipitation

CHO cells stably expressing SORLA variants were transiently transfected with constructs encoding GFP-tagged GGA-1 or HA-tagged PACS-1. After 48 hours, cells were washed and lysed in lysis buffer (50 mM Tris-HCl, 150 mM NaCl, 1 % NP40, 1 % Triton-X, 1 x protease inhibitor cocktail, pH 8.0) on ice. Co-immunoprecipitations were performed using anti-SORLA serum or anti-HA1.1 IgG1 (Covance, USA), and protein G-coupled Sepharose beads (Pierce, USA) according to standard protocols. Briefly, 2 µl antibody was mixed with the antigen in 1 ml immunoprecipitation buffer (IP) (25 mM Tris, 150 mM NaCl, pH 7.2), and 1 x protease inhibitor cocktail for 1 hour at room temperature. 20 µl of settled immobilized protein G was added to the antibody/antigen sample and further incubated 2 hours at room temperature.

The beads were collected by centrifugation (1 min, 8000 x rpm, RT) and washed 6 x with 500 µl IP buffer. The protein-complex was eluted by incubating the beads with 30 µl of SDS-sample buffer (62.5 mM Tris-HCl, 10% glycerol, 2% SDS, 0.01 mg/ml bromphenol blue, pH 6.8) 5 min at 95°C. Finally, the sample was resolved by SDS-PAGE.

3.5.3 Fluorescence activated cell sorting (FACS)

CHO cells stably expressing APP protein and SORLA variants were harvested by non-enzymatic formulation for gently dislodging adherent cell types from plastic surface (CDS, Sigma-Aldrich Co, Germany) and gently centrifugation (3 min, 800 x rpm, RT). The cell pellet was resuspended in 800 µl ice-cold FACS-fix (0.1 % fetal calf serum, 3.5% formaldehyd in phosphate-buffered saline (Invitrogen, UK)) and seperated into 150 µl aliquots. After collecting the cells by centrifugation (2 min, 3000 x rpm, 4°C), they were incubated in 100 µl FACS-fix (non-permeabilizing condition) or 100 µl FACS-fix with 0.1% saponin (permeabilizing condition) for 20 min on ice. After washing with 100 µl ice-cold PBS (+/- saponin) the cells were incubated with the anti-SORLA antiserum or anti-APP (α-SORLAgt, 6E10, dilution 1:40) 30 min on ice. The cells were washed twice and stained with Alexa488- or Alexa 555-conjugated secondary antibody (dilution 1:100, Molecular Probes, USA) in ice-cold PBS (+/- saponin) 15 min on ice in the dark. The cells were washed again and resuspended in 100 µl FACS-fix before being subjected to FACS analysis (10,000 events/ gate) using program BD Biosciences CellQuest Pro Version 5.2.1.

3.5.4 Immunofluorescence microscopy

Cellular localization of proteins was detected by sequential scanning confocal immunofluorescence microscopy. SH-SY5Y or CHO cells were grown on glass coverslips coated with 0.1% gelatine in phosphate-buffered saline (PBS) (Invitrogen, UK) and fixed with 3% formaldehyd (10 min, RT). After washing, the cells were either permeabilized 10 min in 0.25% Triton-X/PBS or kept in PBS (cell surface staining). Thereafter, all unspecific protein binding sites were blocked with 5% not

fat milk in PBS for 1 hour at room temperature and stained with primary antibody over night at 4°C. The next day, the cells were washed twice and stained with Alexa488-, Alexa 555- or Alexa 633-conjugated secondary antibody (dilution 1:2000, Molecular Probes, USA) 2 hours at room temperature in the dark. After staining, the cells were washed 6 x 10 min with PBS and mounted on object holder with fluorescence mounting medium (DAKO, Denmark). Confocal images were made with a 100x Plan-Apochromat oil objective on a Zeiss Laser Scanning Microscope (LSM510 Meta, Carl Zeiss AG, Germany).

Disruption of the Golgi complex was performed by treating the cells with 10 mM nocodazole (Sigma, Germany) in medium while growing. This antimitotic agent disrupts microtubules by binding to β-tubulin and thus causes fragmentation of the Golgi complex. Nocodazole was removed after 2 hours and the cells were washed, fixed, and stained (see above).

3.5.5 Subcellular localization of proteins in eukaryotic cells

Cells were grown and stained according to standard protocol (3.5.4 Immunofluorescence microscopy). Primary antibodies were used as follows:

Table 5: Antibodies for immunofluorescence microscopy.			
antibody	epitope/localization	dilution	Provided by
1227	C-terminal of APP	1:1000	J. Gliemann (University of Aarhus, Denmark
6E10	N-terminal of Aβ	1:1000	Signet Lab., USA
solSORLA	N-terminal of SORLA	1:2000	J. Gliemann (University of Aarhus, Denmark
SORLAgt	N-terminal of SORLA	1:1000	J. Gliemann (University of Aarhus, Denmark
Vti1a	early endos./TGN/PM	1:200	BD Transduction Lab., USA
Vti1b	Golgi complex/TGN	1:200	BD Transduction Lab., USA

GM130	cis-Golgi	1:200	BD Transduction Lab., USA
Mannosidase II	medial-trans Golgi	1:200	Chemicon, USA
p230	TGN	1:200	BD Transduction Lab., USA
AP1/γ-adaptin	early endosomes/TGN	1:200	BD Transduction Lab., USA
EEA1	early endosomes	1:200	BD Transduction Lab., USA
PDI	endoplasmic reticulum	1:200	Stressgen, USA

3.5.6 Surface staining of proteins and internalization experiments

Cells were grown on glas coverslips until the proper density was achieved and then chilled on ice for 30 min. Ice-cold medium with primary antibody (α-SORLA, α-APP, 1:1000) was added to the cells and kept 2 hours on ice. For timepoint "zero" (cell surface staining), the cells were fixed, blocked and incubated with the secondary antibody according to the protocol (3.5.4 Immunofluorescence microscopy). For internalization assay, cells were replaced into the incubator at 37°C for various timepoints (10 min, 20 min, 30 min, 60 min, 120 min) to allow internalization of fluorescent marked cell surface proteins before fixation.

3.5.7 Deglycosylation assay

For deglycosylation studies, 4 µl protein extracts were mixed with 10 mU neuraminidase (Roche, Germany) and/or 1mU O-glycosidase (Roche, Germany) in 60 mM Na-acetate pH 5.5 and water to fill up to a final volume of 25 µl. The sample was incubated over night at 16°C. The next day, the reaction was stoped by adding 8µl SDS-sample buffer, and protein analysis was performed by SDS-PAGE and Western blot analysis.

3.5.8 Enzyme-linked immunosorbent assay (ELISA)

Quantification of Aβ peptides were performed using an ELISA-kit (Biosource, Belgium) according to manual instructions. Briefly, 50 μl of sample or Aβ standard with 50 μl detection antibody was placed into the antibody-coated well. After incubation over night at 4°C, the wells were washed 4 x with washing buffer. Aβ peptids were detected by adding 100 μl anti-rabbit IgG-HRP solution into the wells. After 30 min incubation at room temperature, the wells were washed again 4 times and the staining performed by subjecting the wells with 100 μl of stabilized chromogen. After 30 min incubation at room temperature, the reaction was stopped with 100 μl stop solution. The OD was monitored at 450 nm wavelength.

4. Results

4.1 Interaction of SORLA and APP *in vivo*

4.1.1 Localization of SORLA and APP in the mouse brain

The amyloid presursor protein (APP) interacts with a number of neuronal proteins which possible influence the onset and progression of Alzheimer´s Disease (AD). Only little is known about the role of such interactions *in vivo*. To elucidate the relevance and function of SORLA in this respect, I performed *in vivo* studies in mice to gain insights into the influence of SORLA on AD progression. First, I mapped the distribution of SORLA expressing in the brain using immunohistology analysis and compared it with the distribution of APP. On sagital brain sections of paraffin
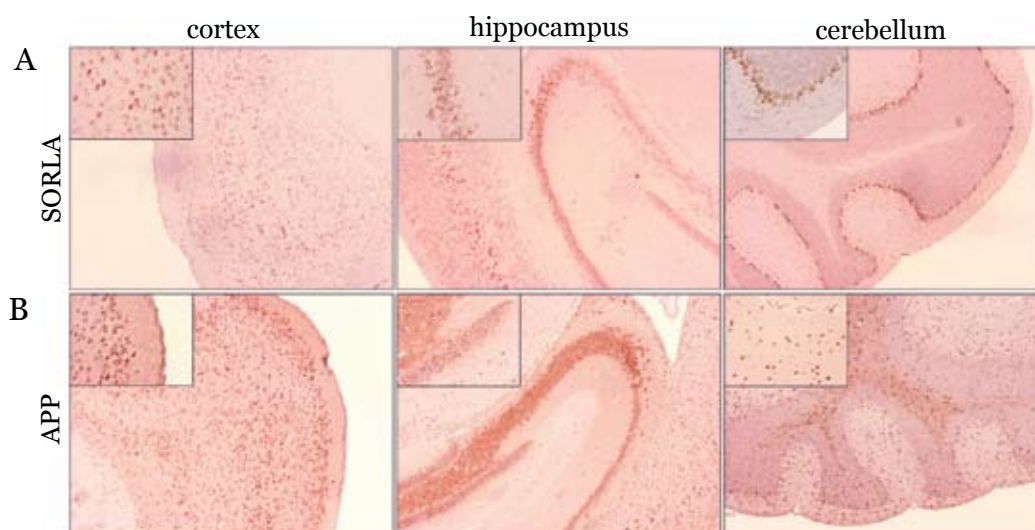
Figure 11: Localization of SORLA and APP in the mouse brain.
Immunodetection of SORLA (A, α-solSORLA) and APP (B, α-CT15) in different brain areas (cortex, hippocampus, cerebellum) of 4μm paraffin sections is shown. SORLA and APP display a diffuse staining throughout the cortex and hippocampus. In the cerebellum, localization of SORLA is restricted to the Purkinje and molecular cell layers whereas APP can be found in all neurons.

embedded tissues, SORLA immunoreactivity was seen almost exclusively in neurons. The immunostaining in neurons was granular and cytoplasmic. In particular, a strong but diffuse neuronal staining for SORLA (figure 11A) and APP (figure 11B) was detectable throughout the cortex and hippocampus with most prominent localization of the receptor in the pyramidal cells of CA1, CA2, CA3 and CA4 regions of the hippocampus and the granule cells of the dentate gyrus. In the cerebellum, however, the patterns of both proteins were different. Whereas APP exhibited a diffuse localization throughout the tissue, SORLA was only seen in the Purkinje and molecular cell layer and to a lesser extent in the granular cell layer of the cerebellum.

4.1.2 Characterization of the *Sorla*-deficient mouse

To test whether SORLA has an influence on APP processing our laboratory previously established a mouse model of targeted *Sorla* gene disruption. Mice homozygous for the disrupted *Sorla* allele lacked SORLA expression as shown by immunohistology (figure 12A) and western bloting (figure 12D) of brain tissues. SORLA-deficient mice were viable and fertile with no obvious alterations in overall APP levels in the cerebral cortex (figure 12B,D). However, a distinct increase in neuron-associated Aβ immunoreactivity (figure 12C) in brain homogenates was evident at 10 months of age. This increase in Aβ was confirmed by ELISA measurements from cortical brain extracts for endogenous Aβ40 and Aβ42, demonstrating an ≈ **30**% increase in murine Aβ levels in *Sorla*-deficient versus control mice (figure 12E).
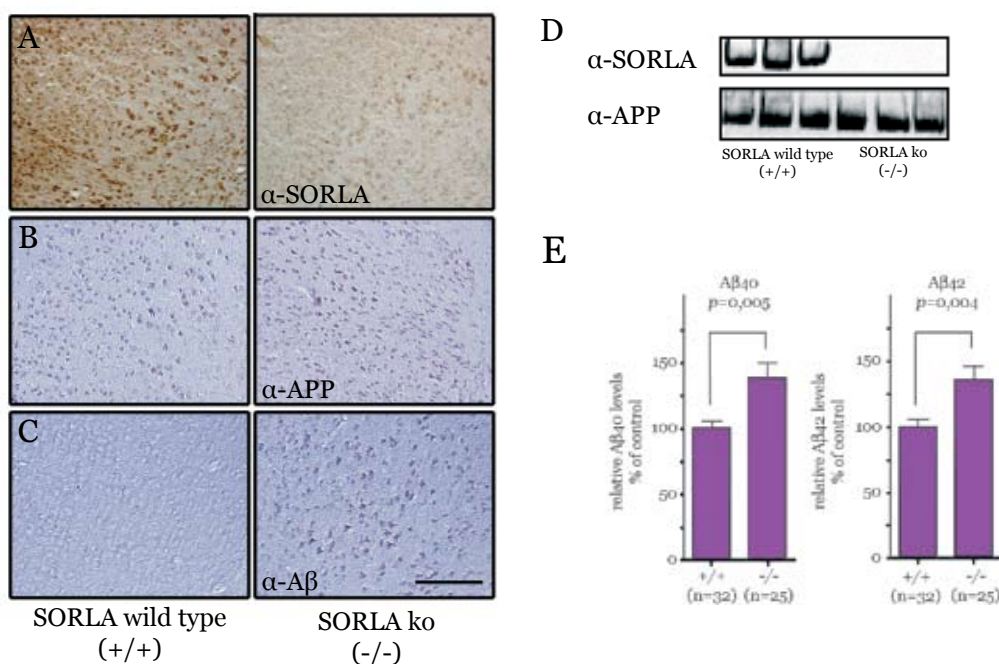
Figure 12: APP metabolism in *Sorla*-deficient mice.
(A,B,C) Immunodetection of SORLA (A, α-solSORLA), APP (B, α-CT695) and Aβ (C, α-4G8) in the frontal cortex of wild type (+/+) and *Sorla*-deficient (-/-) mice. Representative data from experiments in three *Sorla* -/- mice and three control mice are shown (scale bar: 100μm). (D) Loss of SORLA expression in *Sorla* -/- mice (α-solSORLA) did not affect the total levels of APP (α-CT15) as shown by Western blot analysis of brain homogenates. (E) Quantification of the increase in murine Aβ40 and Aβ42 in cortex extracts from 10-month-old *Sorla* -/- mice compared with wild type controls (mean value set as 100%) using ELISA. *P* values were determined by equal-variance *t* test. *n*, number of mice.

4.1.3 Characterization of the *Sorla*-deficient PDAPP mouse

Because soluble murine Aβ peptides do not form aggregates, *Sorla*-deficient mice do not represent a faithful mouse model to investigate the consequence of receptor deficiency for senile plaque formation *in vivo*. To address this question, we generated a new mouse model by crossed the *Sorla*-deficient animals with the PDAPP mouse line. This mouse line overexpresses the human *App* transgene with the Indianer mutation (Val717—›Phe). The PDAPP mouse model is a well characterized and often used model to investigate Alzheimer´s disease processes since these mice

exhibit extensive deposition of Aβ and neurite plaques, accompanied by loss of synapsis, astrocytosis and microgliosis. Also, these mice present impairment in a variety of different learning and memory tests, indicative of AD-related dementia. Using immunohistology I examined mice genetically deficient for *Sorla* and expressing the *App* transgene (SORLA$^{-/-}$ x PDAPP) and compared the results to PDAPP mice expressing SORLA (SORLA x PDAPP). The SORLA$^{-/-}$ x PDAPP mice showed an increased Aβ deposition (figure 13A) compared to PDAPP control mice (figure 13B). Also, these animals suffered from elevated amyloid plaque load (figure 13C,D) as shown by thioflavine-S staining.
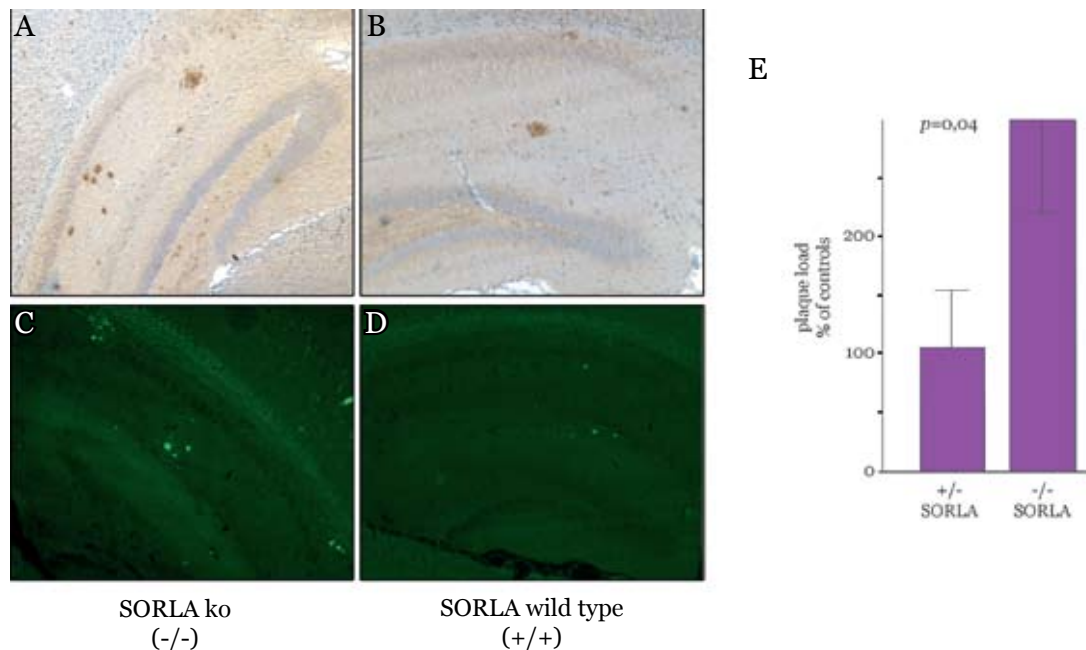
Figure 13: APP metabolism in (SORLA $^{-/-}$ x PDAPP) mice.
Immunodetection of human Aβ (A, α-4G8) and senile plaque load (C, thioflavine-S) in *Sorla*-deficient mice expressing the *App* transgene, compared with PDAPP mice (B,D). Loss of SORLA expression in *Sorla* $^{-/-}$ mice causes an increase in Aβ staining as well as amyloid plaque burden (E) in the hippocampus and the subiculum of 10-month-old mice (mean value set as 100%). *P* values were determined by equal-variance *t* test.

4.2 Interaction of SORLA and APP in cells

4.2.1 Subcellular localization of SORLA and APP in neuronal SH-SY5Y cells

The *in vivo* studies described above demonstrated that SORLA expression influences APP processing with low levels of receptor activity correlating with enhanced amyloidogenic processing and plaque deposition. To elucidate the function of SORLA in APP metabolism and AD progression in more detail I examined whether both proteins can functionally interact in cells. Initially, I used the human neuroblastoma cell line SH-SY5Y which expresses endogenous level of APP_{695} and SORLA (figure 14). The immunofluorescence detection showed co-localization of APP and SORLA in the perinuclear region and in distinct vesicles in the cytoplasm. A similar co-localization were also seen in cells stably expressing $SORLA^{wt}$ construct and transiently expressing APP_{695} (figure 15).
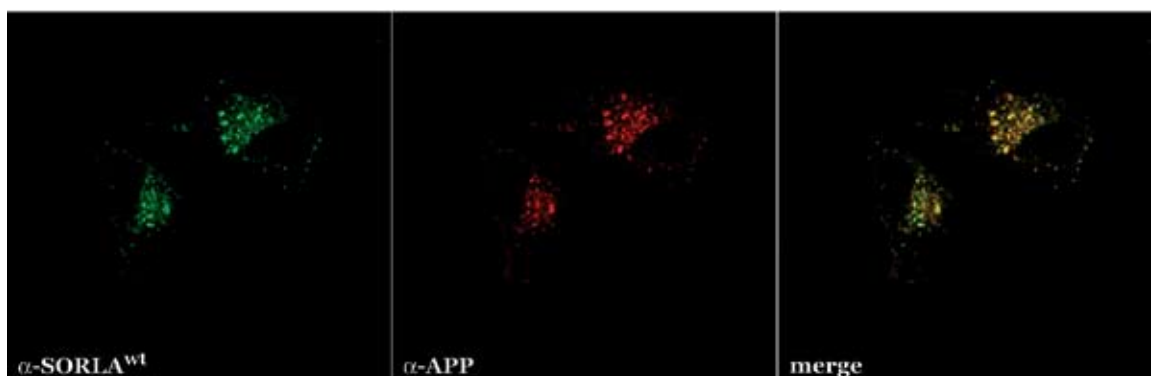

Figure 14: Immunodetection of endogenous APP and SORLA in SH-SY5Y cells.
SH-SY5Y cells were grown on coverslips, fixed and incubated with antibodies against SORLA (solSORLA, green) and APP (6E10, red). Distinct co-localization were seen in the perinuclear region as well in cytoplasmic vesicles (yellow).
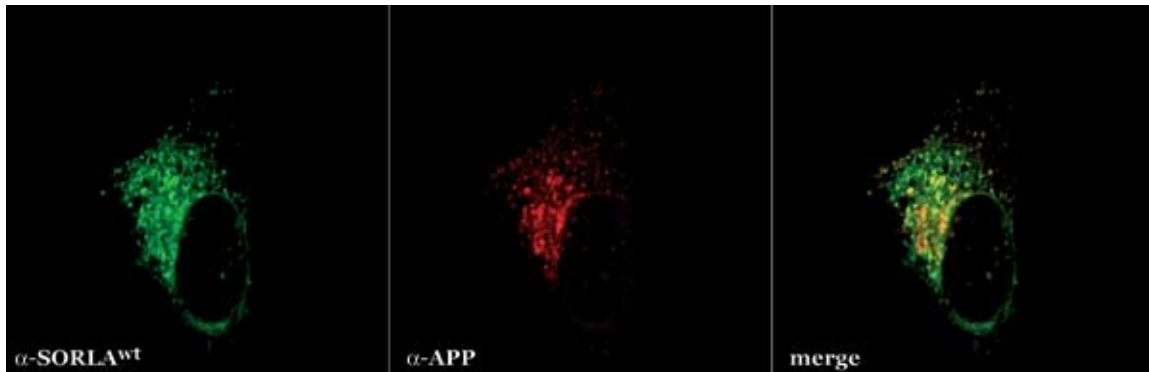
Figure 15: Detection of overexpressed APP and SORLA^wt in SH-SY5Y.
Cells stably expressing a SORLA^wt transgene were grown on coverslips and transiently transfected with an APP expression construct. Thirty six hours later, the cells were fixed and incubated with antibodies against SORLA (solSORLA, green) and APP (6E10, red). Both signals were confined to the perinuclear region where they co-localized.

Next, I wanted to test whether SORLA and APP localize in the same subcellular compartments. Therefore, I first examined the exact localization of SORLA in SH-SY5Y cells by confocal laser-scanning microscopy. By use of antibodies directed against marker proteins of various cellular compartments I was able to determine the organelles where SORLA resides. As shown in figure 16 SORLA^wt predominantly co-localizes with marker of the medial to trans-Golgi compartment (positive for mannosidase II) and trans-Golgi network (positive for p230). Also, co-localization with early endosomes (positive for EEA1, not shown) was detectable, albeit to a weaker extent. In contrast, there was no co-localization with markers indicative for lysosomes (positive for lamp1, not shown), endoplasmic reticulum (positive for PDI, not shown) and cis-Golgi (positive for GM130). To test whether APP resided in the very same compartments as SORLA I performed co-localization studies of APP with the same markers. In these studies, APP predominantly resided in the Golgi region and in the endocytic compartments (figure 17). Taken together, all data presented above, suggested co-localization of SORLA and APP in late Golgi and early endosomal compartments.
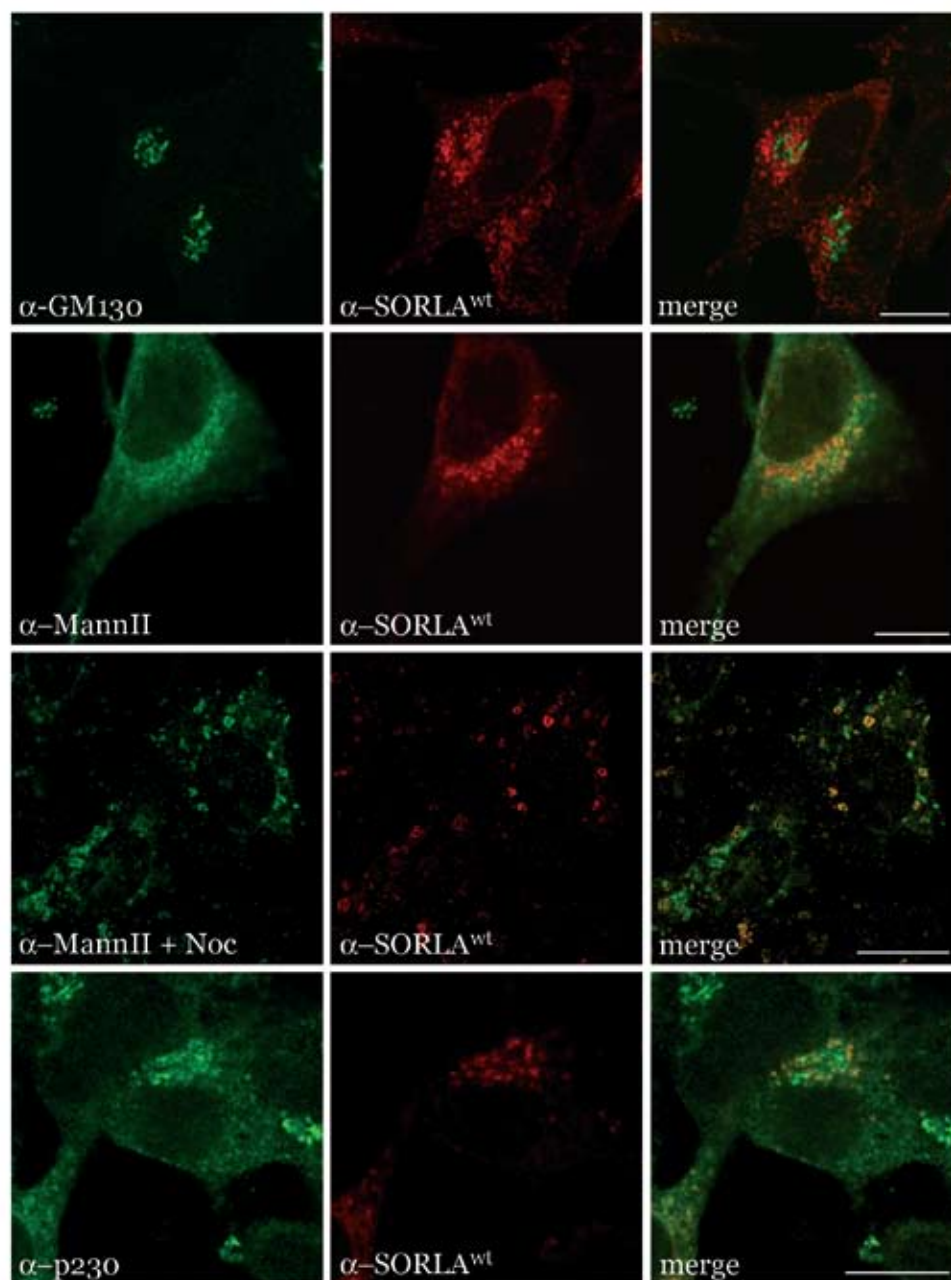
Figure 16: Subcellular localization of SORLA^wt in stably transfected SH-SY5Y cells. Confocal immunofluorescence microscopy identified co-localization of SORLA^wt (solSORLA, red) with marker of the medial-Golgi (mannosidase II) and trans-Golgi / trans-Golgi network (p230) but not with markers of cis-Golgi (golgi matrix protein 130, GM130). Co-localization of SORLA^wt with mannosidase II in the medial-Golgi was confirmed in cells treated with nocodazol (MannII + Noc) that disintegrates the Golgi structure. Scale bar 10 µm.
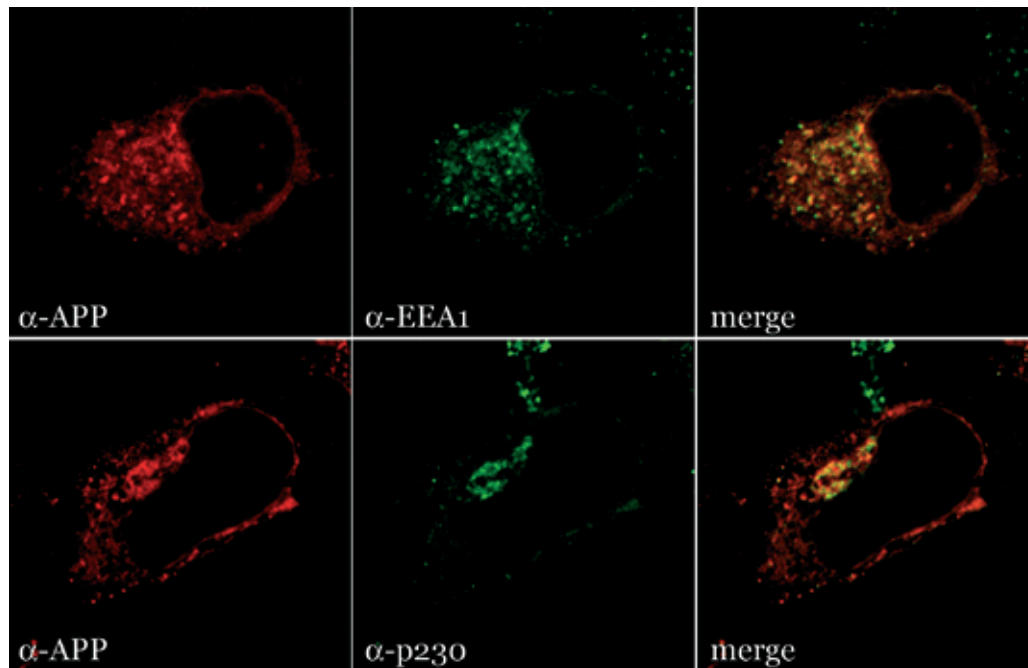
Figure 17: Subcellular localization of endogenous APP$_{695}$ in SH-SY5Y cells.
The confocal immunofluorescent picture shows APP (6E10, red) in the perinuclear region where it colocalizes with the trans-Golgi network marker (p230, green) and early endosomal marker (EEA1, green).

4.2.2 Subcellular localization of SORLA and APP in CHO cells

To circumvent technical problems in handling of the neuroblastoma cell line SH-SY5Y I switched to a more robust cell system to study the APP metabolism for further studies. I choose Chinese hamster ovarey (CHO) cells, a non-neuronal cell culture system commonly used in the APP field. To proof that APP and SORLA distributed equally in CHO cells as they did in SH-SY5Y cells, I initially repeated the experiments discussed for SH-SY5Y above. Because CHO cells do not express detectable levels of endogenous SORLA and APP I established a cell line stably overexpressed human SORLA and human APP$_{695}$ (CHO-A/S). Western blot analysis demonstrated significant and stable expression of both recombinant proteins in these cell lines (figure 18). Further immunofluorescence analysis showed co-localization of APP and SORLA in a vesicular pattern in the cytoplasm and in perinuclear regions simi-

lar to the situation seen in SH-SY5Y cells (figure 19).
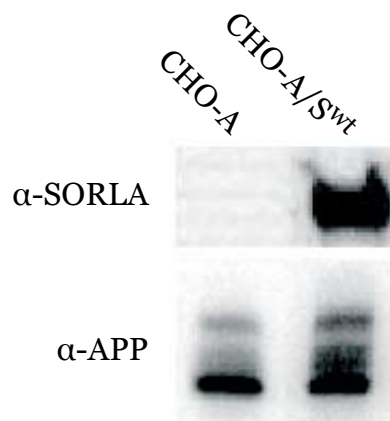
Figure 18: Detection of SORLA and APP in CHO cell lysats.
Extracts of CHO cells stably expressing human APP695 (CHO-A) alone or APP with
SORLA^{wt} construct were subjected to Western blot analysis using antisera directed against
SORLA (α-SORLAgt) or APP (α-1227).
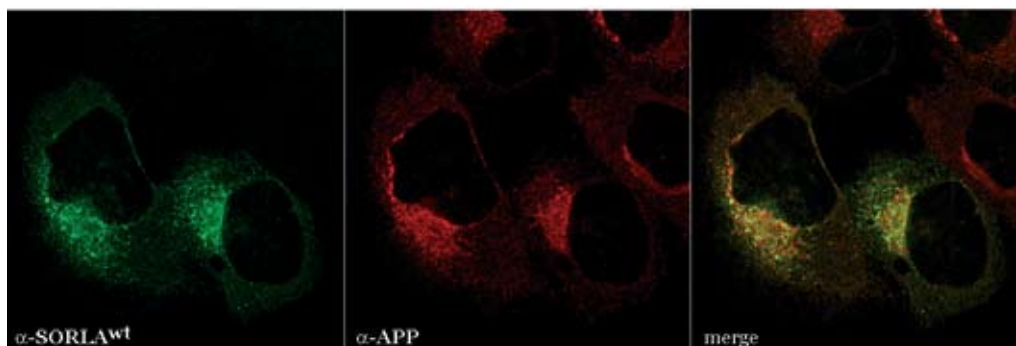
Figure 19: Immunodetection of APP and SORLA^{wt} in CHO cells.
CHO cells stably expressing APP (red) and wild-type SORLA (green) were grown on cover-
slips, fixed and incubated with α-APP (6E10) and α-SORLA (solSORLA) antibody, respec-
tively. Both signals display predominant and overlapping staining in the perinuclear region
(yellow).

To finally conclude indentical distribution of APP and SORLA in neuronal and non-neuronal cell types, I used subcellular markers to pinpoint SORLA in CHO cells overexpressing SORLA protein (figure 20). SORLA was predominantly seen in the perinuclear region identified by markers of VTI1A (trans-Golgi network) and VTI1B (medial/trans-Golgi). Some co-localization with early andosomes (EEA1) was also detectable. SORLA staining was also seen in cytosolic vesicles proposed to traffic between trans-Golgi network and endosomes (positive for SNX1 and AP1). In contrast, no co-localization was seen with the endoplasmic reticulum (ER) and early (cis)-Golgi compartment or late endosomes and lysosomes (data not shown). To test whether APP also resides in the same compartments in CHO cells, I did triple staining for SORLA, APP and the relevant markers. Again, both receptor proteins co-localize to the perinuclear area and vesicular structures identified as trans-Golgi and early endosomal compartments (figure 21).
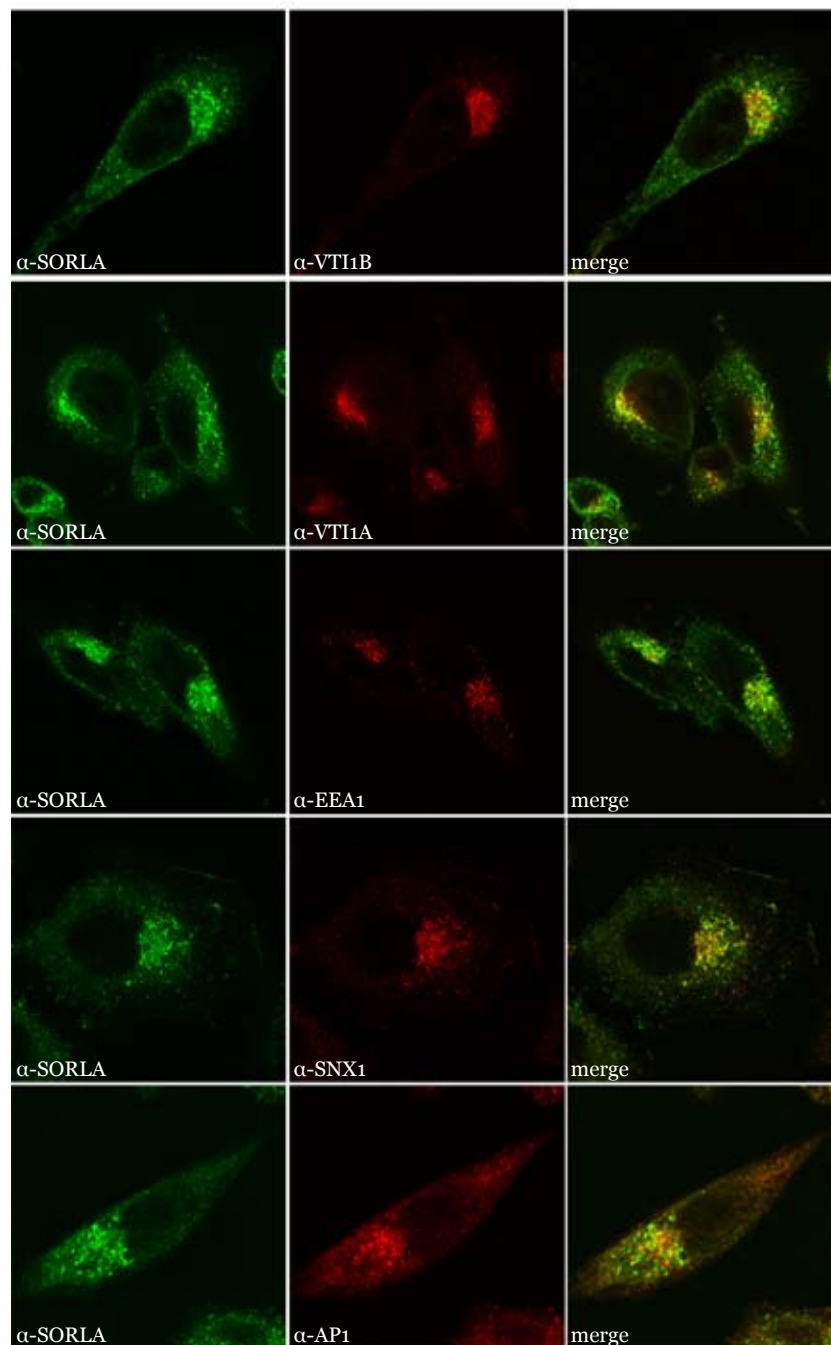
Figure 20: Co-staining of SORLA and subcellular compartments.
Detection of SORLA[wt] (SORLAgt, green) and various subcellular marker (red) in stably transfected CHO-A/S[wt] cell line using confocal immunofluorescence microscopy. SORLA[wt] is predominantly localized in the perinuclear region and cytosolic trafficking vesicles. VTI1B (medial/trans-Golgi), VTI1A (trans-Golgi network), EEA1 (early endosomes), SNX1, AP1 (trafficking vesicles).
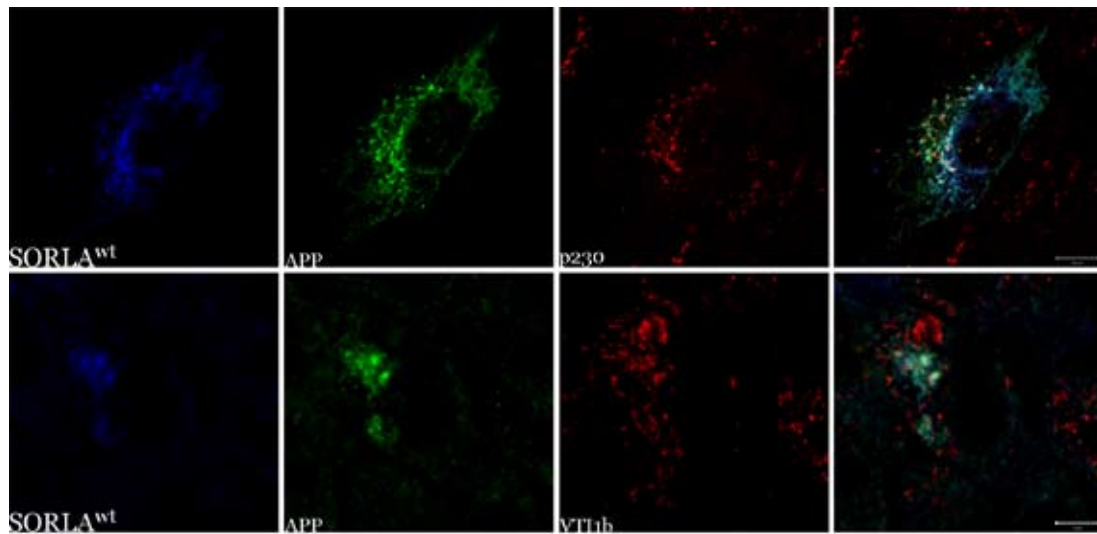
Figure 21: Co-staining of SORLA, APP and subcellular compartments.
Co-staining of SORLA (SORLAgt, blue) and APP (1227, green) with marker for trans-Golgi network (p230) and medial to trans-Golgi compartment (VTI1B) in CHO-A/S cells. Both proteins co-localize in the perinuclear region identified as Golgi compartments seen in white colour.

4.2.3 Interaction of SORLA and APP in CHO cells

Next, I tested whether co-localization of SORLA and APP seen in fluorescence microscopy could be confirmed by documentation of direct protein interaction in cells. To do so, I co-immunoprecipitate SORLA and APP from CHO cells stably expressing both proteins. By Western blot analysis I demonstrated that SORLA interacts with APP since I was able to co-immunoprecipitate APP from cell extracts containing SORLA protein (figure 22).
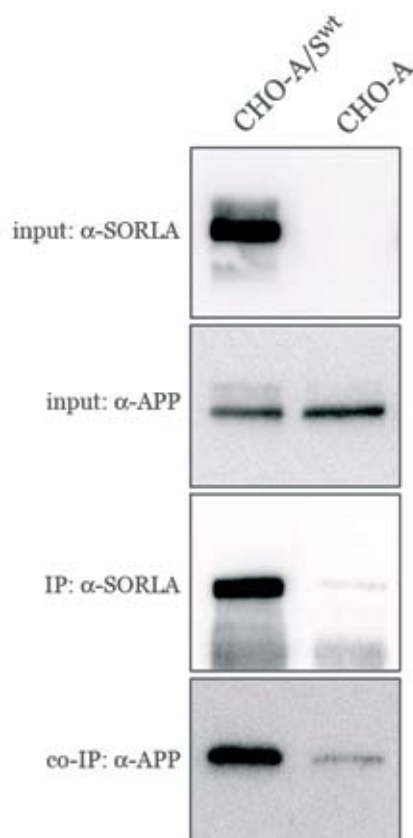
Figure 22: Co-immunoprecipitation of SORLA and APP in CHO cells.
SORLA was co-immunoprecipitated with APP from the indicated CHO cell lines. Panel input represents Western blots for SORLA (input: α-SORLAgt) and APP (input: α-WO2) in cell extracts prior to immunoprecipitation of CHO cells stably expressing APP and SORLA (CHO-A/S) or only APP (CHO-A). Panel IP are Western blots for SORLA and APP in fractions immunoprecipitated with anti-SORLA IgG. SORLA receptor can co-precipitate APP from CHO-A/S cell extracts. For control, immunoprecipitations were also performed in cells lacking SORLA (CHO-A). A weak background signal for SORLA in APP immunoprecipitats from CHO-A was likely due to low levels of endogenous SORLA expression in parental CHO cells.

4.2.4 Altered glycosylation of APP in CHO cells expressing SORLA

Since SORLA and APP predominantly co-localize in Golgi compartments I wanted to investigate whether SORLA may influence APP maturation in this organelle. Western blot analysis showed that overexpression of SORLA resulted in accumulation of mature APP molecules in CHO-A cells compared to CHO-A/S^{wt} cells (figure 18). To characterize export of nascent APP molecules from the ER I subsequently studied acquisition of carbohydrate modifications on APP, indicative of subsequent ER and Golgi maturation steps. In CHO cell lysates, APP immunoreactivity was seen in three distinct bands (figure 23A). Treatment of cell extracts with neuraminidase and *O*-glycosidase uncovered that the high molecular weight band (sensitive to neuraminidase) represented the mature protein, carrying terminally modified *N*- and *O*-linked carbohydrates. The intermediate sized band corresponded to APP carrying complex *O*-linked carbohydrates as it was sensitive to *O*-glycosidase. The lowest molecular weight band represented the immature precursor in the ER as it was resistant to neuraminidase and *O*-glycosidase treatment. No qualitative differences in this pattern were seen when comparing CHO cells stably expressing human APP$_{695}$ (CHO-A) and APP$_{695}$ with SORLA (CHO-A/S^{wt}) (figure 23A). However, CHO-A/S^{wt} cells showed an increase in *O*-glycosylated APP products (middle and upper protein bands) compared to CHO-A cells (bracket), suggesting accumulation of the mature protein in the presence of SORLA (ratio mature/immature APP: 0.67 ± 0.06 in CHO-A/S^{wt} versus 0.46 ± 0.06 in CHO-A, p=0.04). This effect was also seen when comparing parental SH-SY5Y cells and SY5Y cells overexpressing human SORLA^{wt} (figure 23B). In summary, these experiments indicate that SORLA causes a retention of APP in the Golgi compartment resulting in accumulation fully glycosylated mature APP in cells overexpressing this sorting receptor.
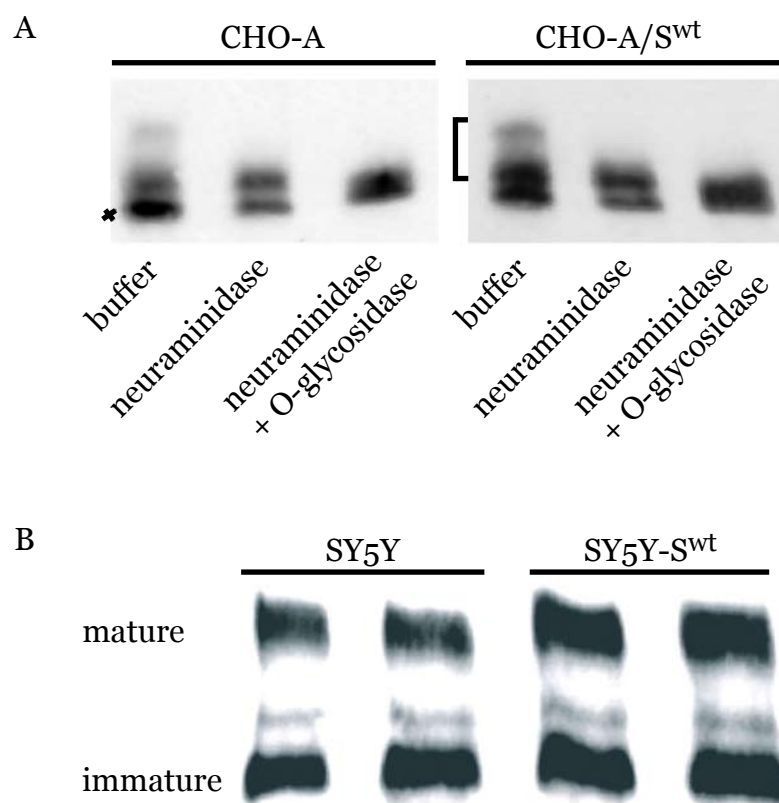
Figure 23 : Glycosylation of APP in CHO cells with and without SORLA.
(A) Extracts of CHO cells expressing APP (CHO-A) or APP and SORLA (CHO-A/S^{wt}) were incubated with buffer only or with buffer containing neuraminidase or neuraminidase and *O*-glycosidase. Subsequently, extracts were subjected to Western blot analysis using anti-APP antiserum 1227. The bracket indicates glycosylated APP isoforms accumulating in CHO-A/S^{wt}. The asterisk denotes the precursor in the ER. (B) Extracts of human neuronal SH-SY5Y cells expressing endogenous APP alone (SY5Y) or APP with human SORLA (SY5Y-S^{wt}).

4.2.5 APP retention in the ER by SORLA^{KKLN} variant

So far, my studies had uncovered a critical function for SORLA as trans-Golgi/TGN localized receptor controlling APP exit from these compartments. To conceptually prove the ability of SORLA to act as retention factor for APP anywhere in the cell, I generated a receptor variant that carried four extra amino acid residues (KKLN) at the carboxyl terminus (SORLA^{KKLN}). This dilysine peptide sequence acts as ER
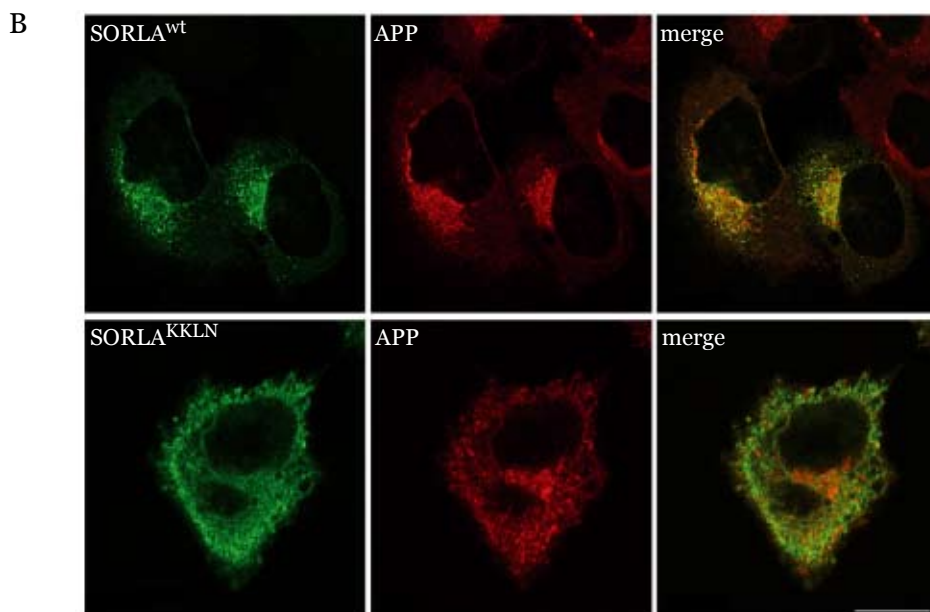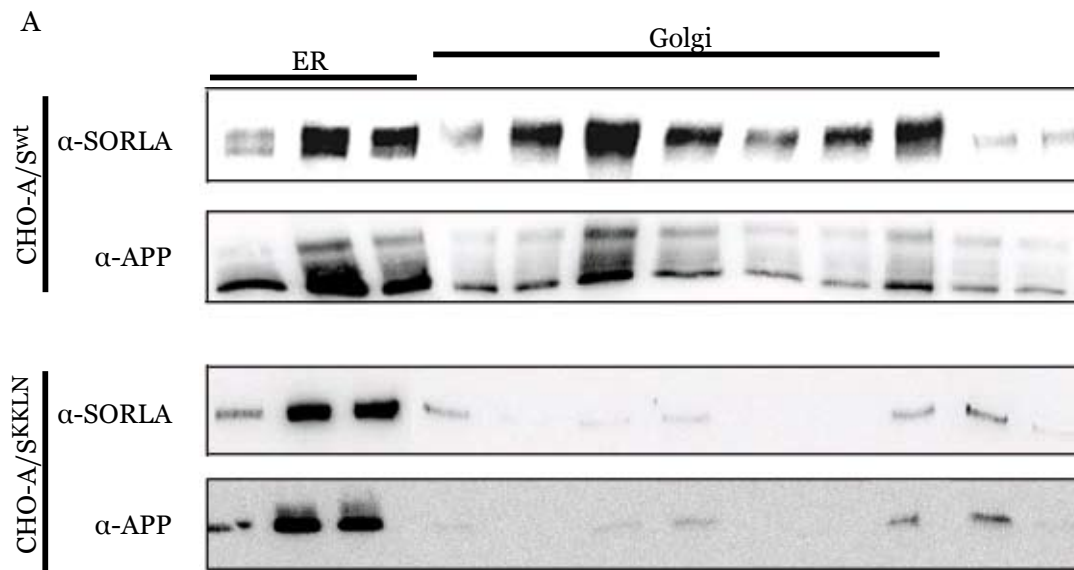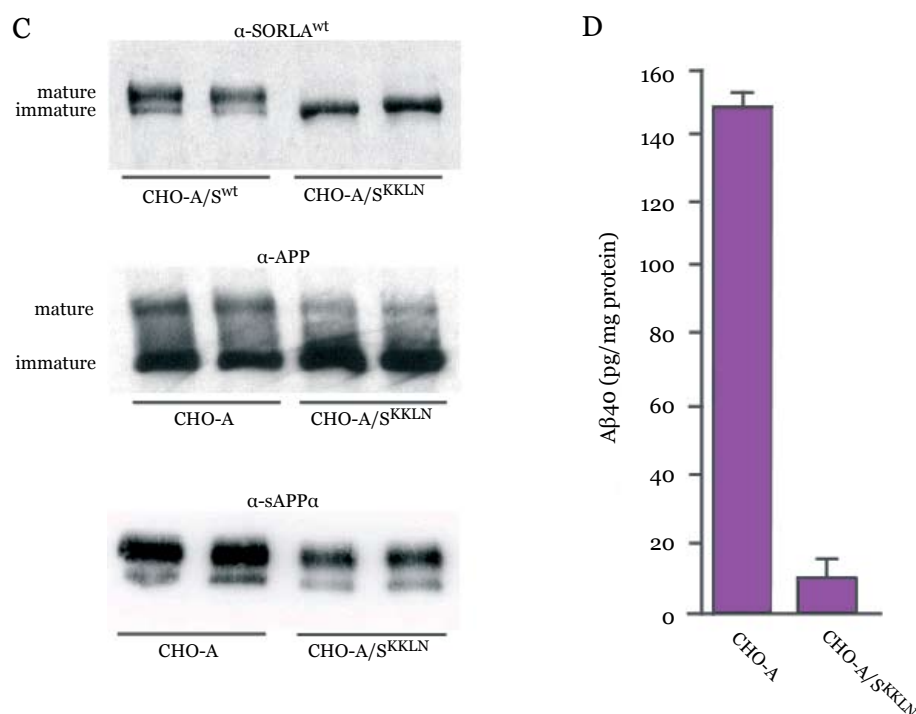
Figure 24: Blockade of APP export from the ER by SORLA^{KKLN}.
(A) Subcellular fractionation by density gradient ultracentrifugation detects APP and SORLA in fractions enriched in ER and in Golgi in cells expressing APP and SORLA^{wt} (CHO-A/S^{wt}). In contrast in cells expressing APP and SORLA^{KKLN} (CHO-A/S^{KKLN}), both proteins are only seen in ER but not in Golgi fractions. Markers used to identify the subcellular compartments are given in the legend to figure 31 (beneath). (B) In cells expressing APP and SORLA^{KKLN} (CHO-A/S^{KKLN}) both proteins exhibited an overlapping disperse cytoplasmic pattern, indicative of ER localization compared to the perinuclear (Golgi) signal in cells expressing APP and SORLA^{wt} (CHO-A/S^{wt}). (C, upper panel) Western blot analysis of cell extracts indicated absence of the mature form of SORLA in cells expressing SORLA^{KKLN} (CHO-A/S^{KKLN}) compared with cells expressing SORLA^{wt} (CHO-A/S^{wt}). (C, middel panel) Co-expression of APP with SORLA^{KKLN} resulted in accumulation of immature APP and decrease in the terminally glycosylated form of the protein as well as in a reduction of sAPPα in cell supernatants (C, lower panel) in CHO-A/S^{KKLN} compared to parental CHO-A cells. (D) Quantification by ELISA of the amounts of Aβ40 in the medium from CHO-A/S^{KKLN} and CHO-A cells (p<0.0009).

retention motif in some transmembrane proteins. Accordingly, SORLA^{KKLN} mainly resided in the ER and was blocked from exit to the Golgi in stably transfected CHO cells as indicated by subcellular fraction studies (figure 24A). Aberrant sequestration of SORLA^{KKLN} in the ER caused redistribution of APP to the same compart-

ment as deduced from fractionation studies that uncovered APP in ER and Golgi fractions in cells expressing SORLA^{wt} but only in the ER in SORLA^{KKLN} expressing cells (figure 24A). The shift in localization was also seen in immunofluorescence experiment where SORLA and APP were stained in CHO-cells stably expressing SORLA^{wt} (CHO-A/S^{wt}) or SORLA^{KKLN} (CHO-A/S^{KKLN}) together with APP (figure 24B). Whereas SORLA^{wt} showed an perinuclear localization SORLA^{KKLN} displays a disperse pattern characteristic of ER localization. Sequestration of SORLA^{KKLN} in the ER was also demonstrated by faster electrophoretic mobility in SDS-PAGE (figure 24C, upper panel) compared to SORLA^{wt}, indicating absence of terminal glycosylation. In line with a SORLA^{KKLN}-dependent blockade of ER exit of APP, accumulation of immature and decrease of mature forms of the protein was seen in cells expressing SORLA^{KKLN} (CHO-A/S^{KKLN}) compared to cells without SORLA (CHO-A) (figure 24C, middle panel) (ratio mature/immature APP: 0.43 ± 0.06 versus 0.57 ± 0.03, $p=0.02$). Finally, the inability of APP to enter distal secretory compartments harboring secretase activities was confirmed by a $66\% \pm 4.8$ decrease in its processing to sAPPα (figure 24C, lower panel; $p<0.001$) and 95% reduction in conversion to Aβ40 (figure 24D; $p<0.0009$) that was not seen in CHO-A cells. Similar findings were obtained in SH-SY5Y cells expressing SORLA^{KKLN} (figure 25). However, the reduction of sAPPα and Aβ was less pronounced than in CHO cells. This difference was likley due to the fact that the SY5Y-SORLA^{KKLN} not only expressed the mutated SORLA polypeptide, but also considerable levels of the endogenous wild-type SORLA protein.
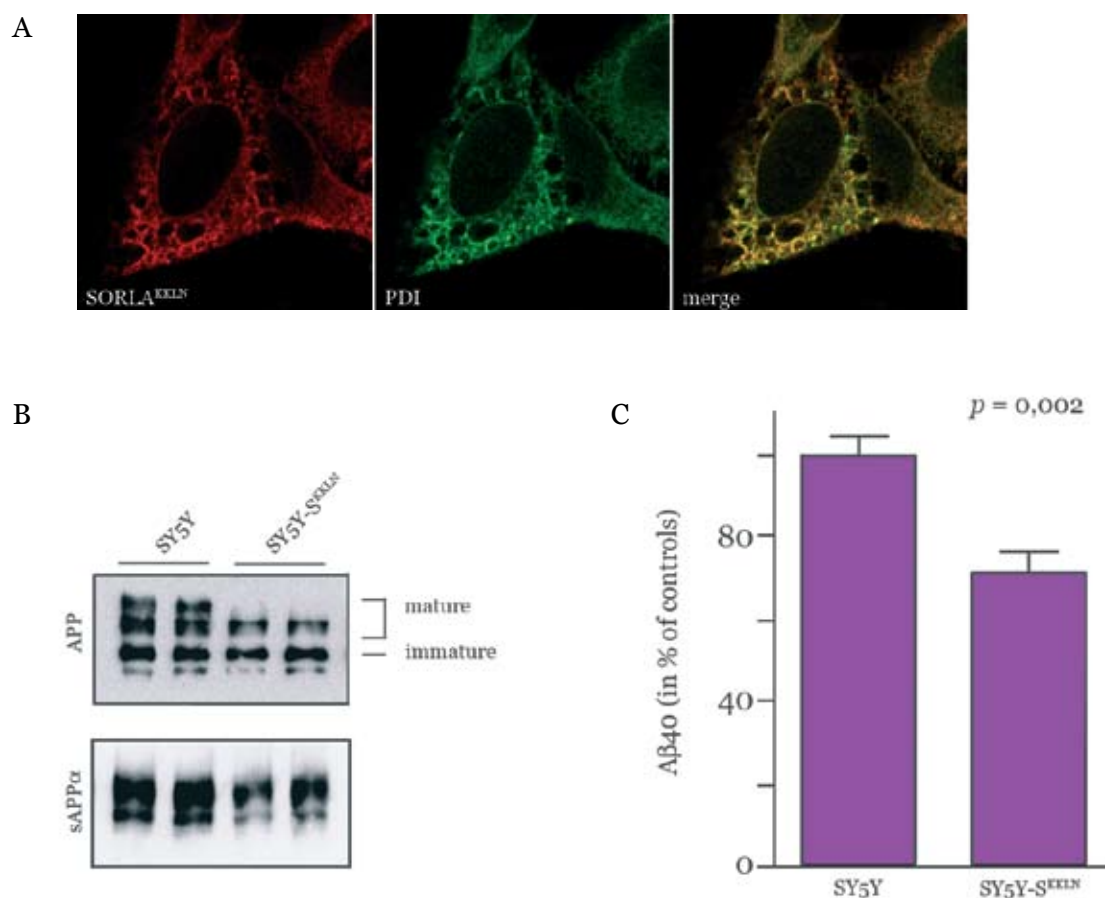
Figure 25: Processing of APP in SH-SY5Y cells expressing SORLA^KKLN.
(A) Immunofluorescent staining of SORLA^KKLN with the ER marker PDI (Protein Disulfide Isomerase) showed overlapping disperse cytoplasmic pattern. (B) Western blot analysis displayed a decrease in mature forms of APP in replicate extracts from SH-SY5Y cells expressing SORLA^KKLN (SY5Y-S^KKLN) compared with control cells (SY5Y) (upper panel). Also, the amount of sAPPα products secreted into the medium was reduced in the presence of SORLA^KKLN (lower panel). (C) Quantification by ELISA indicated a reduction in Aβ40 production in SY5Y-S^KKLN (71.6 ± 5.4; $p = 0.002$) compared with SY5Y cells (set at 100%).

4.2.6 Characterization of wild type and mutant forms of SORLA

As already mentioned APP processing by different secretases occurs in distinct cellular compartments. To test whether SORLA localization may influences not only APP localization but also APP processing, I constructed various SORLA mutants by introducing point mutations in the cytosolic tail sequence of the receptor. The mutated sequences were proposed to function as recognition motives for adaptor proteins which are known to regulate protein trafficking between cell compartments (figure 26A). For example, a number of cellular mechanisms are known that target proteins to and from the TGN including interaction with sorting adaptors GGA and PACS-1. Binding of GGA-1 and -2 to a tetrapeptide motif DVPM in the tail of SORLA has been demonstrated before (L. Jacobsen, 2002). An acidic cluster that may serve as binding site for PACS-1 is also present in the cytoplasmic receptor domain. Thus, I generated mutants lacking the acidic cluster (SORLA^{acidic}) or the GGA binding site (SORLA^{GGA}), or the entire cytoplasmic domain (SORLA$^{\Delta cd}$) (figure 26A). Activity of these mutants was compared to SORLA^{wt}. In Western blot analysis I showed that all SORLA mutants were stably expressed to a similar level as the wild-type receptor in parental CHO-A cells (figure 26B). In detail, SORLA levels were analyzed by two different antibodies directed against human SORLA. α-SORLA$_{ext}$ represents immunodetection with an antibody against the luminal domain of SORLA whereas α-SORLA$_{tail}$ recognizes only the cytoplasmic tail of the receptor variants. All SORLA variants gave significant signal with α-SORLA$_{ext}$ antibody. When the α-SORLA$_{tail}$ antibody was used, all but the CHO-A/S$^{\Delta cd}$ reacted, consistent with deletion of the tail domain from the latter receptor from. Furthermore, SORLA^{acidic} protein reacted poorly with this antiserum, suggesting that the antibody epitope partially overlapped with the peptide motif mutagenized in SORLA^{acidic}. Remarkably, coexpression with SORLA^{wt} but with no other SORLA variant caused accumulation of mature APP in CHO cells, indicating loss of protective function of SORLA by any of the modifications (figure 26B).

A

B
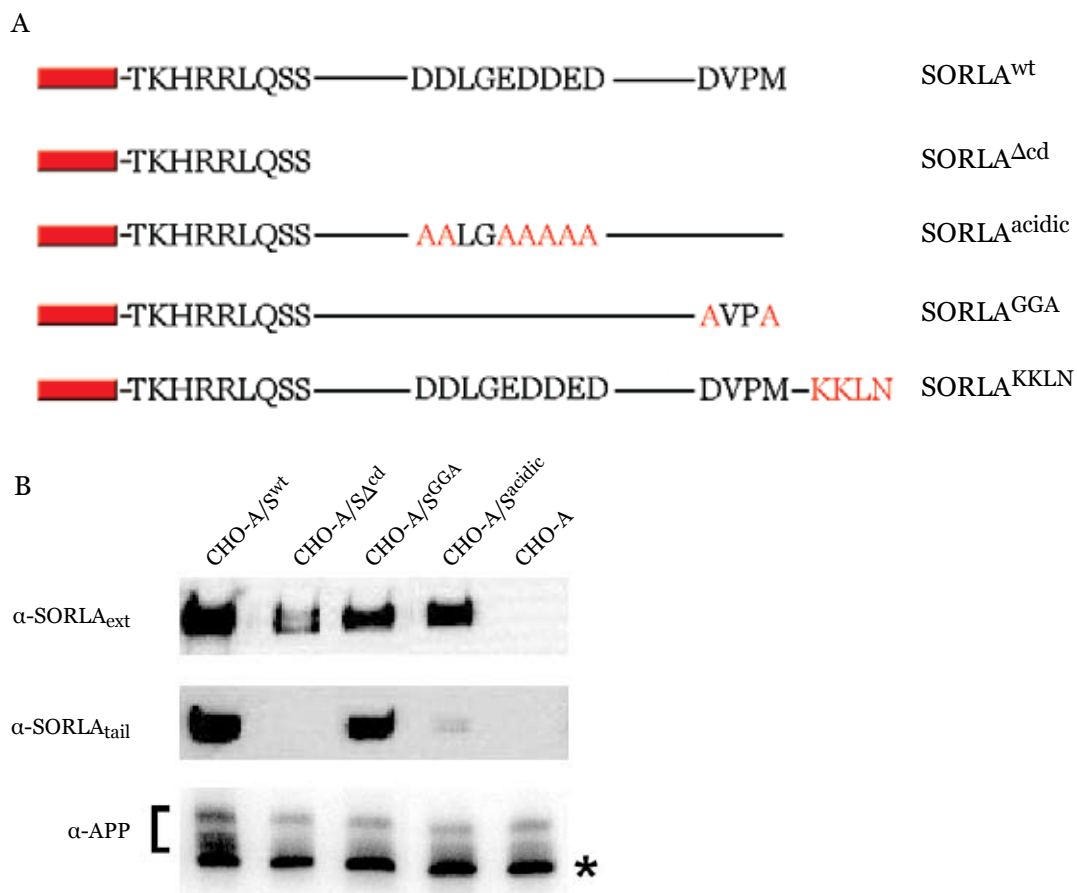
Figure 26: Characterization of wild-type and mutant forms of SORLA.
(A) Amino acid sequence elements in the cytoplasmic domains of wild type (wt) and mutant forms of SORLA are indicated. Solid lines represent the authentic peptide sequences. Boxes indicate the transmembrane domains. The mutated sequence is shown in red. (B) Extracts of CHO cells expressing human APP_{695} (CHO-A) alone or with the indicated variants of SORLA were subjected to Western blot analysis using antisera directed against the extracellular (α-SORLA$_{ext}$) or the intracellular domain (α-SORLA$_{tail}$) of SORLA, or against APP (α-APP). The bracket indicates mature forms of APP accumulating in CHO-A/S^{wt} but in no other cell line. The asterisk highlights immature APP.

The inability of mutant receptors to protect APP from processing was not due to impaired interaction with the precursor protein as all SORLA variants were able to co-immunoprecipitate APP (figure 27). However, SORLA^{GGA} and SORLA^{acidic} failed to co-immunoprecipitate GGA-1 (figure 28A) and PACS-1 (figure 28B), respectively, consistent with disruption of the individual adaptor binding sites in these mutants. An inability to interact with both GGA-1 and PACS-1 was also seen for SORLA$^{\Delta cd}$ that lacked the entire receptor tail (figure 28A,B).
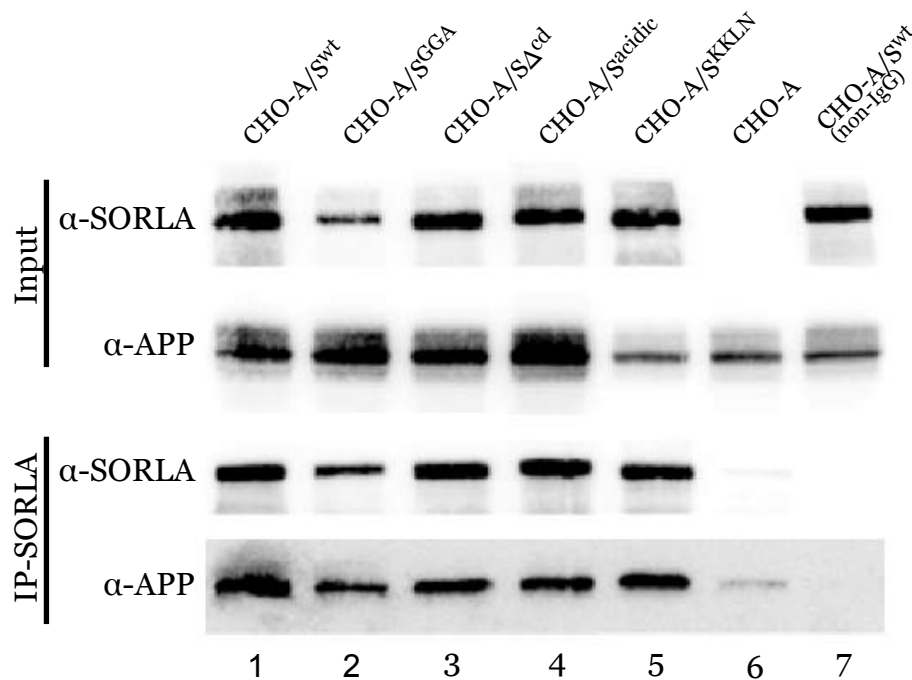
Figure 27: Co-immunoprecipitation of wild type and mutant forms of SORLA. SORLA was co-immunoprecipitated with APP from the indicated CHO cell lines. Panel Input represents Western blots for SORLA and APP in cell extracts prior to immunoprecipitation. Panel IP-SORLA is a Western blot analysis for SORLA and APP in fractions immunoprecipitated with anti-SORLA IgG. All receptor variants co-precipitate APP (lanes 1-5). For control, immunoprecipitations were also performed in cells lacking recombinant SORLA (CHO-A; lane 6) or in CHO-A/S^{wt} cells without specific IgG (non-IgG control; lane 7). A weak background signal for APP immunoprecipitation in CHO-A was due to low levels of endogenous SORLA expression in parental CHO cells.
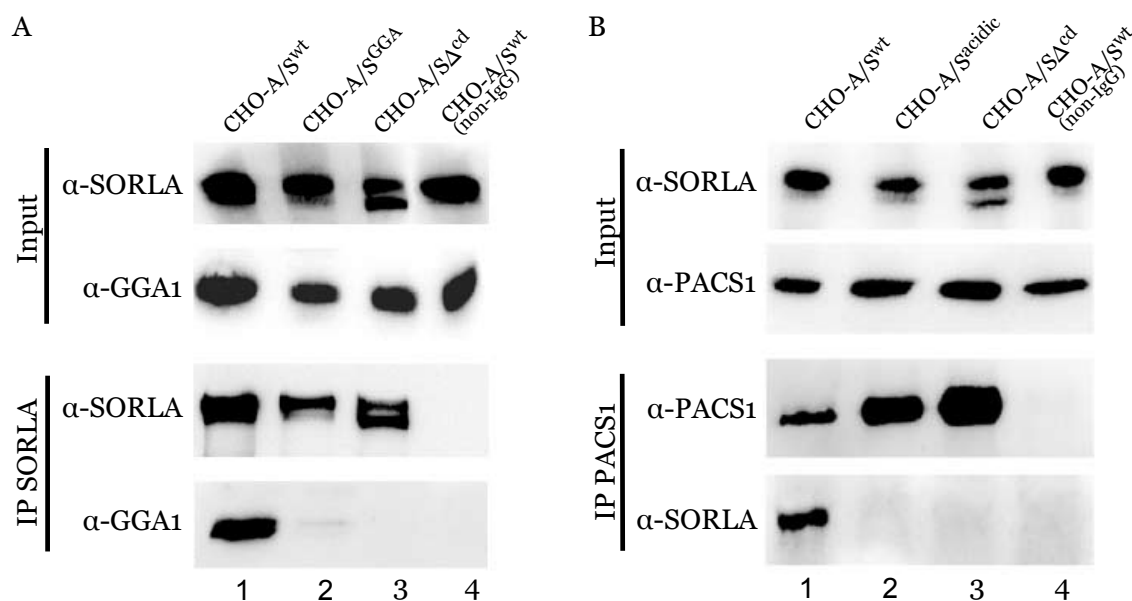
Figure 28: Co-immunoprecipitation of SORLA^{wt} or mutant receptor forms with GGA1 and PACS1.

(A) Cells expressing SORLA^{wt} , SORLA^{GGA}, and SORLA$^{\Delta cd}$ were transfected with an expression construct for GFP-tagged GGA1 and immunoprecipitated using anti-SORLA IgG. Panel Input represents Western blots for SORLA and GFP-GGA1 in cell extracts prior to immunoprecipitation. Panel IP-SORLA is a Western blot analysis for SORLA and GFP-GGA1 in fractions immunoprecipitated with anti-SORLA IgG (lanes 1-3). Co-precipitation of GFP-GGA1 is only seen with SORLA^{wt} (lane 1). As a negative control, immunoprecipitations were also performed in CHO-A/S^{wt} cells without specific IgG (lane 4). (B) Cells expressing SORLA^{wt} , SORLA^{acidic}, and SORLA$^{\Delta cd}$ were transfected with an expression construct for HA-tagged PACS1 and immunoprecipitations performed using anti-HA IgG. Panel Input represents Western blots for SORLA and HA-PACS1 in cell extracts prior to precipitation. Panel IP-PACS1 represents Western blot analysis for HA-PACS1 and SORLA in fractions immunoprecipitated with anti-HA antibody (lanes 1-3). Co-precipitation with HA-PACS1 is only seen for SORLA^{wt} (lane 1). Immunoprecipitations were also performed in CHO-A/S^{wt} cells without specific IgG (lane 4).

4.2.7 Subcellular localization of SORLA variants in CHO cells

So far, my experiments revealed an effect of SORLA mutants on APP. To test the consequences of the SORLA tail mutations on cellular trafficking of the receptor polypeptide and its target APP I investigated the subcellular localization of the various SORLA constructs and its influence on APP. All SORLA variants exhibited partial co-localization with APP in the perinuclear region and in some vesiclular structures as shown by immunofluorescence microscopy of permeabilized cells (figure 29), however, a clear distinction in two receptor categories was shown by surface staining of cells not permeabilized prior to antibody incubation (figure 29, insets). While cell lines expressing SORLA$^{\Delta cd}$ and SORLA^{acidic} exhibited pronounced signals for SORLA and APP on the plasma membrane, little cell surface staining was observed in cells expressing SORLA^{wt} and SORLA^{GGA}. Quantification of surface exposure by fluorescence activated cell sorting (FACS) analysis revealed statistical significant differences ($p<0.004$) for SORLA$^{\Delta cd}$ ($51.2 \pm 6.8\%$ receptor on cell surface) and SORLA^{acidic} ($42.9 \pm 3.9\%$) compared with SORLA^{wt} ($20.1 \pm 5.4\%$) (figure 30).

Finally, aberrant surface localization of SORLA$^{\Delta cd}$ and SORLA^{acidic} was also confirmed by subcellular fractionation of CHO cell lines using Western blot analysis (figure 31A). As reference, the presence of marker proteins for specific cell compartments was evaluated in parallel (figure 31B). In all cell lines, distinct peaks for SORLA were seen in fractions containing markers of ER (Glucose-related protein 78, Grp78; fractions 3-4) and Golgi (Golgi SNARE 28, GS28; fractions 4-11). While only 3% of SORLA^{wt} protein was detected in the peak fractions of the plasma membrane (β1-integrin; fractions 15-16), accumulation of variants SORLA$^{\Delta cd}$ and SORLA^{acidic} in this compartment was evident (23-28% of total protein). This finding was in line with predominant surface localization of these two mutants seen in immunofluorescence (figure 29) and FACS sorting (figure 30) experiments. Surprisingly, in addition to ER and Golgi peak fractions, SORLA^{GGA} was also enriched in fractions 16 and 17 that contained endosomes, but partially also overlapped with the plasma membrane (peak fraction 15 and 16). The ratio of SORLA^{GGA} protein mass in endosomal versus plasma membrane fractions was increased to approximately 1:1 compared to other receptor variants (approximately 1:3).

76
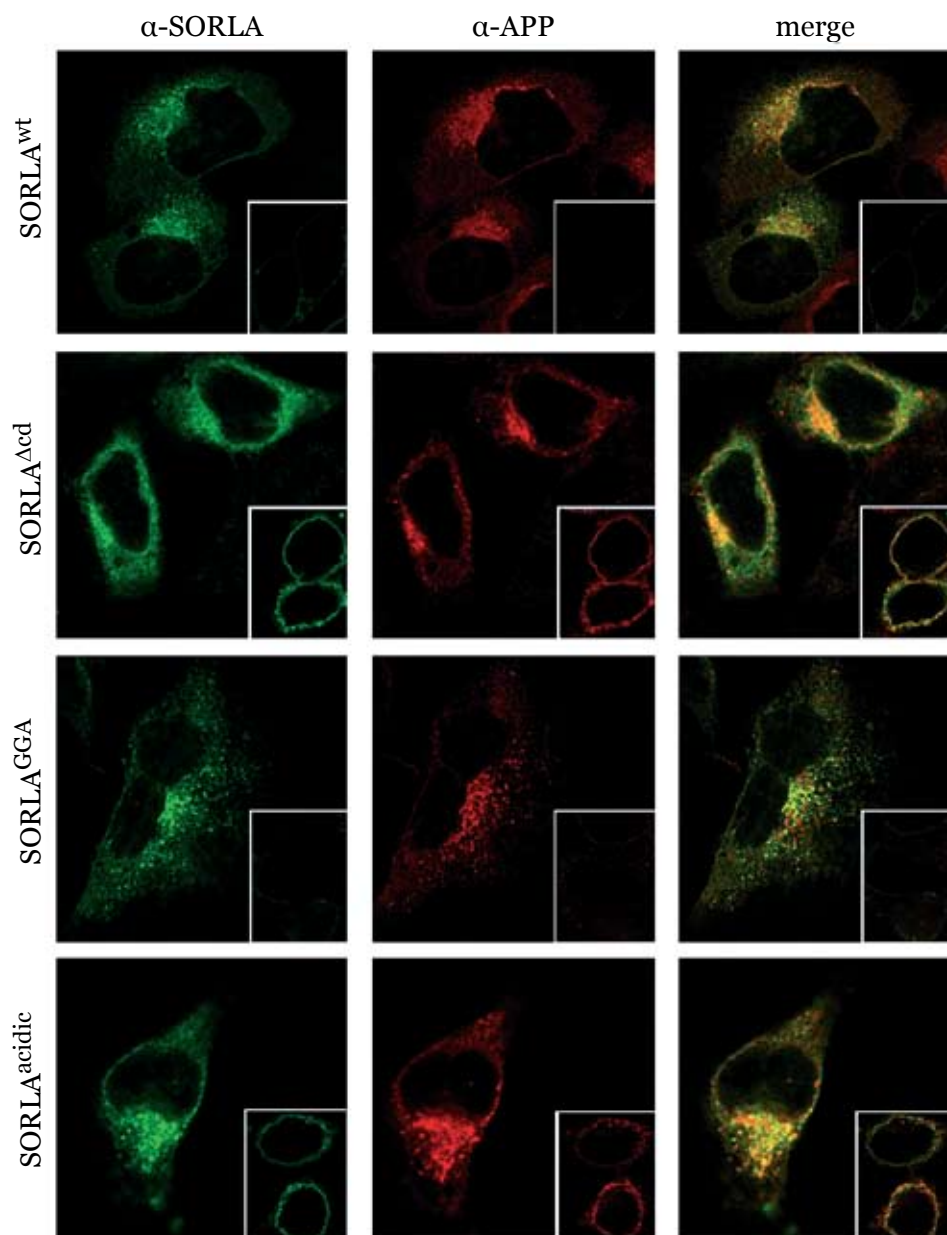
Figure 29: Co-localization of APP and SORLA variants in CHO cells.
Detection of APP and SORLA variants in stably transfected CHO cell lines using confocal immunofluorescence microscopy. The cells were fixed and permeabilized with TritonX-100 before incubation with antibodies against SORLA (α-SORLAgt) and APP (α-6E10). The stainings indicate co-localization of SORLA and APP in the perinuclear region of all lines. The insets depict analyses of the same cell lines not permeabilized with TritonX-100 prior to antibody incubation, demonstrating co-localization of APP with SORLA$^{\Delta cd}$ and SORLA^{acidic}, but not with SORLA^{wt} and SORLA^{GGA} on the cell surface.
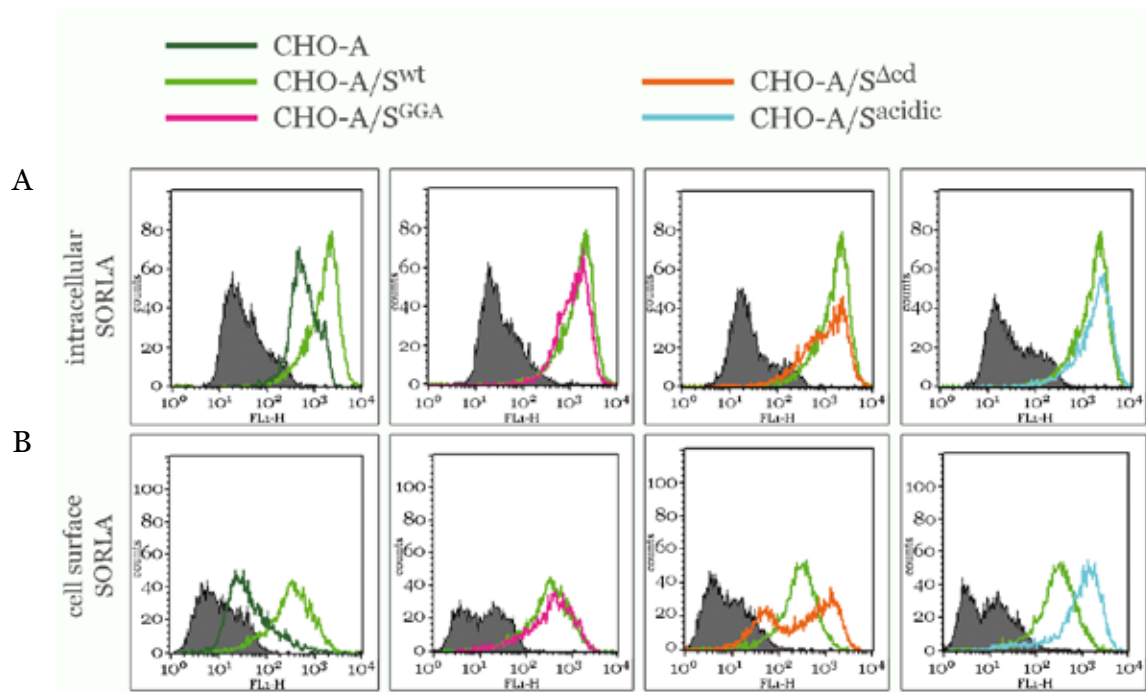
Figure 30: Quantitative measurements of SORLA signal by fluorescence activated cell sorting (FACS). Cells stably expressing APP only (CHO-A) or APP and SORLA variants were harvested and incubated in FACS buffer without (surface staining) or with 0,1% saponin (total staining), followed by incubation with primary anti-SORLA (α-SORLAgt), and Alexa Fluor 488-conjugated secondary IgG. The grey curve corresponds to cells without antibody incubation. CHO-A (dark-green) served as negative control for antibody background staining, while CHO-A/S^{wt} (light green) was a reference value for comparison with all SORLA mutant constructs (CHO-A/S^{GGA}, pink, CHO-A/S$^{\Delta cd}$, orange; CHO-A/S^{acidic}, blue). All SORLA receptor variants were equally expressed within the cell (A), however, only CHO-A/S$^{\Delta cd}$ and CHO-A/S^{acidic} showed an extensive increase in cell surface exposure (B).
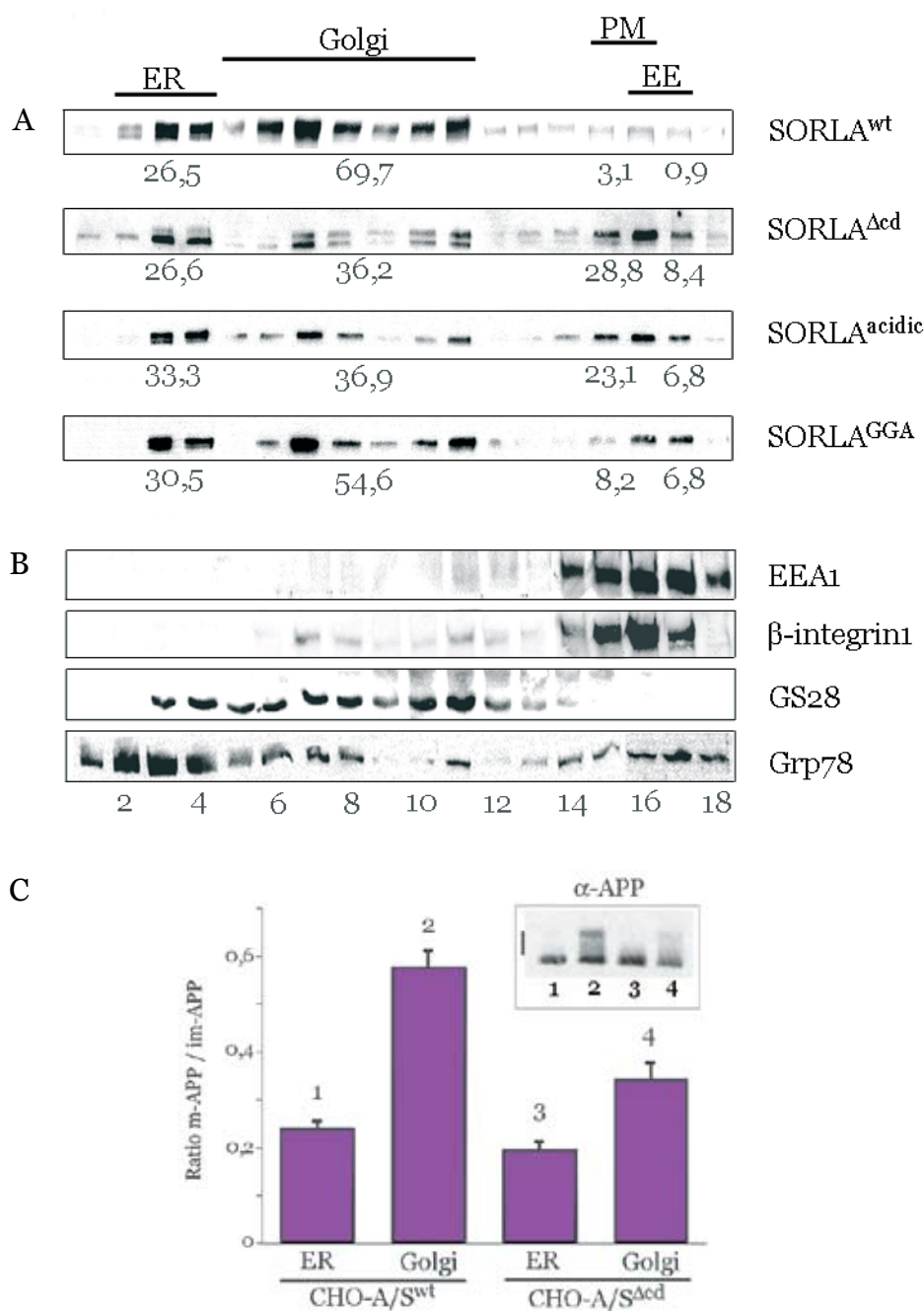
Figure 31: Subcellular localization of APP and SORLA variants.
Cells expressing APP and the indicated SORLA variants were subjected to subcellular fractionation using density gradient ultracentrifugation. Immunodetection of SORLA variants (A) as well as markers (B) β1-integrin (plasma membrane; PM), Grp78 (endoplasmic reticulum; ER), GS28 (all Golgi cisternae), and EEA1 (early endosomes) in the fractions is depicted. All SORLA variants are seen in ER (fractions 3-4) and Golgi (fractions 5-11). In

addition, variants SORLA$^{\Delta cd}$ and SORLA^{acidic} accumulate on the cell surface (fractions 15-16), while SORLA^{GGA} is also enriched in fractions 16-17, containing endosomes as well as plasma membrane. The numbers underneath the fractions indicate percent of total receptor immunoreactivity found in the individual cellular compartments. (C) Fractions enriched in ER (fraction 3) or Golgi (fraction 7) from panel A were tested for APP using Western blot analysis (inset) and densitometric scanning thereof. Mature APP (highlighted by bracket in inset) accumulates in Golgi fractions of CHO-A/S^{wt} (lane 2) but not CHO-A/S$^{\Delta cd}$ cells (lane 4) ($p<0.01$). No mature APP is seen in the ER of either cell line (lanes 1 and 3) ($p=0.1$).

4.2.8 Detailed localization of SORLA^{GGA} with subcellular marker in CHO cells

Because no obvious difference in subcellular localization (figure 31) and immunofluorescent staining between SORLA^{GGA} and SORLA^{wt} (figure 29) was seen, I mapped the localization of both proteins more precisely using different markers. In line with my previous results, SORLA^{GGA} displayed the same subcellular localization as SORLA^{wt} demonstrated by confocal immunofluoresce microscopy (figure 32). CHO-A/S^{GGA} cells were grown on glass coverslips, fixed and stained for SORLA (α-SORLAgt) and markers of the Golgi compartment (positive for VTI1b), early endosomes (positive for EEA1) and trafficking vesicles (positive for SNX1 and gamma adaptin). No SORLA co-localization was seen with a marker of the cis-Golgi compartment (GM130, not shown). The only subtle but consistent difference was seen with Rab11. Rab11 is present in recycling endosomal vesicles and trafficking vesicles of the trans-Golgi network, where it regulates trafficking of cargo containing vesicle to the plasma membrane. Rab11 partially co-localized with SORLA^{GGA} but to a lesser extent with the wild type protein (figure 33). Quantification of a total of 700 peripheral vesicles for each cell lines that stained positive for SORLA identified $22.0 \pm 1.6\%$ co-localization with Rab11 in SORLA^{wt} but $43.6 \pm 3.6\%$ in SORLA^{GGA} ($p=0.0004$). This feature suggested faulty recycling to the plasma membrane (rather than retrograde trafficking to the TGN or anterograde trafficking to the endosomal compartments) for SORLA^{GGA}.
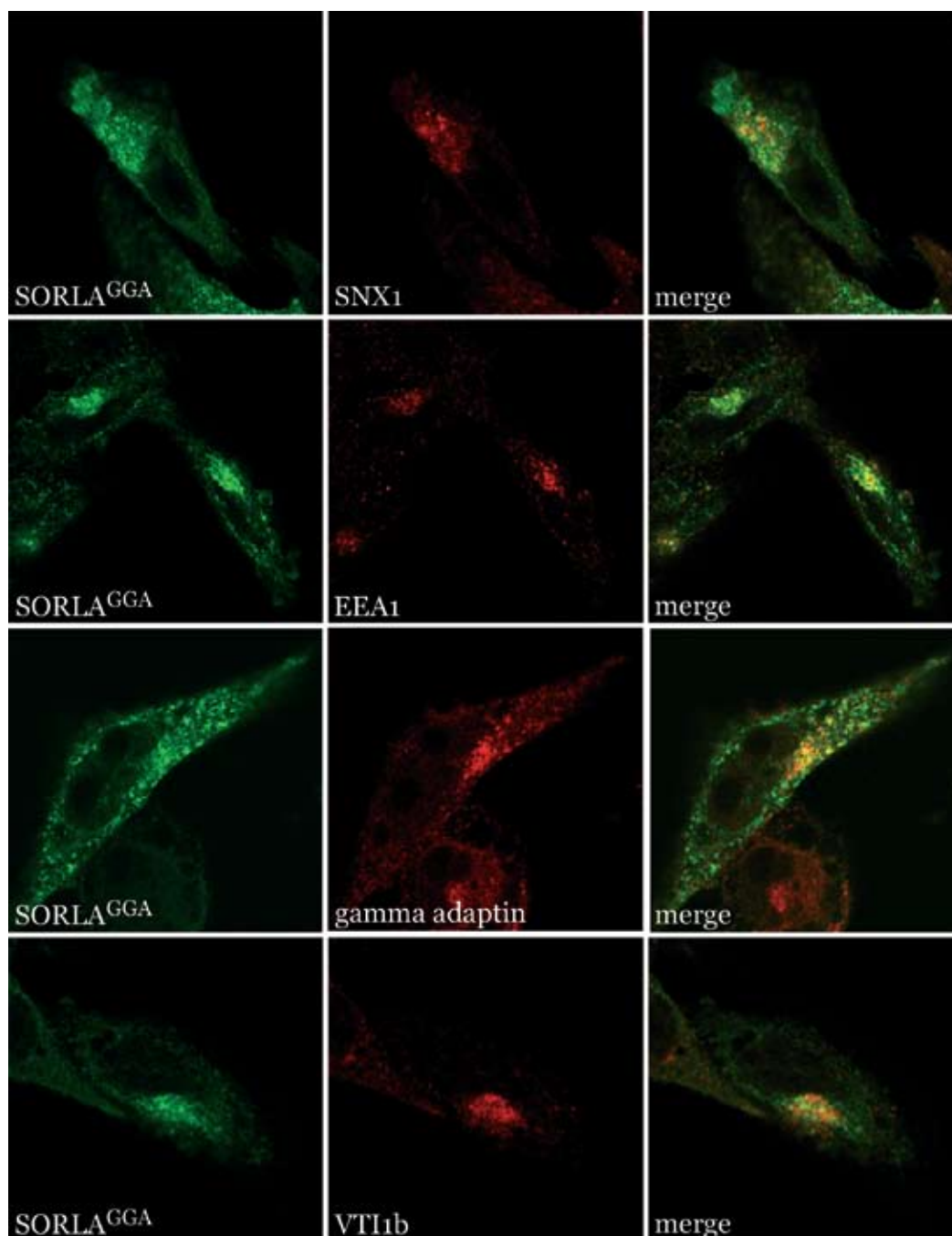
Figure 32: Subcellular localization of SORLA$^{\text{GGA}}$ in stably transfected CHO cells. Confocal immunofluorescence microscopy identified co-localization of SORLA$^{\text{GGA}}$ (green) with marker of medial to trans-Golgi (VTI1b) and early endosomes (EEA1) as well as trafficking vesicles SNX1 (retromer) and gamma adaptin (Adaptor protein 1).
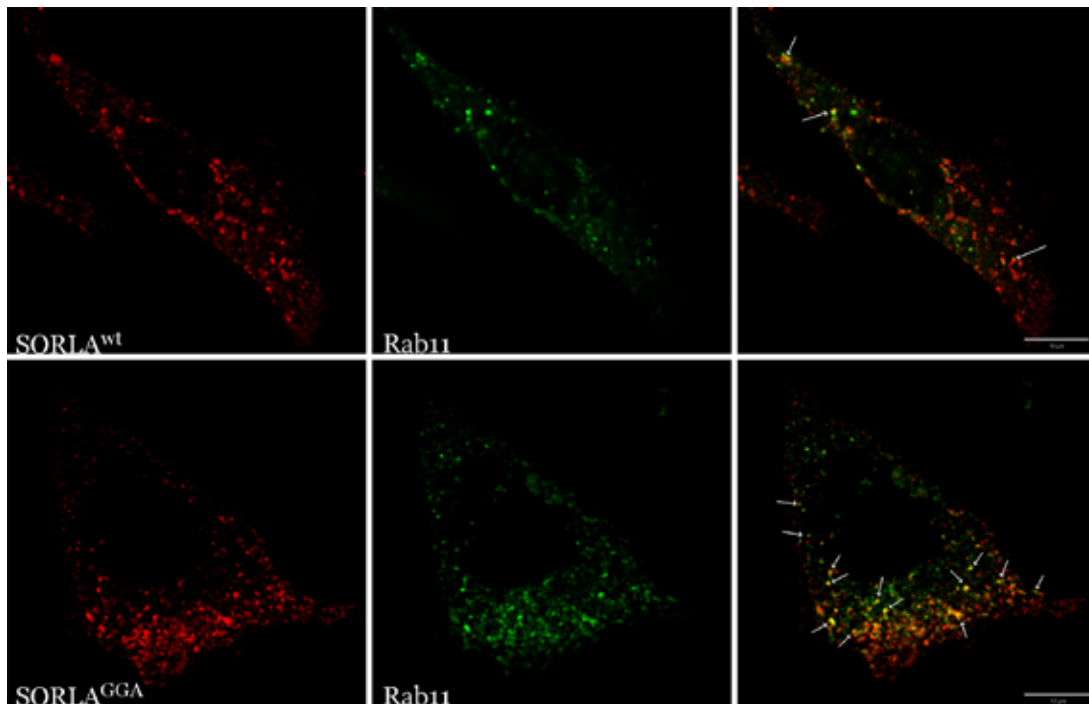
Figure 33: Immunodetection of SORLA^{wt} and SORLA^{GGA} in trafficking vesicles.
Confocal immunofluorescence microscopy in CHO cells indicates partial co-localization of SORLA^{GGA} but to a lesser extend of SORLA^{wt} with marker Rab11 in peripheral vesicles (arrows). Scale bar 10 μm.

4.2.9 SORLA ectodomain shedding in CHO cells

Cell surface trafficking of SORLA^{GGA} was supported independently by the appearance of some shedded extracellular domains of this receptor variant in the cell supernatant (figure 34). Typically, the ectodomain is released by proteolysis of SORLA by metalloproteases (W. Hampe *et al.*, 2000), an effect seen most pronounced for the cell surface variants SORLA$^{\Delta cd}$ and SORLA^{acidic}, but not for the wild type form of the receptor under these conditions (figure 34).
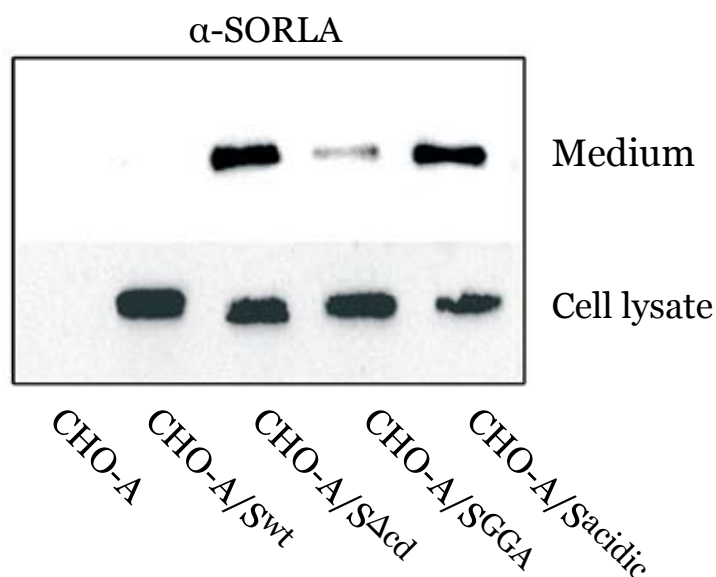
Figure 34: SORLA ectodomain shedding in CHO cells.
Western blot analysis of full-length SORLA in total cell lysates and of the soluble receptor ectodomain in the medium of the indicated cell lines. Some ectodomain shedding can be observed in SORLA^{GGA} as compared to SORLA^{wt}, indicating extended residence time at the plasma membrane. As a positive control, substantial accumulation of the receptor ectodomain was detected in media of cell surface variants SORLA$^{\Delta cd}$ and SORLA^{acidic}. No expression of recombinant SORLA was seen in parental CHO-A cells.

4.2.10 Processing of APP in CHO cell lines expressing SORLA^{wt} and SORLA^{GGA}

Given the distinct distribution of various SORLA mutants in either trans-Golgi/TGN, the recycling compartments, or at the plasma membrane, I investigated the effects of these variants on APP processing. When the subcellular fractions of CHO cells in figure 31A were probed for the presence of APP, accumulation of the mature protein species was seen exclusively in Golgi fractions of CHO-A/S^{wt} cells but not in this compartment or any other compartment of CHO-A/S$^{\Delta cd}$ ($p < 0.01$; figure 31C) or other mutant cell lines (data not shown). This finding confirmed that SORLA^{wt} has the unique property to accumulate mature APP molecules in the Golgi, most likely by extending the transit time of the precursor through this compartment. SORLA

mutants that lack the ability to interact with GGA and PACS-1 did not parallel such activity.

Consequently, I analyzed how altered localization of SORLA (and APP) may affect the generation of APP processing products, initially focusing on the two intracellular variants SORLA^wt and SORLA^GGA. Consistent with my earlier observations, co-expression of APP with SORLA^wt resulted in significantly reduced secretion of sAPPα (figure 35A,B; $p < 0.001$) and Aβ40 peptide (figure 35C; $p = 0.01$), the products of non-amyloidogenic and amyloidogenic processing, respectively, compared to cells expressing APP only (CHO-A). In contrast, SORLA^GGA caused a reduction in Aβ40 ($p = 0.01$) but a distinct increase in sAPPα production ($p < 0.05$) (figure 35A-C). This observation was independently confirmed by measuring C83 (CTFα) and C99 (CTFβ), the carboxyl terminal fragments (CTF) of APP that arise as co-products of α-secretase and β-secretase processing, respectively. The ability of SORLA^GGA to promote α-secretase processing was demonstrated by an increase in C83 as compared to parental CHO-A cells. In contrast, SORLA^wt impaired C83 production as shown by a decrease in the respective protein band (figure 35D). The amount of C99 was reduced by both SORLA variants, demonstrating that these receptors exert their inhibitory effect on amyloidogenic processing via blockade of β-secretase activity (figure 35E).

4.2.11 Internalization of APP and SORLA variants from the cell surface

As well as studying the effect of intracellular localization of SORLA on APP processing, I also investigated the consequences of wrongful targeting of the receptor to the cell surface with mutants SORLA^Δcd and SORLA^acidic. Both proteins are predominantly localized to the plasma membrane. In comparison to SORLA^wt , SORLA^Δcd should be unable to undergo endocytosis due to the lack of internalization signals in the cytoplasmic domain. To proof this assumption, I preincubated the cells on ice to arrest endocytosis and stained for SORLA to visualize plasma membrane bound SORLA receptor molecules. After chasing the cells by incubation at 37°C SORLA^Δcd was unable to internalize (figure 36) whereas SORLA^wt in CHO-A/S^wt cells was seen in the perinuclear region already after 30 min chase.
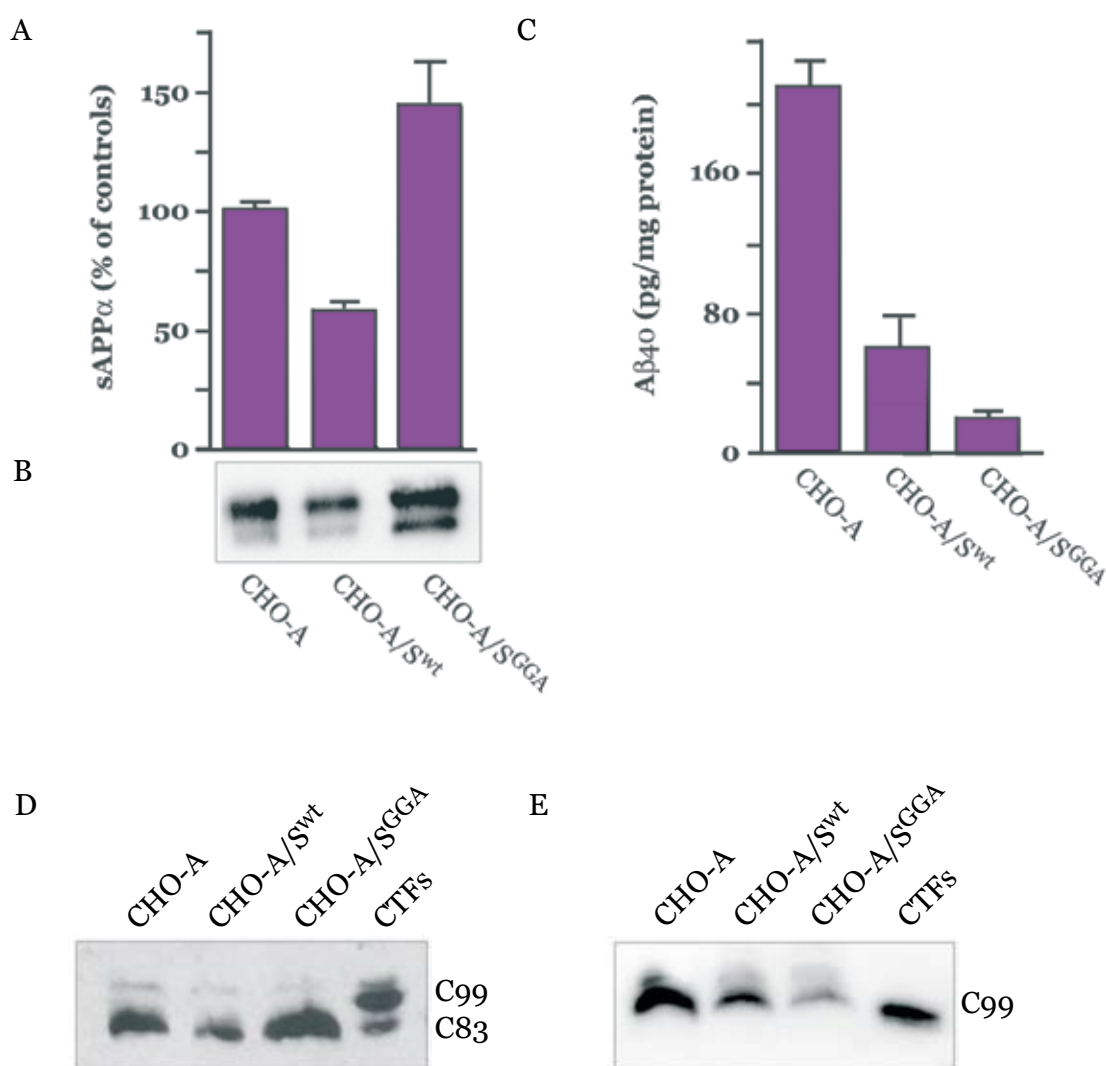
Figure 35: Processing of APP in CHO cell lines expressing SORLA^{wt} and SORLA^{GGA}. (A, B) Amount of sAPPα products in medium of the indicated CHO cell lines was determined by densitometric scanning of Western blots exemplified in panel B, and expressed as percent of processing product seen in cells without SORLA set at 100% (CHO-A). The data in panel A are the mean (± SEM) of 4 individual experiments. (C) Amount of Aβ40 in the medium of the cell lines as determined by ELISA (mean ± SEM of 3 experiments). (D, E) Immunodetection of C83 and C99 in cell lysates using antiserum 1227 that recognizes both CTFs (D), or antiserum WO2 recognizing C99 only (E). For comparison, electrophoretic mobility of recombinant CTFs was evaluated in parallel. Data in D indicate decreased levels of C83 in CHO-A/S^{wt} but increased levels in CHO-A/S^{GGA} cells compared with CHO-A. Levels of CTF C99 are decreased in CHO-A/S^{GGA} and CHO-A/S^{wt} compared with parental cells (E).

As mentioned before I demonstrated that overexpression of SORLA^{wt} coincided with sequestration of APP in the Golgi and reduced cell surface exposure. In contrast, cells overexpressing SORLA$^{\Delta cd}$ showed increased levels of APP on the cell surface which may be due to reduced APP internalization in this cell line. To elucidate
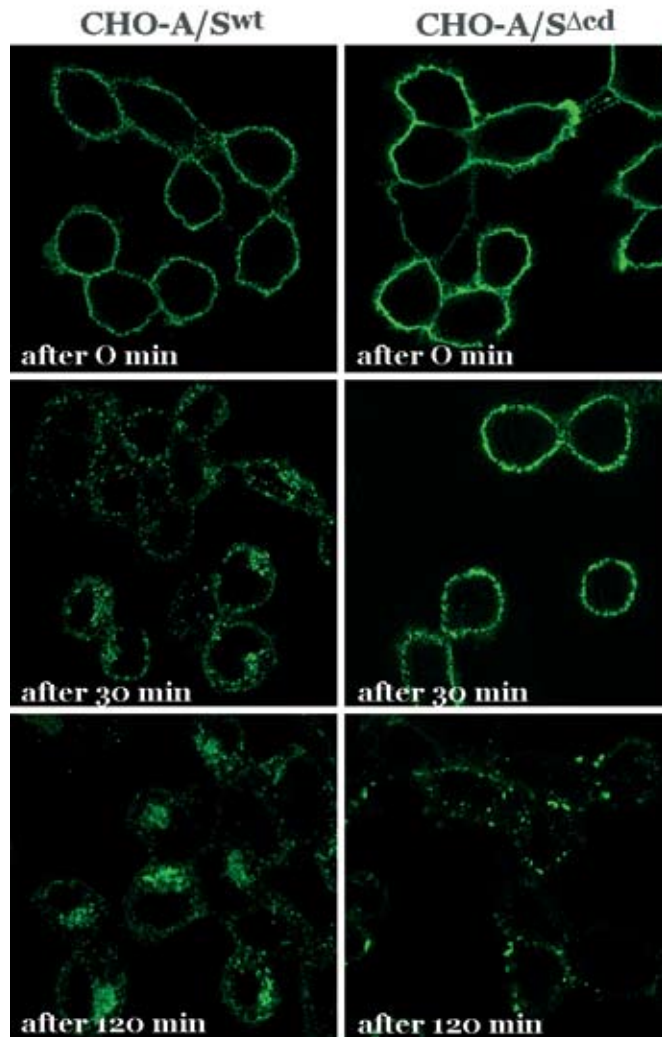
Figure 36: Internalization of SORLA receptor variants from the cell surface.
Internalization of SORLA variants was evaluated in CHO-A/S$^{\Delta cd}$ and CHO-A/S^{wt} by pre-incubating the cells at 4°C for 30 minutes to arrest endocytosis, and by subsequent labeling of SORLA molecules exposed on the plasma membrane. When the cells were chased by incubation at 37°C for 30 or 120 min, surface-labeled SORLA^{wt} relocated to endocytic compartments (30 min) or to the Golgi region (120 min) whereas SORLA$^{\Delta cd}$ remained cell surface bound.

whether SORLA may act as an endocytic receptor mediating the internalization of cell surface APP I analysed the uptake of cell surface labeled APP in cells overexpressing SORLA^{wt} or SORLA$^{\Delta cd}$ (figure 37). No altered internalization behavior was seen for APP coexpressed with SORLA^{wt} or SORLA$^{\Delta cd}$. These data indicate that SORLA activity does not influence APP uptake from the cell surface but rather affects the kinetics of APP trafficking through the Golgi.
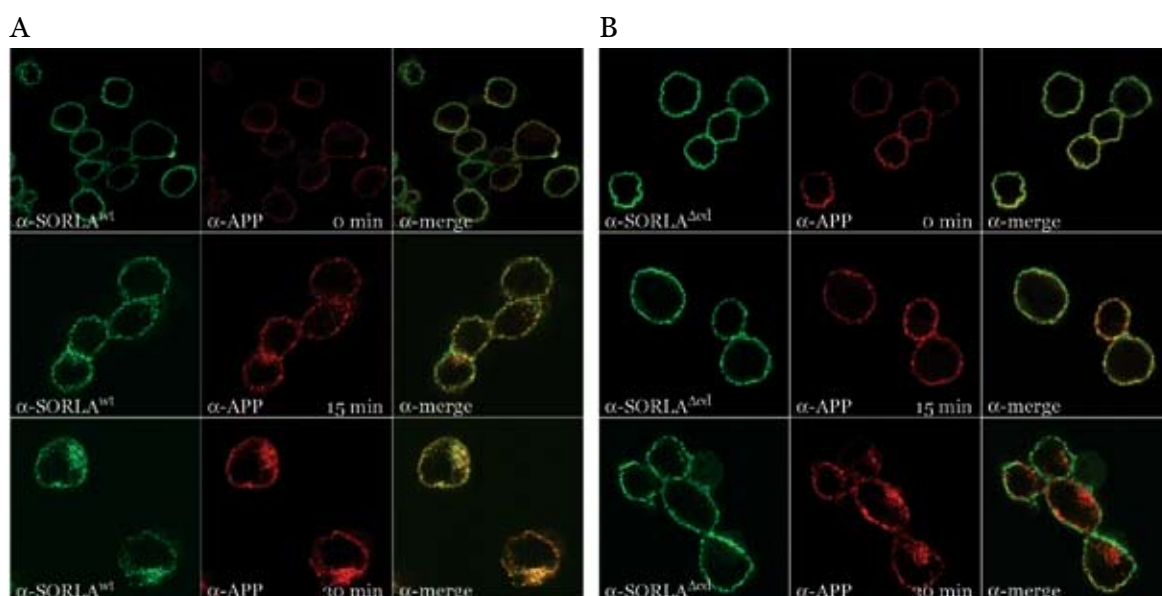
Figure 37: Internalization of APP is independent of SORLA activity.
Internalization of SORLA (green) and APP (red) was blocked by keeping CHO cells at 4°C. Subsequently, cell surface proteins were stained using antiserum directed against SORLA (α-SORLAgt) and APP (α-6E10). After 2h incubation the cells were chased at 37°C for the indicated periods of time. (A) In CHO-A/S^{wt} cells both proteins were able to internalize as indicated by a perinuclear localization after 30 min. In cells overexpressing SORLA$^{\Delta cd}$, only cell surface labeled APP molecules reached the perinuclear region whereas SORLA$^{\Delta cd}$ proteins remained at the cell surface (B).

4.2.12 Processing of APP in CHO cell lines expressing cell surface variants of SORLA

In line with my results that SORLA^{wt} and SORLA^{GGA} displayed an effect on APP processing (figure 35) I assumed that other SORLA variants which were stuck to the cell surface may also influence the generation of APP processing products. To test this hypothesis, APP cleavage products were measured in CHO-A/S$^{\Delta cd}$ and CHO-A/S^{acidic} cells by Western blot analysis and ELISA and were compared to data in CHO-A/S^{wt} and CHO-A. Whereas sAPPα levels were unchanged in SORLA$^{\Delta cd}$ and SORLA^{acidic} compared to CHO-A (figure 38A,B), both SORLA variants caused a massive increase in Aβ40 levels as shown by ELISA (figure 38C; SORLA^{acidic} p<0.02; SORLA$^{\Delta cd}$ p = 0.03). The stimulatory effect on amyloidogenic processing was also seen by determination of Aβ42 levels which were below detection limit
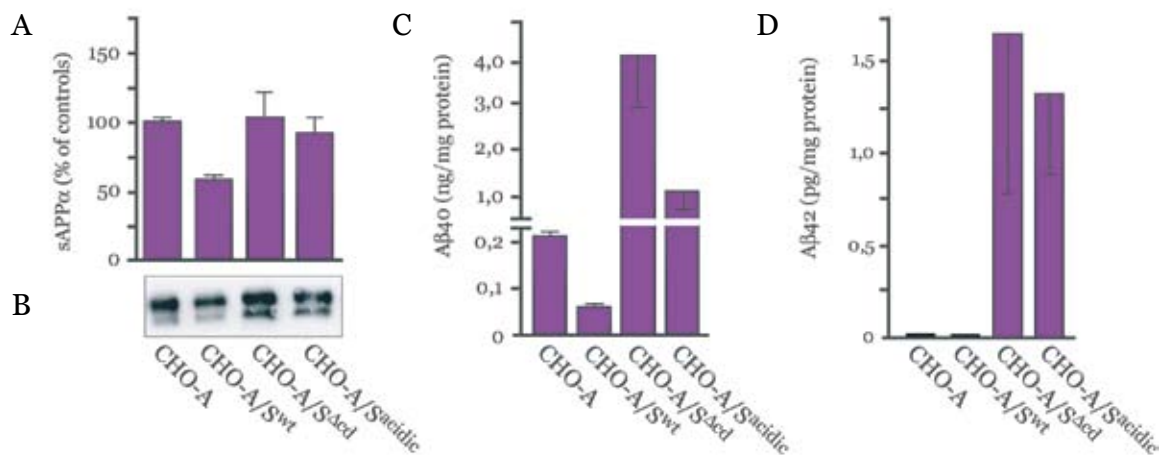
Figure 38: Processing of APP in CHO cell lines expressing cell surface variants of SORLA. (A, B) Amount of sAPPα in the medium of the indicated CHO cell lines was determined by densitometric scanning of Western blots exemplified in panel B, and expressed as percent of processing products seen in CHO-A (set at 100%). The data in panel A are the mean (± SEM) of 4 individual experiments. (C, D) Amount of Aβ40 (C) and Aβ42 (D) in media of the indicated CHO cell lines as determined by ELISA (mean ± SEM of 3 to 6 experiments).

in parental CHO-A and CHOA/S^{wt} cells, in agreement with Aβ42 representing less than 10% of the total amyloid peptide production in CHO cells. In contrast to CHO-A and CHOA/S^{wt} cells, Aβ42 was easily detectable in CHO-A/S$^{\Delta cd}$ and CHO-A/S^{acidic} (figure 38D).

Moreover, the increase in Aβ production was independently confirmed by Western blot analysis that demonstrated substantial amounts of the amyloid peptide in supernatants from CHO-A/S$^{\Delta cd}$ and CHO-A/S^{acidic}, but not from CHO-A or CHOA/S^{wt} cells (figure 39A). Finally, enhanced amyloidogenic activity with SORLA cell surface variants was also documented by detection of significant amounts of sAPPβ (the co-product of β-secretase cleavage) in cell media of the latter cell lines compared with CHO-A. In contrast, levels of sAPPβ in CHOA/S^{wt} cells were reduced compared with CHO-A in accordance with the protective function of the wild type receptor (figure 39B).
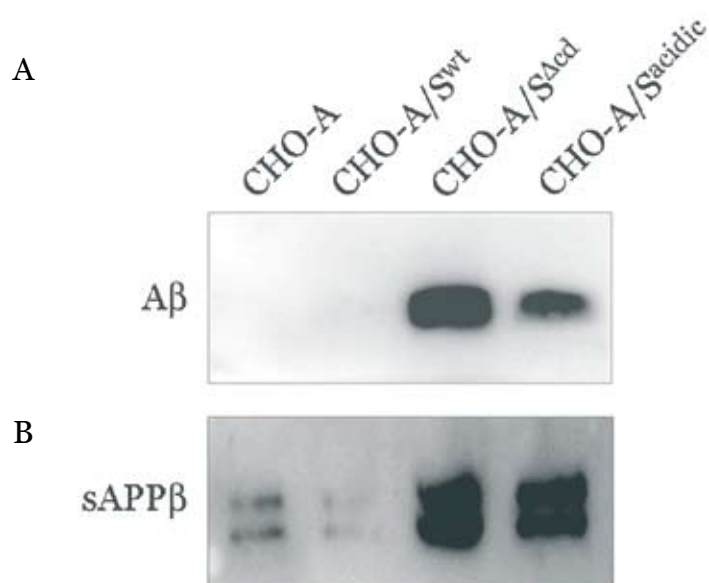
Figure 39: Aβ and sAPPβ production in CHO cell lines expressing cell surface variants of SORLA. (A) Western blot analysis of cell supernatants of the indicated CHO cell lines demonstrated accumulation of Aβ (IgG WO2) in CHO-A/S$^{\Delta cd}$ and CHO-A/S^{acidic} mutants. No Aβ proteins were detectable in cells expressing SORLA^{wt} or APP only. (B) Massiv production of sAPPβ (IgG JP18957) is seen CHO-A/SORLA$^{\Delta cd}$ and CHO-A/SORLA^{acidic} cell lines compared to parental CHO-A and CHO-A/SORLA^{wt} cells.

In conclusion, SORLA^{wt} expression had a protective effect on APP metabolism by reducing both the amyloidogenic and nonamyloidogenic APP processing pathway. Altered subcellular localization of SORLA variants and their distinct effects on APP processing are summarized in table 6. These data have identified some of the molecular mechanisms regulating intracellular trafficking of the receptor, and they have substantiated the physiological relevance of this sorting pathway in determination of APP processing fates in the cell types analyzed here.

Table 6: Effect of SORLA variants on APP processing compared with CHO-A				
	Preferential localization	**mature APP**	**sAPPα**	**Aβ**
SORLA^{wt}	trans-Golgi / TGN some early endosomes	↑	↓	↓
SORLA^{GGA}	trans-Golgi / TGN some recycling/secretory vesicles	→	↑	↓
SORLA^{acidic}	cell surface	→	→	↑
SORLA^{Δcd}	cell surface	→	→	↑
SORLA^{KKLN}	endoplasmic reticulum	↓	↓	↓

5. Discussion

In my study, I have characterized a novel neuronal sorting receptor SORLA that interacts with APP and that affects trafficking and proteolytic processing of the precursor protein in cultured cells and in the brain. I demonstrated that a lack of SORLA activity coincides with altered APP processing and enhanced Aβ production, whereas the presence of receptor function impaires APP processing and amyloidogenic plaque formation. By using wild type and trafficking defective mutants of SORLA I obtained detailed insights into the molecular mechanisms governing the intracellular transport route of this receptor and their relevance for APP transport as well as the generation of amyloidogenic Aβ peptides. These findings uncovered a novel regulatory pathway in the cell biology of APP, potentially important for our understanding of pathological mechanisms underlying AD in patients.

5.1 SORLA and APP expression *in vivo*

Initial gene expression profiling studies discovered a loss of SORLA in lymphoblasts from patients who suffer from AD (Scherzer et al., 2004). Subsequently, the same group confirmed this result in AD brain autopsies by measuring *Sorla* mRNA. SORLA is strongly expressed in cortex and hippocampus of the brain, especially CA-region and dentate gyrus of the hippocampus, both regions strongly affected in AD (figure 11). In fact, the hippocampus is one of the first brain regions to suffer damage resulting in memory problems and disorientation. Further, the cortex plays a role in memory, attention, thought, language, and consciousness, all properties which are altered in AD patients. Although APP is ubiquitously expressed in all tissues (http://www.genecards.org/cgi-bin/carddisp.pl?gene=APP&search=app), the receptor is concentrated in neuronal cells of the brain, the same location where SORLA is predominantly expressed. Based on these initial observation, I tested the influence of SORLA on APP metabolism *in vivo* and *in vitro*. In both mouse brain and cultured cells I showed that SORLA and APP localize to the same subcellular compartments (endosomal and Golgi-compartment in cultured cells and neurons of the hippocampus and cortex in mouse brain) (figure 11, figure 21).

Although SORLA and APP are mainly expressed in the same brain areas, I observed,

however, a different pattern in the cerebellum. Whereas APP displays a diffuse expression in the cerebellum, SORLA showed a distinct localization only in the Purkinje and the molecular cell layer suggesting that SORLA may have other roles than the regulation of APP metabolism.

In my study, I demonstrated enhanced amyloidogenic APP processing leading to enhanced Aβ levels in *Sorla* deficient mice and, consequently, more plaque load similar to the situation in AD patients (figure 12, figure 13). Recent publications reported inherited single nucleotid polymorphism (SNP) variants in the SORLA protein that are associated with late-onset AD (Rogaeva et al., 2006; Bettens et al., 2008; Kolsch et al., 2008). This findings further supports a critical role of SORLA in AD processes. Potentially, a dysfunctional receptor or reduced receptor expression due to certain SNP variants could promote spontaneous Alzheimer disease. Unfortunately, none of the SNPs resulted in dysfunctional SORLA protein. Neither the amino acid sequence of the receptor nor the splicing sites of the gene were affected. Further investigations must follow to elucidate the influence of these SORLA variants on neuron-specific transcriptional regulation, RNA destabilization, or protein stability. Not all genetic studies confirmed the association of the *Sorla* gene within AD. This inconsistency could be due to the problems associated with population-based studies. These studies contend against large genetic heterogeneity, rare variants of large effects, phenotypic variability, and the question of adequate coverage. Because SORLA levels were normal in patients with familial AD, one can exclude that reduced SORLA level is a secondary effect of amyloid accumulation or other AD related neuropathologic changes (Dodson et al., 2006). This leads me to the assumption that SORLA expression plays an important and preventative role in development of Alzheimer´s dementia.

5.2 SORLA influences APP transport

Based on its homology to sorting receptors that shuttle between Golgi compartments and endosomes/lysosomes, I proposed a model whereby SORLA acts as a sorting receptor for APP that determines transport of the precursor into pathways less favorable for processing. Data obtained in this thesis fully support such a working model. In particular, SORLA seems to confine APP to the Golgi compartment and to impair its transition to the cell surface (figure 23). This may be achieved by either impairing transition of nascent APP molecules en route through the Golgi to the plasma membrane or by re-routing internalized precursors from early endosomes back to the Golgi compartment. By using life cell imaging, our group demonstrated that SORLA blocks transit of APP through the secretory pathway. Trafficking of APP from the perinuclear region into more distal compartments was reduced in SORLA overexpressing cells compared to cells expressing APP only (Schmidt et al. 2007). A role for SORLA in re-routing internalized precursor molecules from early endosomes back to the TGN seems less likely as retrograde trafficking of APP was not affected by the presence of the receptor. A retention of APP in the Golgi is expected to cause accumulation of mature APP molecules in the cell. In my study, CHO cells co-expressing APP and SORLA proteins displayed enhanced levels of mature APP molecules compared to control cells expressing no SORLA (figure 23). In fact, I demonstrated that SORLA[wt] positive CHO cells have the unique property to present higher ratio of mature APP to immature APP compared to cells without SORLA or cells expressing SORLA trafficking mutants (figure 31). This result was independent of total APP levels in the various cell lines (figure 27). This findings implies that the exit of APP from the ER to the Golgi was normal but the ability of further transit to more distal compartments was blocked by SORLA[wt] proteins and thereby increasing the amount of fully glycosylated APP molecules in the cell. This model is supported by the fact that SORLA[wt] inhibits APP processing and, consequently, reduces the turnover rate of mature APP. Others showed that retrograde transport of APP from TGN to early Golgi compartment or the extended retention period within the Golgi is of importance for maturation of the holoprotein. An inhibition of retrograde transport causes a reduction of APP maturation (Selivanova et al., 2006). APP is *N*- and *O*-glycosylated in CHO cells. Proper glycosylation of proteins is relevant for correct assembly and folding, surface expression, protection of

proteins from proteolytic degradation, cellular recognition and adhesion, transport activity, and protein stability.

To conceptually prove the ability of SORLA to act as retention factor for APP, I generated the SORLA^{KKLN} mutant which was unable to exit the ER (figure 24; figure 25). I showed that cells co-expressing APP and SORLA^{KKLN} displayed altered APP localization. The majority of all APP molecules were sequestered in the ER by this SORLA variant. The altered localization also changed the proteolytic fate of APP. Only a small fraction of APP molecules moved through the early secretory pathway and become processed by α-, β-, or γ-secretases. Surprisingly, already immature non-glycosylated SORLA molecules seem to interact with immature APP molecules suggesting that SORLA may exhibit its protective function on APP already early in the secretory compartment.

5.3 SORLA trafficking mutants alter APP processing

Anterograde and retrograde transport are controlled by different sorting motifs in the cytoplasmic tail of SORLA (and related receptors). These sorting motifs interact with specific adaptor proteins including GGAs, PACS1 and the retromer complex which shuttle their cargo to the final destination. Using immunofluorescence microscopy and subcellular frationation studies I demonstrated that SORLA^{wt} predominantly resides in trans-Golgi/TGN and early endosomal compartments (figure 20, figure 31). There was also evidence that SORLA co-localizes with SNX1 and AP1 positive vesicles suggesting that SORLA may use those adaptor protein containing vesicles to shuttle between the endosomal compartment and trans-Golgi network (data not shown). A similar localization pattern was seen in FLIM analysis (Spoelgen et al., 2006). APP also predominantly localizes to trans-Golgi/TGN compartments. It is likely that this organelle is the main compartment where both proteins interact and where SORLA exerts its protective impact on APP (figure 40). Although there are some inconsistencies concerning the localization and activity of the secretases within cells, it is widely-accepted that BACE1 cleaves APP in the early and late secretory pathway (TGN and multi vesiclular bodies) and endocytic pathway (endosomes). The same is true for γ-secretases except that this enzyme is also active in
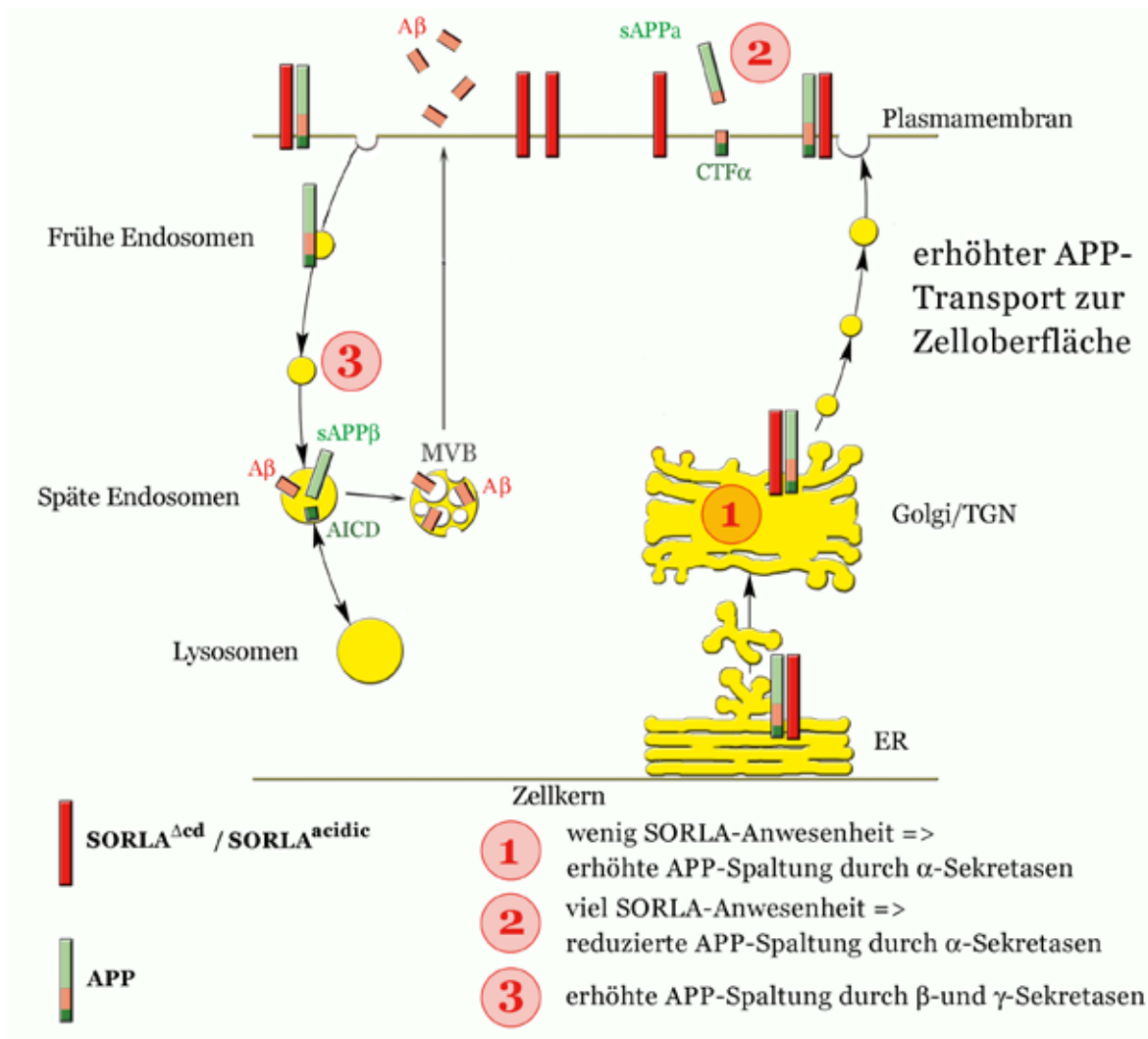
Figure 40: APP trafficking and processing in cells expressing SORLA$^{\Delta cd}$ and SORLA^{acidic}. APP (green) and SORLA (red) are synthesized in the ER. On the way to the cell surface APP is cleaved by α- and β-secretases (step 1). The cell surface transport and processing of APP is enabled by the absence of SORLA in the Golgi/TGN. At the cell surface APP is cleaved by α-secretases (step 2). Whereas APP can internalize and, consequently, become proteolytic cleaved by β- and γ-secretases (step 3), SORLA mutants remain on the plasma membrane. Aβ peptids which are produced in late endocytic compartments are secreted via exosomes/MVB. Abbreviation: ER, endoplasmic reticulum; TGN, trans-Golgi network; PM, plasma membrane; MVB, multi vesicular body; CTF, c-terminal fragment.

the ER. Proteolytic processing of APP by γ-secretase only succeeds once the large luminal APP domain was cleaved by α- or β-secretase. α-Secretases are supposed to cleave APP mainly in the TGN and at the cell surface (figure 40).

The regulated transport of SORLA, APP, and of all secretases and their interaction in one compartment is crucial for the balance of amyloidogenic and non-amyloidogenic pathway. Aberrant SORLA trafficking interferes with this balance. The SORLA$^{\Delta cd}$ construct which lacks the whole cytoplasmic domain and, by that means, all sorting motifs is produced in the ER and passes the Golgi compartment until it arrives at the cell surface (figure 40). This construct is unable to undergo internalisation and resides at the plasma membrane (figure 36). Thus, SORLA$^{\Delta cd}$ is not able to exert its protective effect on APP processing in endosomes by preventing transport of APP to late endocytic compartments that harbor β- and γ-secretase activity (figure 37, figure 40). In contrast, APP can enter endocytic vesicles and become degraded in late endosomes. A massive production of Aβ peptides was oberserved in this cell line due to increased β-secretase cleavage (documented by an enhancement in sAPPβ and C99 fragments (figure 39)). Sortilin, a member belonging to the same gene family like SORLA, has also the possibility to alter APP processing by affecting BACE1. Overexpression of sortilin decreases Aβ, whereas a sortilin mutant construct lacking the cytoplasmic domain similar to SORLA$^{\Delta cd}$ is able to increase Aβ secretion (Finan et al., 2006, poster abstract).

Similar results as for SORLA$^{\Delta cd}$ were seen for SORLA^{acidic} construct (figure 40). SORLA^{acidic} exhibits alterations of the amino acid sequence of the cytoplasmic domain where PACS-1 interacts. PACS-1 binding to SORLA regulates endosomal-to-Golgi retrograde trafficking after receptor endocytosis. In fact, the mutation in the SORLA^{acidic} variant not only causes retrograde trafficking defects, but also a drastically reduction of the internalization rate as shown by Nielsen et al., 2007. These authors conclude that the acidic cluster constitutes the most important endocytic motif in SORLA. Similar observation was seen for the endopeptidase furin. Furin undergoes cycling between plasma membrane and TGN. It was demonstrated that the acidic cluster in the cytoplasmic tail of furin is sufficient to induce endocytosis (Voorhees et al., 1995). Other proteins including the human cytomegalovirus glycoprotein B (Tugizov et al., 1999) and insulin-regulated aminopeptidase (Johnson et

al., 2001) also exhibit an acidic cluster motif which, when deleted, leads to deficits in endocytosis. Many studies confirmed PACS1 as the adaptor protein which binds this acidic peptide motif. Surprisingly, PACS1 is not involved in endocytosis of proteins derived from the plasma membrane but is rather implicated in retrograde trafficking of proteins from endosomal recycling compartment (ERC) to the TGN. In terms of SORLA, PACS1 knockdown in cells did not affect internalization. However, a knockdown of the adaptor protein-2 (AP2), a protein involved in clathrin-mediated endocytosis of many proteins, lead to a complete disruption of SORLA endocytosis (Nielsen et al., 2007). This observation raises the question where exactly the binding of AP2 to the cytoplasmic domain of SORLA may occur? AP2 typically interacts with sequences similar to the NPxY motif, dileucin, or YxxΦ (X represents any amino acid and Φ represents a large hydrophobic residue). The latter two motifs are not present in the SORLA tail and the putative NPxY motif is not involved in SORLA endocytosis (Nielsen et al., 2007). I propose that AP2 binds to a yet unknow sequence within close proximity to the acidic cluster. Thus, mutation of the latter sequence in SORLA$^{\text{acidic}}$ may cause a conformational change of the cytoplasmic domain and interfere with AP2 binding to its target sequence. A complex formation between AP2 and PACS1 can be excluded because PACS1 interacts only with AP1 and AP3 but not AP2 (Crump et al., 2001).

As well as PACS1 binding, interaction with GGA1 is also required for functional expression of SORLA. Based on the trafficking route of other proteins targeted by GGAs (e.g., mannose 6 phosphate receptors, sortilin, BACE1), one may speculate that lack of GGA1 interaction interferes with the ability of SORLA$^{\text{GGA}}$ to shuttle from trans-Golgi network to the endosomal recycling compartment (figure 41). GGAs predominantly localize to the TGN and AP1 positive transport vesicles (Boman et al., 2000). By means of interaction with clathrin and other accessory proteins GGAs bind their cargos in the TGN and transport them to endosomes. The disrupted GGA-binding motif drives SORLA$^{\text{GGA}}$ to an altered trafficking route. Because the direct access to the endosomes from the TGN is blocked, SORLA$^{\text{GGA}}$ seems to be redirected to the plasma membrane. This situation would lead to an enhanced SORLA expression on the cell surface which, in fact, was also observed for this construct by FACS analysis and ectodomain shedding (figure 30, figure 34). Although GGA proteins are known to mediate anterograde transport, they may have an impact on PACS1 medi-

Figure 41: APP trafficking and processing in cells expressing SORLA^{GGA}.
APP (green) and SORLA (red) are synthesized in the ER. The direct route from Golgi/TGN to the endosomal compartments is blocked by the inability of SORLA^{GGA} to bind GGA proteins in the TGN. On the way to the plasma membrane APP is processed by α- and β-secretases (step 1). At the cell surface APP is further cleaved by α-secretases (step 2). After endocytosis SORLA^{GGA} interferes with APP degradation by re-routing this receptor back to the cell surface. Thereby SORLA^{GGA} prevents proteolytic cleavage of APP to Aβ (step 3). Abbreviation: ER, endoplasmic reticulum; TGN, trans-Golgi network; CTF, c-terminal fragment; ERC, endocytic recycling compartment.

ated retrograde transport as well. From studies with mannose 6 phosphate receptor it is known that PACS1 directly binds GGA and that this interaction is required for release of GGAs from endosomal membranes (Scott et al., 2006). Binding and release of GGA or PACS1 proteins are regulated by phosphorylation events of their autoinhibitory domains. A phosphorylation of GGA1 protein by the phosphotase PP2A in the TGN causes a relieve of the autoinhibition and allows GGA1 to interact with its cargo. Once at the endosomal membrane PACS1 links casein kinase-2 (CK2) to GGA1 to form a multimeric complex. GGA1 becomes phosphorylated and thereby inactive. Consequently, the cargo is released from GGA1. Simultaniously, PACS1 becomes activated by CK2 phosphorylation and interacts with the cargo protein to introduce retrograde transport until a new cycle of binding and release at the TGN starts. The role of CK2 and PP2A in controlling multiple sorting steps in the TGN/ endosomal system and the cooperation of many different adaptors and accessory proteins involved indicates that the distribution of cargo proteins is tightly regulated. Disturbing or altering one factor would inevitably interfere with cargo transport. One can envision such a scenario for SORLA. Suggesting that SORLA^{GGA} mutant is unable to undergo retrograde transport this receptor has only two possibilities for further transport: SORLA could remain in endosomal compartments and follows the endosomal/lysosomal degradation pathway, or SORLA undergoes enhanced recycling to the plasma membrane. In my studies I saw increased colocalization of SORLA^{GGA} with RAB11 proteins, a marker for secretory vesicles derived from endosomes or TGN (figure 33). This observation suggests an increased SORLA^{GGA} recycling. Because SORLA^{GGA} exhibits intensified endosomal and diminished Golgi localization (figure 31) I observed increased sAPPα and decreased Aβ peptid secretion (figure 35). This could be due to a blockade of β-secretase activity of APP in endocytic compartments by SORLA^{GGA} and increased access of α-secretases to APP in the TGN and at the cell surface (figure 41).

In contrast, cells overexpressing SORLA^{wt} proteins showed reduced amyloidogenic and non-amyloidogenic processing of APP (figure 35). SORLA^{wt}-mediated accumulation of APP in the trans-Golgi/TGN results in impairment of α- and β-secretase cleavage. One may speculate that SORLA re-route internalized precursor molecules from endocytic recycling compartment (ERC) to the TGN to avoid APP cleavage by BACE1 in the endocytic compartments (figure 42). However, no discernable differ-

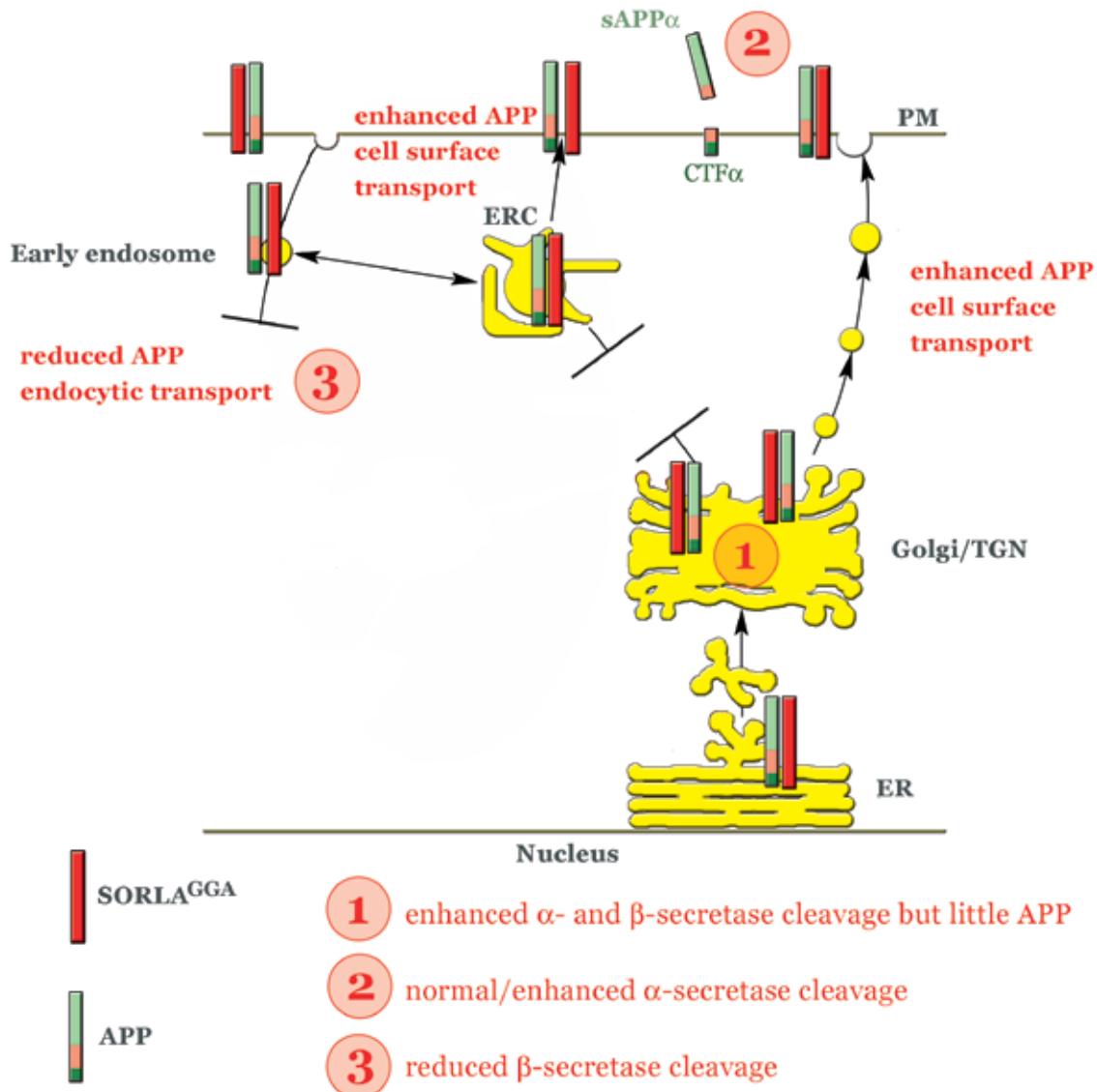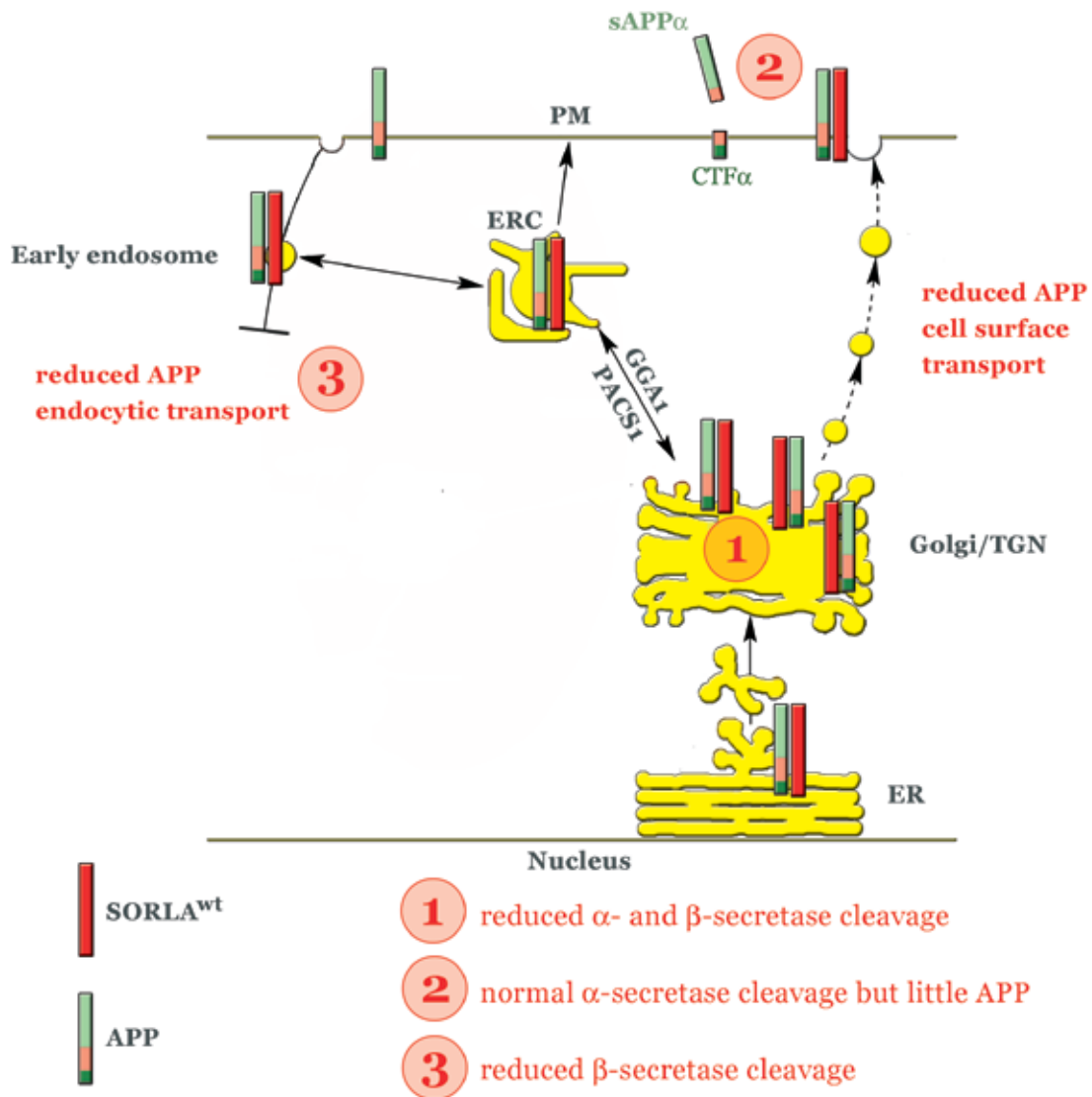**Figure 42: APP trafficking and processing in cells expressing SORLA^{wt}.**
APP (green) and SORLA (red) are synthesized in the ER. Due to binding to GGA proteins SORLA^{wt} shuttles directly from Golgi/TGN to the endosomal compartments. Once there, GGA proteins become substitute by PACS1 proteins and the receptor shuttles back to the Golgi. Only a small fraction of SORLA molecules arrives the cell surface. The accumulation of SORLA^{wt} molecules in the Golgi/TGN causes a decrease of APP transport to the plasma membrane and reduced access of α- and β-secretases to the precursor (step 1). Consequently, only little APP molecules arrive the cell surface and become cleaved by α-secretases (step 2). After APP internalization SORLA picks up the precursor and continues preventing APP degradation by assisting re-routing this receptor back to the Golgi/TGN (step 3). Abbreviation: ER, endoplasmic reticulum; TGN, trans-Golgi network; CTF, c-terminal fragment; ERC, endocytic recycling compartment.

ences were seen for the amount of APP in endosomes or in trans-Golgi/TGN when comparing cells with and without SORLA, indicating that endocytic uptake and retrograde targeting of APP were not influenced by this receptor (Schmidt et al., 2007). We are just beginning to understand the molecular concepts that govern interaction of SORLA with APP. To fully appreciate the complexity of this regulatory pathway, one has to consider numerous other factors that participate in it as well. Beside the well-known secretases and some of the adaptors discussed above, other candidate interaction partners need to be considered as well. For example, X11 and ubiquilin are two *in vivo* regulators of APP. The X11/Mint protein family consists of three mammalian members: neuron-specific X11α and X11β, and ubiquitously expressed X11γ. The first two isoforms are found in amyloid plaques of AD patients. It was shown that increased X11α and X11β expression leads to reduced secretion of Aβ peptids by increasing the steady-state level of APP. It does so by altering the maturation fate in the secretory pathway by changing endocytic trafficking of APP (King et al., 2003). Co-transfection of APP and X11 stabilizes cellular full-length APP and down-regulates sAPPα and Aβ secretion suggesting that APP-X11 interaction plays a role in the regulation of APP processing (Sastre et al., 1998). Furthermore, X11 leads to a cytoplasmic retention of AICD via direct binding (Gross et al., 2008).

Ubiquilin1, another gene that is linked to AD, is found in neurofibrillary tangles and alters APP levels and Aβ secretion by modulating APP trafficking. Downregulation of ubiquilin1 increases the ratio of APP mature/immature forms, increases levels of full-length APP on the cell surface, and enhances the secretion of sAPPα, sAPPβ, and Aβ generation (Hiltunen et al., 2006).

Furthermore, it was reported that PAT1 (Protein Interacting with APP Tail 1), a microtubule-interacting protein which recognizes the basolateral sorting signal of APP, may control the intracellular localization of APP. PAT1 may be involved in the translocation of APP along microtubules toward the cell surface and, by these means, also influences the proteolytic cleavage of this protein. It was shown that PAT1 promotes APP processing. Cells overexpressing PAT1 showed elevated levels of surface APP, increased sAPPs, CTFs, and Aβ levels. It is still unclear how PAT1 regulates APP trafficking but scientists propose that PAT1 either facilitates APP transport to the cell surface or reduce the endocytosis rate of APP (Kuan et al., 2006).

5.4 Sorting defects may lead to late-onset Alzheimer´s disease

The sorting of SORLA, APP, BACE1, and other transmembrane receptors among the different compartments of the Golgi, plasma membrane and endosomes is a highly regulated process. Already slight modifications may cause an imbalance between amyloidogenic and non-amyloidogenic processing of APP and, accordingly, enhanced Aβ production. Various studies implicate the link of late-onset Alzheimer´s disease to proteins which are involved in trafficking mechanisms. So far, they showed aberrant expression levels of SORLA, ubiquilin1, X11, GGA1, and GGA3 in human AD brains. Also reduced VPS35 and VPS26 (two components of the retromer complex) were observed in late-onset Alzheimer´s disease. Animal models suggest that retromer deficiency can contribute to Alzheimer pathogenesis since retromer-deficient mice display enhanced Aβ levels accompanied with synaptic dysfunction. Since SORLA can interact with the retromer complex, mutations in the binding motif may also cause altered APP trafficking and processing. It was shown that defects in retromer leads to increased residence time of APP and/or BACE1 in the endosomal compartments and, by this means, enhancing Aβ secretion. In the end, protein sorting represents one of the key mechanism in Alzheimer´s cell biology and, when altered, may contribute to late-onset pathology.

5.5 SORLA-APP interaction *in vitro*

By subcellular fractionation and immunofluorescence microscopy studies in cells I was able to demonstrate that SORLA and APP are found in the same cellular compartments and that both proteins come in close proximity (figure 21, figure 22). This observation was confirmed by fluorescence lifetime imaging analysis (FLIM) that was performed in collaboration with Robert Spoelgen, Harvard Medical School in Boston (Spoelgen et al., 2006). Moreover, I substantiated a direct interaction between these two proteins by using co-immunoprecipitation studies (figure 22). I pulled down APP with SORLA when both proteins were overexpressed in the same cell. In addition, colleagues from our group (2006) exactly deciphered the specific binding region of both proteins using surface plasmon resonance analysis. This study revealed the involvement of the complement-type domain of SORLA which binds to two regions in APP, the growth factor-like domain (GFLD) and carbohydrate domain (E2). Since the E2 domain is conserved in the APP gene family it may possible that SORLA could also bind to APLP1 and APLP2 and thereby exerts other cellular function. It is interesting to note that the complement-type domain of SORLA is the APP binding site. This domain is a typical ligand interacting domain found in all members of the LDLR family. The receptor associated protein RAP is able to bind to the complement-type domain. RAP is a chaperone that is especially designed to assist in the biosynthesis and intracellular transport of endocytic receptors. Studies suggest that RAP acts as a receptor antagonist and prevents association of newly synthesized receptors with their ligands during transport to the cell surface. Assuming a similar role for RAP in the biology of SORLA, one may envision a scenario where RAP could inhibit binding of immature APP to SORLA in the endoplasmic reticulum and the early Golgi (Bu et al., 1995). Since APP can be cleaved by α-secretase in the early secretory pathway and on the cell surface, one can envision that an interaction between the E2-domain containing sAPPα molecules and SORLA holoproteins may function as an impulse which leads to an intracellular signaling cascade. In contrast, shedded SORLA fragments by α-secretase cleavage might have the possibility to bind APP holoprotein on the plasma membrane inducing signal transduction.

Full length APP exists as a balanced populations of monomers and dimers in the cell. The dimerization occurs shortly after synthesis in the ER and influences sorting

of this receiver during the passage through the Golgi and secretory compartment. It was shown that the N-terminal GFLD domain (residues 91-111) and the E2 domain (residus 448-465) are sufficient for homodimerization. Thus, it may be possible that specific APP ligands may regulate this interaction (Kienlen-Campard et al., 2008). Intriguingly, it is exactly these two domains in APP that are responsible for binding SORLA. Two amino acid residues of the RERMS motif in the E2 domain are directly involved in the APP-APP dimerization. Once a protein binds to this sequence, the motif is no longer available for other interacting proteins. Thus, SORLA might interfere with APP-APP homodimerization and maybe also with APP-APLP heterodimerization. A trimeric complex formation can be excluded because molecular mass analysis revealed a 1:1 stoichiometric complex between the E2-domain of APP and the complement-type domain of SORLA (Andersen et al., 2006).

It is plausible that the various APP functions might be regulated by this dimerization and dissociation. It was shown that APP of one cell forms a complex with APP, APLP1 or APLP2 of another cell to promote trans-cellular adhesion in a homo- and heterotypic fashion (Soba et al., 2005). In this study it was also demonstrated that all members of the APP family are enriched in synaptic membranes and that APP/ APLP1 heterocomplexes exist in synaptic compartments. This trans-cellular APP/ APLP1 interaction may be involved in regulating synaptogenesis since APP and APLP2 are enriched at the presynapse and APLP1 at the postsynapse of neurons (Lyckmann et al., 1998).

APP dimers appear to be sequestered in specific domains of the lipid bilayer that are enriched in cholesterol and sphingolipids - the so-called lipid rafts. Lipid rafts also appear to contain Aβ dimers, of which a significant fraction is supposed to remain in the plasma membrane (Kawarabayashi et al., 2004). In fact, the simplest interpretation is that the Aβ dimers are generated from the APP dimers. According to some studies, the formation of Aβ dimers are the first step of amyloid formation which starts intracellularly and is believed to have a strong toxic effect on neuronal cells (Dyrks et al., 1992; El-Agnaf et al., 2000). This hypothesis raises the question how Aβ dimers are stabilized in the lipid bilayer? APP exhibits three glycine-xxx-glycine/alanine (GxxxG or GxxxA) motifs in its Aβ domain (figure 43). Such motifs are known to promote dimerization of peptides via close apposition of transmem-

brane sequences (Bormann et al., 1989). The GxxxG/A motif mediates dimerization between transmembrane α-helices by direct glycine-glycine contacts. Mutation of one of the GxxxG motifs leads to less dimerization efficiency which is completely abolished when all motifs are mutated (Munter et al., 2007). Moreover, it was demonstrated that GxxxG motifs play a role in the assembly, trafficking and activity of multiple proteins of the γ-secretase complex (Edbauer et al., 2004). The fact that APP possesses three GxxxG motifs suggests that the Aβ sequence may be involved in interaction also with other proteins as it is proposed for the interaction of Aβ with Aph-1 (Marchesi, 2005). Aph-1 is a subunit of the γ-secretase complex which is essential for complex assembly. Marchesi presumes that the γ-secretase complex might be disrupted by intramembranous Aβ (Marchesi, 2005). Since Aph-1 exhibits transmembrane GxxxG motifs Marchesi hypothesizes that Aph-1 can form a heterodimer with Aβ and prevents stabilizing the γ-secretase complex which would lead
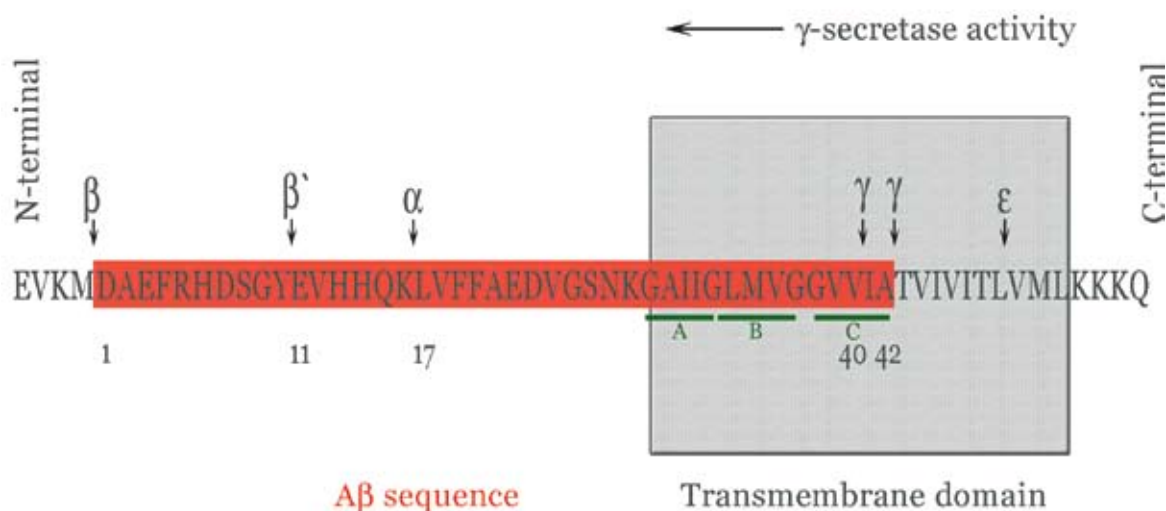

Figure 43: Sequence of the Aβ and transmembrane domain of APP.
Aβ domain shaded in red and the transmembrane domain is highlighted in grey. The major sites of cleavage by α-, β-, and γ-secretases are indicated along with Aβ numbering from the N-terminus of Aβ. The GxxxG/A motifs are underlined in green.

to a reduction of enzyme function. Such Aβ interacting partner could also include SORLA since it has a transmembrane segment (GVGFA) similar to the c-terminal end of Aβ$_{42}$ (GVVIA). In fact, both represent a GxxxA motif. So far, there are only speculations how Aβ exert its neurotoxicity in AD. In the end, it needs further investigations to find out which forms of Aβ (amyloid plaques, Aβ oligomers, soluble intraneuronal Aβ or intramembranous Aβ) mediates neuroinflammation and neurodegeneration. Perhaps all Aβ-forms contribute their share to neurotoxicity. Studies have de-monstrated that intramembranous Aβ peptids can generate membrane pores by self-assembly via their GxxxG motifs and that these Aβ-channels lead to neuronal cell death (Kim et al., 2005). SORLA might interfere with Aβ oligomerization when interacting with this peptide and thereby reducing its cytotoxic effect on neurons (figure 44).

It is known that Aβ42 is the most toxic agent in AD because its overproduction strongly correlates with familial AD. APP dimerization is important for Aβ production and APP dimers are the substrates for γ-secretases (Munter et al., 2007). Disruption of the G33xxxG29 motif to diminish APP dimerization revealed a reduction of secreted Aβ40 and Aβ42 peptides (Munter et al., 2007; Kienlen-Campard, 2008). β-Cleavage was not inhibited, and reduction of Aβ secretion resulted from inhibition of γ-cleavage at the N-terminus of the transmembrane domain due to insufficient dimerization of this part. AICD production was unaltered in this study since the first cleavage of the γ-secretase occurs at the ε-site C-terminal of the three GxxxG/A motifs (figure 43). It is known that the γ-secretase possesses sequential activity. The enzyme starts at the ε-site and cuts each third amino acid towards the N-terminal part of the transmembrane domain (figure 43). APP interacting proteins such as SORLA which might interupt the homodimerization of APP via binding to APP could directly inhibit the access of γ-secretase to its substrat, the APP dimer (figure 44).

There are also additional evidences that dimerization of proteins are involved in neurodegenerative processes. The oligomeric forms of the prion protein PrP facilitates rapid conversion of PrPc (cellular prion protein isoform) into PrPSc (scrapie prion protein isoform) in scrapie pathogenesis (Turk et al., 1988). Studies inducing dimerization of cellular APP increases the level of soluble Aβ 7-fold suggesting that the dimerization of APP could regulate APP processing (Scheuermann et al., 2001).
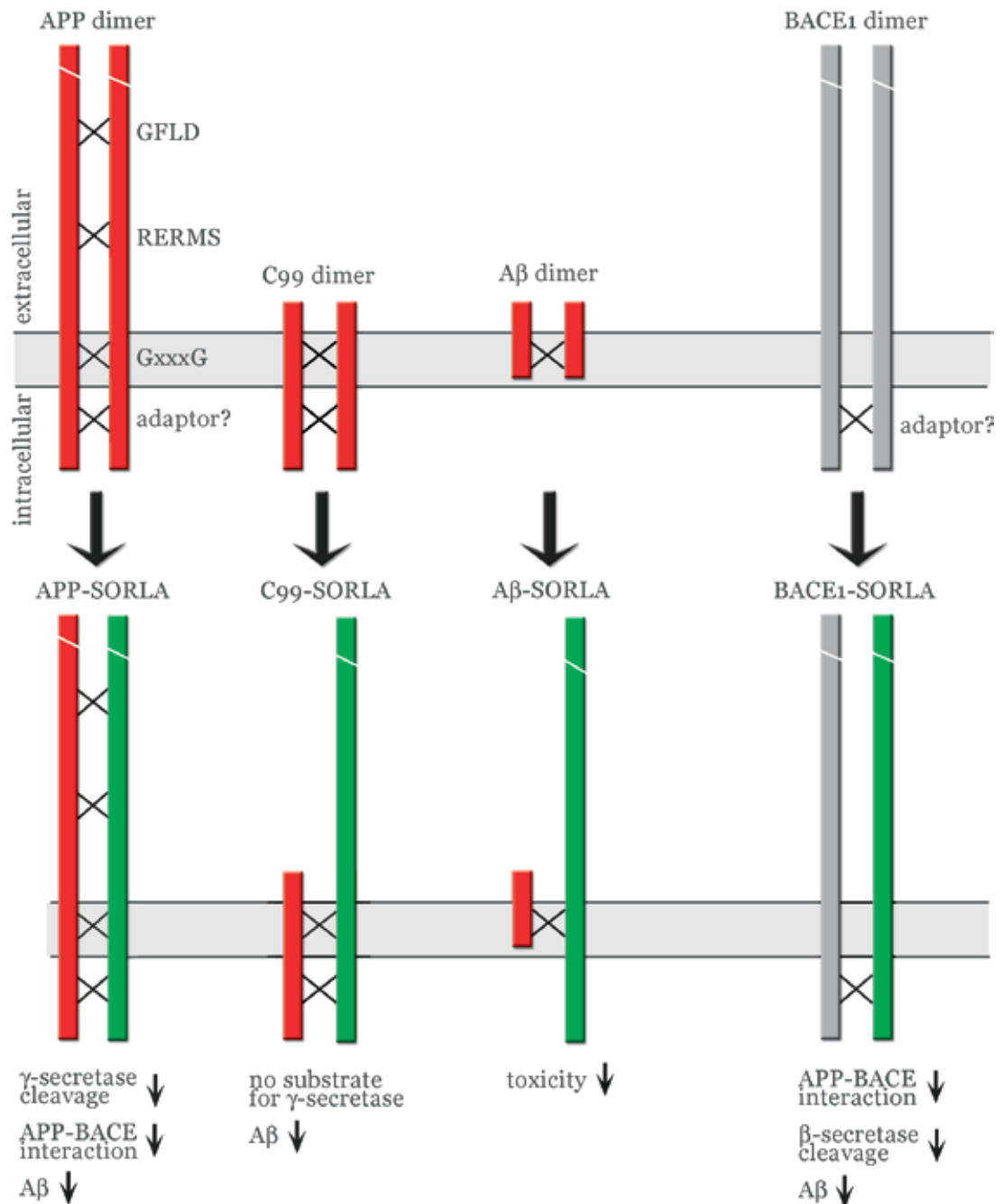
Figure 44: Putative function of SORLA on APP- and BACE1-dimers.
APP holoprotein and APP fragments (red), SORLA (green), and BACE1 (grey) are shown in colour. Possible interacting domains are highlighted as cross. SORLA may influence the homodimerization of all molecules by generating heterodimers which all reduce Aβ level and, consequently, the cytotoxic effect on neurons.

One can now speculate what happens when this dimerization of APP is inhibited by SORLA leading to a SORLA-APP formation rather than an APP-APP interaction (figure 44). In my experiments I showed that cells overexpressing SORLA^{wt} construct led to a significant reduction of Aβ peptids (figure 35). It is possible that the dimerization of APP is inhibited by SORLA. Further, SORLA might interfere with APP-BACE1 interaction by binding to either BACE1 or APP (figure 44). BACE1 is the main β-secretase which cleaves APP at the β-site to generate soluble APPβ and the CTFβ fragment. CTFβ can be further cleaved by γ-secretase which leads to Aβ generation. In SORLA^{wt} overexpressing cells I saw a reduction of Aβ, sAPPβ, and CTFβ fragment (figure 35, figure 39). One reason for the impact of SORLA on specifically β-secretase activity could be that SORLA inhibits APP and BACE1 complex formation by either directly interacting with APP and thereby preventing that BACE1 gets access to APP and/or by interacting with APP and routing this receptor in cell compartments less favorable for β-secretase activity. Using FLIM studies, we and others observed less interaction of APP and BACE1 in cells overexpressing SORLA compared to mock transfected cells (Spoelgen et al., 2006). Interaction of SORLA with BACE1 was also shown by additional experiment. SORLA/BACE1 complex formation was localized to the early Golgi compartment because by co-immunoprecipitation of SORLA and BACE1 mainly immature and non-glycosylated BACE1 proteins were immunoprecipitated. An interaction of SORLA and BACE1 in early Golgi that prevents APP/BACE1 complex formation could also lead to reduced β-site cleavage of APP (figure 44).

It was shown that BACE1 forms homodimer in ER/cis-Golgi compartments (Westmeyer et al., 2004; Schmechel et al., 2004). BACE1 dimers revealed a higher affinity and turnover rate towards APP in comparison to soluble monomeric BACE1 suggesting that this enzyme acts as a dimer. Proteins interfering with BACE1 dimerization may alter Aβ production. So far, there is no evidence that the interaction of SORLA and BACE1 is directly via their luminal domains or cytoplasmic tails. However, Spoelgen and colleagues saw an effect on APP processing in cells overexpressing only the cytoplasmic tail of SORLA. They demonstrated that SORLA-tail inhibits β-secretase cleavage by showing reduced Aβ levels in those cells. This fact means, SORLA must exhibit another binding site for BACE1 situated in the cytoplasmic tail. The GGA proteins may represent a linker because they interact with the

cytoplasmic tails of both SORLA and BACE1 proteins. The fact that not only the luminal part but also the cytoplasmic domain of SORLA interacts with other receptors was also shown for SORLA binding to APP or LRP1, as well as for the cytoplasmic interaction between APP and LRP1 (Kinoshita et al. 2001). Further, it was demonstrated that SORLA interacts with C99, the cytoplasmic fragment after β-site cleavage and that this interaction occurred in Golgi compartments and in the endosomes (Spoelgen et al., 2006). Because this interaction is thought to occur indirectly, other proteins like Fe65 could act as linker between APP and SORLA cytoplasmic tails similar to the situation seen for APP/LRP1. Fe65 binds to the NPxY motif in the tail of APP and it is possible that also SORLA can interact with Fe65 because the SORLA cytoplasmic domain exhibits a sequence similar to the NPxY motif seen in APP. It is likely that the cytoplasmic tails of both proteins interact via different NPxY binding adaptors. However, it was also shown that the SORLA/C99 complex formation was not affected by deletion of the NPxY motif in the C99 construct suggesting that other adaptor proteins are necessary for binding or, as mentioned before, the GxxxG motifs in the transmembrane domains can substitute this role. C99 also forms dimers and dimerization correlates with Aβ42 production. This observation means that the γ-secretase complex needs C99-dimers to generate Aβ42 peptids. Compounds interfering with the dimerization of C99 might decrease Aβ production in humans and it is possible that SORLA is one candidate to affect this process (figure 44).

Taking together, an inhibition of APP or C99 homodimerization by SORLA could lead to altered transport and/or processing of APP and, subsequently, decreased Aβ production. Preventing dimerization of Aβ peptides reduces the toxic effect on neurons. Moreover, an interaction of SORLA with BACE1 and maybe sequestration of this complex in early Golgi compartments or influencing BACE1 trafficking may also interfere with APP/BACE1 complex formation and thereby diminishing β-site cleavage of APP in compartments where actually BACE1 activity is suggested.

5.6 Concluding remark

The mechanisms that regulate APP trafficking to and from the Golgi are poorly understood, but all of my experimental evidence suggests that SORLA activity represents an important determinant in this process. It is likely that SORLA^wt prevents both amyloidogenic and non-amyloidogenic processing pathways by sequesters APP in the Golgi/TGN and interfering with APP dimerization and/or inhibit binding of APP to α- and β-secretases. SORLA^wt is mainly localized to the Golgi where it binds to BACE1 or APP early in the secretory pathway. Consequently, BACE1 cannot interact with APP to execute the first cleavage for Aβ generation. Early binding to APP also prevents α-secretase cleavage. That means, interacting of SORLA^wt with APP may block the access of both secretases to APP in the Golgi compartment. Also the presence of SORLA in the endocytic compartment is crucial. Binding to APP may prevent further degradation and Aβ production. That APP processing is disturbed by only protein binding was shown for different shaperons in the ER. For instance, overexpression of Grp78, a chaperon assisting the folding of proteins, leads to decreased Aβ production only by binding to APP (Hoshino et al., 2007).

The relevance of SORLA for APP processing and AD progression is supported by the observation that the receptor binds APP as ligand and that patients with AD exhibit significantly reduced expression of the receptor in the brain. The reason for reduced SORLA expression by, for instance, SNP analysis in these individuals remains to be determined, but I suggest that low levels of the receptor may be a primary cause of accelerated Aβ production and senile plaque formation. However, this process is slow and Aβ peptides cumulates over decades until plaque burdens appear. Thus, altered SORLA activity is an important risk factor for develope AD. The possibility that SORLA could serve as diagnostic marker before diagnose AD in individuals and finding ways of pharmacological interventions that increase receptor activity as early as possible in life may represent a therapeutic approach for treating this devastating disease.

6. Bibliography

Ancolio, K., Dumanchin, C., Barelli, H., Warter, J. M., Brice, A., Campion, D., Frebourg, T., and Checler, F. (1999) Proc. Natl. Acad. Sci. U. S. A. 96, 4119-4124

Andersen, O. M., Reiche, J., Schmidt, V., Gotthardt, M., Spoelgen, R., Behlke, J., von Arnim, C. A., Breiderhoff, T., Jansen, P., Wu, X., Bales, K. R., Cappai, R., Masters, C. L., Gliemann, J., Mufson, E. J., Hyman, B. T., Paul, S. M., Nykjaer, A., and Willnow, T. E. (2005) Proc. Natl. Acad. Sci. U. S. A. 102, 13461-13466

Andersen, O. M., Schmidt, V., Spoelgen, R., Gliemann, J., Behlke, J., Galatis, D., McKinstry, W. J., Parker, M. W., Masters, C. L., Hyman, B. T., Cappai, R., and Willnow, T. E. (2006) Biochemistry 45, 2618-2628

Arighi, C. N., Hartnell, L. M., Aguilar, R. C., Haft, C. R., and Bonifacino, J. S. (2004) J. Cell Biol. 165, 123-133

Ashley, J., Packard, M., Ataman, B., and Budnik, V. (2005) J. Neurosci. 25, 5943-5955

Bankaitis, V. A., Johnson, L. M., and Emr, S. D. (1986) Proc. Natl. Acad. Sci. U. S. A 83, 9075-9079

Baulac, S., LaVoie, M. J., Kimberly, W. T., Strahle, J., Wolfe, M. S., Selkoe, D. J., and Xia, W. (2003) Neurobiol. Dis. 14, 194-204

Bettens, K., Brouwers, N., Engelborghs, S., De Deyn, P. P., Van, B. C., and Sleegers, K. (2008) Hum. Mutat. 29, 769-770

Bilodeau, P. S., Winistorfer, S. C., Allaman, M. M., Surendhran, K., Kearney, W. R., Robertson, A. D., and Piper, R. C. (2004) J. Biol. Chem. 279, 54808-54816

Blacker, D., Wilcox, M. A., Laird, N. M., Rodes, L., Horvath, S. M., Go, R. C., Perry, R., Watson, B., Jr., Bassett, S. S., McInnis, M. G., Albert, M. S., Hyman, B. T., and Tanzi, R. E. (1998) Nat. Genet. 19, 357-360

Bodovitz, S. and Klein, W. L. (1996) J. Biol. Chem. 271, 4436-4440

Boels, K., Glassmeier, G., Herrmann, D., Riedel, I. B., Hampe, W., Kojima, I., Schwarz, J. R., and Schaller, H. C. (2001) J. Cell Sci. 114, 3599-3606

Bohm, C., Seibel, N. M., Henkel, B., Steiner, H., Haass, C., and Hampe, W. (2006) J. Biol. Chem. 281, 14547-14553

Boman, A. L., Zhang, C., Zhu, X., and Kahn, R. A. (2000) Mol. Biol. Cell 11, 1241-1255

Bonifacino, J. S. (2004) Nat. Rev. Mol. Cell Biol. 5, 23-32

Borchardt, T., Camakaris, J., Cappai, R., Masters, C. L., Beyreuther, K., and Multhaup, G. (1999) Biochem. J. 344 Pt 2, 461-467

Borg, J. P., Ooi, J., Levy, E., and Margolis, B. (1996) Mol. Cell Biol. 16, 6229-6241

Bormann, B. J., Knowles, W. J., and Marchesi, V. T. (1989) J. Biol. Chem. 264, 4033-4037

Bouras, C., Hof, P. R., Giannakopoulos, P., Michel, J. P., and Morrison, J. H. (1994) Cereb. Cortex 4, 138-150

Breen, K. C., Bruce, M., and Anderton, B. H. (1991) J. Neurosci. Res. 28, 90-100

Brown, M. S., Herz, J., and Goldstein, J. L. (1997) Nature 388, 629-630

Bu, G., Geuze, H. J., Strous, G. J., and Schwartz, A. L. (1995) EMBO J. 14, 2269-2280

Burgoon, M. P., Hazan, R. B., Phillips, G. R., Crossin, K. L., Edelman, G. M., and Cunningham, B. A. (1995) J. Cell Biol. 130, 733-744

Buxbaum, J. D., Koo, E. H., and Greengard, P. (1993) Proc. Natl. Acad. Sci. U. S. A 90, 9195-9198

Canuel, M., Lefrancois, S., Zeng, J., and Morales, C. R. (2008) Biochem. Biophys. Res. Commun. 366, 724-730

Cao, X. and Sudhof, T. C. (2001) Science 293, 115-120

Chen, W. J., Goldstein, J. L., and Brown, M. S. (1990) J. Biol. Chem. 265, 3116-3123

Chen, Z. Y., Ieraci, A., Teng, H., Dall, H., Meng, C. X., Herrera, D. G., Nykjaer, A., Hempstead, B. L., and Lee, F. S. (2005) J. Neurosci. 25, 6156-6166

Chien, K. L., Hsu, H. C., Su, T. C., Hwang, Y. L., Chang, W. T., Sung, F. C., Lin, R. S., and Lee, Y. T. (2001) J. Formos. Med. Assoc. 100, 587-591

Chow, N., Korenberg, J. R., Chen, X. N., and Neve, R. L. (1996) J. Biol. Chem. 271, 11339-11346

Combarros, O., Infante, J., Llorca, J., Pena, N., Fernandez-Viadero, C., and Berciano, J. (2002) Neurosci. Lett. 326, 33-36

Cooper, A. A. and Stevens, T. H. (1996) J. Cell Biol. 133, 529-541

Cooper, B., Gruber, J. A., and McPhaul, M. J. (1996) J. Steroid Biochem. Mol. Biol. 57, 251-257

Corder, E. H., Saunders, A. M., Strittmatter, W. J., Schmechel, D. E., Gaskell, P. C., Small, G. W., Roses, A. D., Haines, J. L., and Pericak-Vance, M. A. (1993) Science 261, 921-923

Crump, C. M., Xiang, Y., Thomas, L., Gu, F., Austin, C., Tooze, S. A., and Thomas, G. (2001) EMBO J. 20, 2191-2201

Crump, C. M., Hung, C. H., Thomas, L., Wan, L., and Thomas, G. (2003) J. Virol. 77, 11105-11113

Daigle, I. and Li, C. (1993) Proc. Natl. Acad. Sci. U. S. A 90, 12045-12049

De, S. B. (2003) Neuron 38, 9-12

Dodel, R. C., Du, Y., Bales, K. R., Gao, F., Eastwood, B., Glazier, B., Zimmer, R., Cordell, B., Hake, A., Evans, R., Gallagher-Thompson, D., Thompson, L. W., Tinklenberg, J. R., Pfefferbaum, A., Sullivan, E. V., Yesavage, J., Alstiel, L., Gasser, T., Farlow, M. R., Murphy, G. M., Jr., and Paul, S. M. (2000) Neurology 54, 438-442

Dodson, S. E., Gearing, M., Lippa, C. F., Montine, T. J., Levey, A. I., and Lah, J. J. (2006) J. Neuropathol. Exp. Neurol. 65, 866-872

Doray, B., Bruns, K., Ghosh, P., and Kornfeld, S. A. (2002) Proc. Natl. Acad. Sci. U. S. A 99, 8072-8077

Doray, B., Ghosh, P., Griffith, J., Geuze, H. J., and Kornfeld, S. (2002) Science 297, 1700-1703

Doray, B., Bruns, K., Ghosh, P., and Kornfeld, S. (2002) J. Biol. Chem. 277, 18477-18482

Dyrks, T., Dyrks, E., Hartmann, T., Masters, C., and Beyreuther, K. (1992) J. Biol. Chem. 267, 18210-18217

Edbauer, D., Kaether, C., Steiner, H., and Haass, C. (2004) J. Biol. Chem. 279, 37311-37315

El-Agnaf, O. M., Mahil, D. S., Patel, B. P., and Austen, B. M. (2000) Biochem. Biophys. Res. Commun. 273, 1003-1007

Esch, F. S., Keim, P. S., Beattie, E. C., Blacher, R. W., Culwell, A. R., Oltersdorf, T., McClure, D., and Ward, P. J. (1990) Science 248, 1122-1124

Farris, W., Mansourian, S., Chang, Y., Lindsley, L., Eckman, E. A., Frosch, M. P., Eckman, C. B., Tanzi, R. E., Selkoe, D. J., and Guenette, S. (2003) Proc. Natl. Acad. Sci. U. S. A 100, 4162-4167

Fassa, A., Mehta, P., and Efthimiopoulos, S. (2005) J. Neurosci. Res. 82, 214-224

Ferri, C. P., Prince, M., Brayne, C., Brodaty, H., Fratiglioni, L., Ganguli, M., Hall, K., Hasegawa, K., Hendrie, H., Huang, Y., Jorm, A., Mathers, C., Menezes, P. R., Rimmer, E., and Scazufca, M. (2005) Lancet 366, 2112-2117

Fiete, D., Mi, Y., Oats, E. L., Beranek, M. C., and Baenziger, J. U. (2007) J. Biol. Chem. 282, 1873-1881

Fiore, F., Zambrano, N., Minopoli, G., Donini, V., Duilio, A., and Russo, T. (1995) J. Biol. Chem. 270, 30853-30856

Fotinopoulou, A., Tsachaki, M., Vlavaki, M., Poulopoulos, A., Rostagno, A., Frangione, B., Ghiso, J., and Efthimiopoulos, S. (2005) J. Biol. Chem. 280, 30768-30772

Furukawa, K., Sopher, B. L., Rydel, R. E., Begley, J. G., Pham, D. G., Martin, G. M., Fox, M., and Mattson, M. P. (1996) J. Neurochem. 67, 1882-1896

Ghosh, P., Griffith, J., Geuze, H. J., and Kornfeld, S. (2003) J. Cell Biol. 163,

755-766

Ghosh, P., Dahms, N. M., and Kornfeld, S. (2003) Nat. Rev. Mol. Cell Biol. 4, 202-212

Ghosh, P. and Kornfeld, S. (2003) J. Biol. Chem. 278, 14543-14549

Golde, T. E., Estus, S., Younkin, L. H., Selkoe, D. J., and Younkin, S. G. (1992) Science 255, 728-730

Goretzki, L. and Mueller, B. M. (1998) Biochem. J. 336 (Pt 2), 381-386

Gotthardt, M., Trommsdorff, M., Nevitt, M. F., Shelton, J., Richardson, J. A., Stockinger, W., Nimpf, J., and Herz, J. (2000) J. Biol. Chem. 275, 25616-25624

Greenberg, S. M., Qiu, W. Q., Selkoe, D. J., Ben-Itzhak, A., and Kosik, K. S. (1995) Neurosci. Lett. 198, 52-56

Gross, G. G., Feldman, R. M., Ganguly, A., Wang, J., Yu, H., and Guo, M. (2008) PLoS. ONE. 3, e2495

Guenette, S., Chang, Y., Hiesberger, T., Richardson, J. A., Eckman, C. B., Eckman, E. A., Hammer, R. E., and Herz, J. (2006) EMBO J. 25, 420-431

Gunawardena, S. and Goldstein, L. S. (2001) Neuron 32, 389-401

Haft, C. R., de la Luz, S. M., Barr, V. A., Haft, D. H., and Taylor, S. I. (1998) Mol. Cell Biol. 18, 7278-7287

Hampe, W., Frank, R. W., Schulze, C., Dehning, I., and Schaller, H. C. (1996) Eur. J. Biochem. 235, 814-820

Hampe, W., Hermans-Borgmeyer, I., and Schaller, H. C. (1999) Results

Probl. Cell Differ. 26, 323-337

Hampe, W., Riedel, I. B., Lintzel, J., Bader, C. O., Franke, I., and Schaller, H. C. (2000) J. Cell Sci. 113 Pt 24, 4475-4485

Hardy, J. and Selkoe, D. J. (2002) Science 297, 353-356

Heber, S., Herms, J., Gajic, V., Hainfellner, J., Aguzzi, A., Rulicke, T., von, K. H., von, K. C., Sisodia, S., Tremml, P., Lipp, H. P., Wolfer, D. P., and Muller, U. (2000) J. Neurosci. 20, 7951-7963

Hermans-Borgmeyer, I., Hampe, W., Schinke, B., Methner, A., Nykjaer, A., Susens, U., Fenger, U., Herbarth, B., and Schaller, H. C. (1998) Mech. Dev. 70, 65-76

Hermey, G., Plath, N., Hubner, C. A., Kuhl, D., Schaller, H. C., and Hermans-Borgmeyer, I. (2004) J. Neurochem. 88, 1470-1476

Herms, J., Anliker, B., Heber, S., Ring, S., Fuhrmann, M., Kretzschmar, H., Sisodia, S., and Muller, U. (2004) EMBO J. 23, 4106-4115

Hesse, L., Beher, D., Masters, C. L., and Multhaup, G. (1994) FEBS Lett. 349, 109-116

Hiltunen, M., Lu, A., Thomas, A. V., Romano, D. M., Kim, M., Jones, P. B., Xie, Z., Kounnas, M. Z., Wagner, S. L., Berezovska, O., Hyman, B. T., Tesco, G., Bertram, L., and Tanzi, R. E. (2006) J. Biol. Chem. 281, 32240-32253

Hinners, I., Wendler, F., Fei, H., Thomas, L., Thomas, G., and Tooze, S. A. (2003) EMBO Rep. 4, 1182-1189

Hirayama, S., Bujo, H., Yamazaki, H., Kanaki, T., Takahashi, K., Kobayashi, J., Schneider, W. J., and Saito, Y. (2000) Biochem. Biophys. Res. Com-

mun. 275, 365-373

Hirst, J., Lindsay, M. R., and Robinson, M. S. (2001) Mol. Biol. Cell 12, 3573-3588

Ho, A. and Sudhof, T. C. (2004) Proc. Natl. Acad. Sci. U. S. A 101, 2548-2553

Horazdovsky, B. F., Davies, B. A., Seaman, M. N., McLaughlin, S. A., Yoon, S., and Emr, S. D. (1997) Mol. Biol. Cell 8, 1529-1541

Hoshino, T., Nakaya, T., Araki, W., Suzuki, K., Suzuki, T., and Mizushima, T. (2007) Biochem. J. 402, 581-589

Houlden, H., Crook, R., Dolan, R. J., McLaughlin, J., Revesz, T., and Hardy, J. (2001) Neurosci. Lett. 313, 93-95

Howell, B. W., Lanier, L. M., Frank, R., Gertler, F. B., and Cooper, J. A. (1999) Mol. Cell Biol. 19, 5179-5188

Hutton, M., Lendon, C. L., Rizzu, P., Baker, M., Froelich, S., Houlden, H., Pickering-Brown, S., Chakraverty, S., Isaacs, A., Grover, A., Hackett, J., Adamson, J., Lincoln, S., Dickson, D., Davies, P., Petersen, R. C., Stevens, M., de, G. E., Wauters, E., van, B. J., Hillebrand, M., Joosse, M.,Kwon, J. M., Nowotny, P., Che, L. K., Norton, J., Morris, J. C., Reed, L. A., Trojanowski, J., Basun, H., Lannfelt, L., Neystat, M., Fahn, S., Dark, F., Tannenberg, T., Dodd, P. R., Hayward, N., Kwok, J. B., Schofield, P. R., Andreadis, A., Snowden, J., Craufurd, D., Neary, D., Owen, F.,Oostra, B. A., Hardy, J., Goate, A., van, S. J., Mann, D., Lynch,T., and Heutink, P. (1998) Nature 393, 702-705

Iqbal, K., Grundke-Iqbal, I., Smith, A. J., George, L., Tung, Y. C., and Zaidi, T. (1989) Proc. Natl. Acad. Sci. U. S. A 86, 5646-5650

Iqbal, K., Alonso, A. C., Gong, C. X., Khatoon, S., Pei, J. J., Wang, J. Z., and Grundke-Iqbal, I. (1998) J. Neural Transm. Suppl 53, 169-180

Iwata, N., Tsubuki, S., Takaki, Y., Shirotani, K., Lu, B., Gerard, N. P., Gerard, C., Hama, E., Lee, H. J., and Saido, T. C. (2001) Science 292, 1550-1552

Jacobsen, L., Madsen, P., Moestrup, S. K., Lund, A. H., Tommerup, N., Nykjaer, A., Sottrup-Jensen, L., Gliemann, J., and Petersen, C. M. (1996) J. Biol. Chem. 271, 31379-31383

Jacobsen, L., Madsen, P., Jacobsen, C., Nielsen, M. S., Gliemann, J., and Petersen, C. M. (2001) J. Biol. Chem. 276, 22788-22796

Jacobsen, L., Madsen, P., Nielsen, M. S., Geraerts, W. P., Gliemann, J., Smit, A. B., and Petersen, C. M. (2002) FEBS Lett. 511, 155-158

Jellinger, K. A. and Attems, J. (2005) Neuropathol. Appl. Neurobiol. 31, 203

Jin, L. W., Ninomiya, H., Roch, J. M., Schubert, D., Masliah, E., Otero, D. A., and Saitoh, T. (1994) J. Neurosci. 14, 5461-5470

Johnson, A. O., Lampson, M. A., and McGraw, T. E. (2001) Mol. Biol. Cell 12, 367-381

Kamal, A., Stokin, G. B., Yang, Z., Xia, C. H., and Goldstein, L. S. (2000) Neuron 28, 449-459

Kamal, A., menar-Queralt, A., LeBlanc, J. F., Roberts, E. A., and Goldstein, L. S. (2001) Nature 414, 643-648

Kanaki, T., Bujo, H., Hirayama, S., Tanaka, K., Yamazaki, H., Seimiya, K., Morisaki, N., Schneider, W. J., and Saito, Y. (1998) DNA Cell Biol. 17, 647-657

Kanaki, T., Bujo, H., Hirayama, S., Ishii, I., Morisaki, N., Schneider, W. J., and Saito, Y. (1999) Arterioscler. Thromb. Vasc. Biol. 19, 2687-2695

Kang, D. E., Pietrzik, C. U., Baum, L., Chevallier, N., Merriam, D. E., Kounnas, M. Z., Wagner, S. L., Troncoso, J. C., Kawas, C. H., Katzman, R., and Koo, E. H. (2000) J. Clin. Invest 106, 1159-1166

Kang, J., Lemaire, H. G., Unterbeck, A., Salbaum, J. M., Masters, C. L., Grzeschik, K. H., Multhaup, G., Beyreuther, K., and Muller-Hill, B. (1987) Nature 325, 733-736

Kawarabayashi, T., Shoji, M., Younkin, L. H., Wen-Lang, L., Dickson, D. W., Murakami, T., Matsubara, E., Abe, K., Ashe, K. H., and Younkin, S. G. (2004) J. Neurosci. 24, 3801-3809

Kawasumi, M., Hashimoto, Y., Chiba, T., Kanekura, K., Yamagishi, Y., Ishizaka, M., Tajima, H., Niikura, T., and Nishimoto, I. (2002) Neurosignals. 11, 236-250

Kayser, S. T., Ulrich, H., and Schaller, H. C. (1998) Eur. J. Cell Biol. 76, 119-124

Kenchappa, R. S., Zampieri, N., Chao, M. V., Barker, P. A., Teng, H. K., Hempstead, B. L., and Carter, B. D. (2006) Neuron 50, 219-232

Kienlen-Campard, P., Tasiaux, B., Van, H. J., Li, M., Huysseune, S., Sato, T., Fei, J. Z., Aimoto, S., Courtoy, P. J., Smith, S. O., Constantinescu, S. N., and Octave, J. N. (2008) J. Biol. Chem. 283, 7733-7744

Kim, S., Jeon, T. J., Oberai, A., Yang, D., Schmidt, J. J., and Bowie, J. U. (2005) Proc. Natl. Acad. Sci. U. S. A 102, 14278-14283

King, G. D., Perez, R. G., Steinhilb, M. L., Gaut, J. R., and Turner, R. S. (2003) Neuroscience 120, 143-154

Kinoshita, A., Whelan, C. M., Smith, C. J., Mikhailenko, I., Rebeck, G. W., Strickland, D. K., and Hyman, B. T. (2001) J. Neurosci. 21, 8354-8361

Kitaguchi, N., Takahashi, Y., Tokushima, Y., Shiojiri, S., and Ito, H. (1988) Nature 331, 530-532

Klein, W. L., Krafft, G. A., and Finch, C. E. (2001) Trends Neurosci. 24, 219-224

Kolsch, H., Jessen, F., Wiltfang, J., Lewczuk, P., Dichgans, M., Kornhuber, J., Frolich, L., Heuser, I., Peters, O., Schulz, J. B., Schwab, S. G., and Maier, W. (2008) Neurosci. Lett. 440, 68-71

Kopan, R., Schroeter, E. H., Weintraub, H., and Nye, J. S. (1996) Proc. Natl. Acad. Sci. U. S. A 93, 1683-1688

Kottgen, M., Benzing, T., Simmen, T., Tauber, R., Buchholz, B., Felician geli, S., Huber, T. B., Schermer, B., Kramer-Zucker, A., Hopker, K., Simmen, K. C., Tschucke, C. C., Sandford, R., Kim, E., Thomas, G., and Walz, G. (2005) EMBO J. 24, 705-716

Kounnas, M. Z., Moir, R. D., Rebeck, G. W., Bush, A. I., Argraves, W. S., Tanzi, R. E., Hyman, B. T., and Strickland, D. K. (1995) Cell 82, 331-340

Kozarsky, K., Kingsley, D., and Krieger, M. (1988) Proc. Natl. Acad. Sci. U. S. A. 85, 4335-4339

Kuan, Y. H., Gruebl, T., Soba, P., Eggert, S., Nesic, I., Back, S., Kirsch, J., Beyreuther, K., and Kins, S. (2006) J. Biol. Chem. 281, 40114-40123

Kurten, R. C., Cadena, D. L., and Gill, G. N. (1996) Science 272, 1008-1010

Lefrancois, S., Zeng, J., Hassan, A. J., Canuel, M., and Morales, C. R. (2003) EMBO J. 22, 6430-6437

Leissring, M. A., Murphy, M. P., Mead, T. R., Akbari, Y., Sugarman, M. C., Jannatipour, M., Anliker, B., Muller, U., Saftig, P., De, S. B., Wolfe, M. S., Golde, T. E., and LaFerla, F. M. (2002) Proc. Natl. Acad. Sci. U. S. A. 99, 4697-4702

Leyssen, M., Ayaz, D., Hebert, S. S., Reeve, S., De, S. B., and Hassan, B. A. (2005) EMBO J. 24, 2944-2955

Li, H. L., Roch, J. M., Sundsmo, M., Otero, D., Sisodia, S., Thomas, R., and Saitoh, T. (1997) J. Neurobiol. 32, 469-480

Li, Y., Lu, W., Marzolo, M. P., and Bu, G. (2001) J. Biol. Chem. 276, 18000-18006

Lin, B. Z., Pilch, P. F., and Kandror, K. V. (1997) J. Biol. Chem. 272, 24145-24147

Lintzel, J., Franke, I., Riedel, I. B., Schaller, H. C., and Hampe, W. (2002) Biol. Chem. 383, 1727-1733

Loewer, A., Soba, P., Beyreuther, K., Paro, R., and Merdes, G. (2004) EMBO Rep. 5, 405-411

Lyckman, A. W., Confaloni, A. M., Thinakaran, G., Sisodia, S. S., and Moya, K. L. (1998) J. Biol. Chem. 273, 11100-11106

Mahley, R. W. (1988) Science 240, 622-630

Makarova, A., Williams, S. E., and Strickland, D. K. (2004) Cell Biochem. Biophys. 41, 139-178

Mandelkow, E. M., Schweers, O., Drewes, G., Biernat, J., Gustke, N., Trinczek, B., and Mandelkow, E. (1996) Ann. N. Y. Acad. Sci. 777, 96-106

Marchesi, V. T. (2005) Proc. Natl. Acad. Sci. U. S. A 102, 9093-9098

Marcusson, E. G., Horazdovsky, B. F., Cereghino, J. L., Gharakhanian, E., and Emr, S. D. (1994) Cell 77, 579-586

Mattera, R., Arighi, C. N., Lodge, R., Zerial, M., and Bonifacino, J. S. (2003) EMBO J. 22, 78-88

Mattson, M. P., Cheng, B., Culwell, A. R., Esch, F. S., Lieberburg, I., and Rydel, R. E. (1993) Neuron 10, 243-254

Mattson, M. P. and Furukawa, K. (1998) Perspect. Dev. Neurobiol. 5, 337-352

Mazella, J., Zsurger, N., Navarro, V., Chabry, J., Kaghad, M., Caput, D., Ferrara, P., Vita, N., Gully, D., Maffrand, J. P., and Vincent, J. P. (1998) J. Biol. Chem. 273, 26273-26276

McPhie, D. L., Coopersmith, R., Hines-Peralta, A., Chen, Y., Ivins, K. J., Manly, S. P., Kozlowski, M. R., Neve, K. A., and Neve, R. L. (2003) J. Neurosci. 23, 6914-6927

Merdes, G., Soba, P., Loewer, A., Bilic, M. V., Beyreuther, K., and Paro, R. (2004) EMBO J. 23, 4082-4095

Meziane, H., Dodart, J. C., Mathis, C., Little, S., Clemens, J., Paul, S. M., and Ungerer, A. (1998) Proc. Natl. Acad. Sci. U. S. A 95, 12683-12688

Miyata, M. and Smith, J. D. (1996) Nat. Genet. 14, 55-61

Molloy, S. S., Thomas, L., Kamibayashi, C., Mumby, M. C., and Thomas, G. (1998) J. Cell Biol. 142, 1399-1411

Motoi, Y., Aizawa, T., Haga, S., Nakamura, S., Namba, Y., and Ikeda, K.

(1999) Brain Res. 833, 209-215

Muller, T., Concannon, C. G., Ward, M. W., Walsh, C. M., Tirniceriu, A. L., Tribl, F., Kogel, D., Prehn, J. H., and Egensperger, R. (2007) Mol. Biol. Cell 18, 201-210

Muller, U., Cristina, N., Li, Z. W., Wolfer, D. P., Lipp, H. P., Rulicke, T., Brandner, S., Aguzzi, A., and Weissmann, C. (1994) Cell 79, 755-765

Munter, L. M., Voigt, P., Harmeier, A., Kaden, D., Gottschalk, K. E., Weise, C., Pipkorn, R., Schaefer, M., Langosch, D., and Multhaup, G. (2007) EMBO J. 26, 1702-1712

Needham, B. E., Wlodek, M. E., Ciccotosto, G. D., Fam, B. C., Masters, C. L., Proietto, J., Andrikopoulos, S., and Cappai, R. (2008) J. Pathol. 215, 155-163

Nielsen, M. S., Jacobsen, C., Olivecrona, G., Gliemann, J., and Petersen, C. M. (1999) J. Biol. Chem. 274, 8832-8836

Nielsen, M. S., Madsen, P., Christensen, E. I., Nykjaer, A., Gliemann, J., Kasper, D., Pohlmann, R., and Petersen, C. M. (2001) EMBO J. 20, 2180-2190

Nielsen, M. S., Gustafsen, C., Madsen, P., Nyengaard, J. R., Hermey, G., Bakke, O., Mari, M., Schu, P., Pohlmann, R., Dennes, A., and Petersen, C. M. (2007) Mol. Cell Biol. 27, 6842-6851

Ninomiya, H., Roch, J. M., Sundsmo, M. P., Otero, D. A., and Saitoh, T. (1993) J. Cell Biol. 121, 879-886

Nishimura, M., Yu, G., Levesque, G., Zhang, D. M., Ruel, L., Chen, F., Milman, P., Holmes, E., Liang, Y., Kawarai, T., Jo, E., Supala, A., Rogaeva, E., Xu, D. M., Janus, C., Levesque, L., Bi, Q., Duthie, M., Rozmahel, R., Mat-

tila, K., Lannfelt, L., Westaway, D., Mount, H. T., Woodgett, J., St George-Hyslop, P., and . (1999) Nat. Med. 5, 164-169

Nothwehr, S. F., Bruinsma, P., and Strawn, L. A. (1999) Mol. Biol. Cell 10, 875-890

Nykjaer, A., Lee, R., Teng, K. K., Jansen, P., Madsen, P., Nielsen, M. S., Jacobsen, C., Kliemannel, M., Schwarz, E., Willnow, T. E., Hempstead, B. L., and Petersen, C. M. (2004) Nature 427, 843-848

Oh, S. Y., Ellenstein, A., Chen, C. D., Hinman, J. D., Berg, E. A., Costello, C. E., Yamin, R., Neve, R. L., and Abraham, C. R. (2005) J. Neurosci. Res. 82, 32-42

Ohno, H., Fournier, M. C., Poy, G., and Bonifacino, J. S. (1996) J. Biol. Chem. 271, 29009-29015

Ohsawa, I., Takamura, C., and Kohsaka, S. (2001) J. Neurochem. 76, 1411-1420

Oltersdorf, T., Ward, P. J., Henriksson, T., Beattie, E. C., Neve, R., Lieber burg, I., and Fritz, L. C. (1990) J. Biol. Chem. 265, 4492-4497

Owen, D. J. and Evans, P. R. (1998) Science 282, 1327-1332

Park, J. H., Gimbel, D. A., GrandPre, T., Lee, J. K., Kim, J. E., Li, W., Lee, D. H., and Strittmatter, S. M. (2006) J. Neurosci. 26, 1386-1395

Perez, R. G., Zheng, H., Van der Ploeg, L. H., and Koo, E. H. (1997) J. Neurosci. 17, 9407-9414

Piguet, V., Wan, L., Borel, C., Mangasarian, A., Demaurex, N., Thomas, G., and Trono, D. (2000) Nat. Cell Biol. 2, 163-167

Ponte, P., Gonzalez-DeWhitt, P., Schilling, J., Miller, J., Hsu, D., Greenberg, B., Davis, K., Wallace, W., Lieberburg, I., and Fuller, F. (1988) Nature 331, 525-527

Puertollano, R., Aguilar, R. C., Gorshkova, I., Crouch, R. J., and Bonifacino, J. S. (2001) Science 292, 1712-1716

Puertollano, R., Randazzo, P. A., Presley, J. F., Hartnell, L. M., and Bonifacino, J. S. (2001) Cell 105, 93-102

Puertollano, R., van der Wel, N. N., Greene, L. E., Eisenberg, E., Peters, P. J., and Bonifacino, J. S. (2003) Mol. Biol. Cell 14, 1545-1557

Puertollano, R. and Bonifacino, J. S. (2004) Nat. Cell Biol. 6, 244-251

Roch, J. M., Masliah, E., Roch-Levecq, A. C., Sundsmo, M. P., Otero, D. A., Veinbergs, I., and Saitoh, T. (1994) Proc. Natl. Acad. Sci. U. S. A 91, 7450-7454

Rogaeva, E., Meng, Y., Lee, J. H., Gu, Y., Kawarai, T., Zou, F., Katayama, T., Baldwin, C. T., Cheng, R., Hasegawa, H., Chen, F., Shibata, N., Lunetta, K. L., Pardossi-Piquard, R., Bohm, C., Wakutani, Y., Cupples, L. A., Cuen co, K. T., Green, R. C., Pinessi, L., Rainero, I., Sorbi, S., Bruni, A., Duara, R., Friedland, R. P., Inzelberg, R., Hampe, W., Bujo, H., Song, Y. Q., Andersen, O. M., Willnow, T. E., Graff-Radford, N., Petersen, R. C., Dickson, D., Der, S. D., Fraser, P. E., Schmitt-Ulms, G., Younkin, S., Mayeux, R., Farrer, L. A., and St George-Hyslop, P. (2007) Nat. Genet. 39, 168-177

Roncarati, R., Sestan, N., Scheinfeld, M. H., Berechid, B. E., Lopez, P. A., Meucci, O., McGlade, J. C., Rakic, P., and D'Adamio, L. (2002) Proc. Natl. Acad. Sci. U. S. A 99, 7102-7107

Rosen, D. R., Martin-Morris, L., Luo, L. Q., and White, K. (1989) Proc. Natl. Acad. Sci. U. S. A 86, 2478-2482

Roses, A. D. (1997) Neurogenetics. 1, 3-11

Rossjohn, J., Cappai, R., Feil, S. C., Henry, A., McKinstry, W. J., Galatis, D., Hesse, L., Multhaup, G., Beyreuther, K., Masters, C. L., and Parker, M. W. (1999) Nat. Struct. Biol. 6, 327-331

Rothman, J. H. and Stevens, T. H. (1986) Cell 47, 1041-1051

Rudenko, G., Henry, L., Henderson, K., Ichtchenko, K., Brown, M. S., Goldstein, J. L., and Deisenhofer, J. (2002) Science 298, 2353-2358

Sabo, S. L., Ikin, A. F., Buxbaum, J. D., and Greengard, P. (2001) J. Cell Biol. 153, 1403-1414

Sabo, S. L., Ikin, A. F., Buxbaum, J. D., and Greengard, P. (2003) J. Neurosci. 23, 5407-5415

Sandbrink, R., Masters, C. L., and Beyreuther, K. (1994) Neurobiol. Dis. 1, 13-24

Sandbrink, R., Masters, C. L., and Beyreuther, K. (1994) J. Biol. Chem. 269, 1510-1517

Sastre, M., Turner, R. S., and Levy, E. (1998) J. Biol. Chem. 273, 22351-22357

Scheinfeld, M. H., Roncarati, R., Vito, P., Lopez, P. A., Abdallah, M., and D'Adamio, L. (2002) J. Biol. Chem. 277, 3767-3775

Schellenberg, G. D. (1995) Proc. Natl. Acad. Sci. U. S. A 92, 8552-8559

Scherzer, C. R., Offe, K., Gearing, M., Rees, H. D., Fang, G., Heilman, C. J., Schaller, C., Bujo, H., Levey, A. I., and Lah, J. J. (2004) Arch. Neurol. 61, 1200-1205

Scheuermann, S., Hambsch, B., Hesse, L., Stumm, J., Schmidt, C., Beher, D., Bayer, T. A., Beyreuther, K., and Multhaup, G. (2001) J. Biol. Chem. 276, 33923-33929

Schmechel, A., Strauss, M., Schlicksupp, A., Pipkorn, R., Haass, C., Bayer, T. A., and Multhaup, G. (2004) J. Biol. Chem. 279, 39710-39717

Schmid, S. L., Fuchs, R., Male, P., and Mellman, I. (1988) Cell 52, 73-83

Schmidt, V., Sporbert, A., Rohe, M., Reimer, T., Rehm, A., Andersen, O. M., and Willnow, T. E. (2007) J. Biol. Chem. 282, 32956-32964

Schroeter, E. H., Kisslinger, J. A., and Kopan, R. (1998) Nature 393, 382-386

Scott, G. K., Gu, F., Crump, C. M., Thomas, L., Wan, L., Xiang, Y., and Thomas, G. (2003) EMBO J. 22, 6234-6244

Scott, G. K., Fei, H., Thomas, L., Medigeshi, G. R., and Thomas, G. (2006) EMBO J. 25, 4423-4435

Seaman, M. N., McCaffery, J. M., and Emr, S. D. (1998) J. Cell Biol. 142, 665-681

Seaman, M. N. (2004) J. Cell Biol. 165, 111-122

Seaman, M. N. (2007) J. Cell Sci. 120, 2378-2389

Selivanova, A., Winblad, B., Farmery, M. R., Dantuma, N. P., and Ankarcrona, M. (2006) Biochem. Biophys. Res. Commun. 350, 220-226

Selkoe, D. J. (1989) Cell 58, 611-612

Selkoe, D. J. (2001) Physiol Rev. 81, 741-766

Shiba, T., Takatsu, H., Nogi, T., Matsugaki, N., Kawasaki, M., Igarashi, N., Suzuki, M., Kato, R., Earnest, T., Nakayama, K., and Wakatsuki, S. (2002) Nature 415, 937-941

Shiba, T., Kametaka, S., Kawasaki, M., Shibata, M., Waguri, S., Uchiyama, Y., and Wakatsuki, S. (2004) Traffic. 5, 437-448

Shiba, Y., Katoh, Y., Shiba, T., Yoshino, K., Takatsu, H., Kobayashi, H., Shin, H. W., Wakatsuki, S., and Nakayama, K. (2004) J. Biol. Chem. 279, 7105-7111

Shioi, J., Anderson, J. P., Ripellino, J. A., and Robakis, N. K. (1992) J. Biol. Chem. 267, 13819-13822

Simons, M., Keller, P., De, S. B., Beyreuther, K., Dotti, C. G., and Simons, K. (1998) Proc. Natl. Acad. Sci. U. S. A 95, 6460-6464

Sisodia, S. S., Koo, E. H., Hoffman, P. N., Perry, G., and Price, D. L. (1993) J. Neurosci. 13, 3136-3142

Small, D. H., Nurcombe, V., Reed, G., Clarris, H., Moir, R., Beyreuther, K., and Masters, C. L. (1994) J. Neurosci. 14, 2117-2127

Soba, P., Eggert, S., Wagner, K., Zentgraf, H., Siehl, K., Kreger, S., Lower, A., Langer, A., Merdes, G., Paro, R., Masters, C. L., Muller, U., Kins, S., and Beyreuther, K. (2005) EMBO J. 24, 3624-3634

Spoelgen, R., von Arnim, C. A., Thomas, A. V., Peltan, I. D., Koker, M., Deng, A., Irizarry, M. C., Andersen, O. M., Willnow, T. E., and Hyman, B. T. (2006) J. Neurosci. 26, 418-428

Steinbach, J. P., Muller, U., Leist, M., Li, Z. W., Nicotera, P., and Aguzzi, A. (1998) Cell Death. Differ. 5, 858-866

Suzuki, N., Cheung, T. T., Cai, X. D., Odaka, A., Otvos, L., Jr., Eckman, C., Golde, T. E., and Younkin, S. G. (1994) Science 264, 1336-1340

Tabert, M. H., Liu, X., Doty, R. L., Serby, M., Zamora, D., Pelton, G. H., Marder, K., Albers, M. W., Stern, Y., and Devanand, D. P. (2005) Ann. Neurol. 58, 155-160

Taira, K., Bujo, H., Hirayama, S., Yamazaki, H., Kanaki, T., Takahashi, K., Ishii, I., Miida, T., Schneider, W. J., and Saito, Y. (2001) Arterioscler. Thromb. Vasc. Biol. 21, 1501-1506

Takehashi, M., Tanaka, S., Masliah, E., and Ueda, K. (2002) Neurosci. Lett. 327, 79-82

Tanahashi, H., Asada, T., and Tabira, T. (2004) Neuroreport 15, 175-179

Tanzi, R. E., McClatchey, A. I., Lamperti, E. D., Villa-Komaroff, L., Gusella, J. F., and Neve, R. L. (1988) Nature 331, 528-530

Theuns, J., Del-Favero, J., Dermaut, B., van Duijn, C. M., Backhovens, H., Van den Broeck, M. V., Serneels, S., Corsmit, E., Van Broeckhoven, C. V., and Cruts, M. (2000) Hum. Mol. Genet. 9, 325-331

Torroja, L., Packard, M., Gorczyca, M., White, K., and Budnik, V. (1999) J. Neurosci. 19, 7793-7803

Townsend, M., Mehta, T., and Selkoe, D. J. (2007) J. Biol. Chem. 282, 33305-33312

Tugizov, S., Maidji, E., Xiao, J., and Pereira, L. (1999) J. Virol. 73, 8677-8688

Turk, E., Teplow, D. B., Hood, L. E., and Prusiner, S. B. (1988) Eur. J. Biochem. 176, 21-30

Turner, P. R., O'Connor, K., Tate, W. P., and Abraham, W. C. (2003) Prog. Neurobiol. 70, 1-32

Ulery, P. G. and Strickland, D. K. (2000) J. Clin. Invest 106, 1077-1079

Van Nostrand, W. E., Schmaier, A. H., Neiditch, B. R., Siegel, R. S., Raschke, W. C., Sisodia, S. S., and Wagner, S. L. (1994) Biochim. Biophys. Acta 1209, 165-170

Vassar, R., Bennett, B. D., Babu-Khan, S., Kahn, S., Mendiaz, E. A., Denis, P., Teplow, D. B., Ross, S., Amarante, P., Loeloff, R., Luo, Y., Fisher, S., Fuller, J., Edenson, S., Lile, J., Jarosinski, M. A., Biere, A. L., Curran, E., Burgess, T., Louis, J. C., Collins, F., Treanor, J., Rogers, G., and Citron, M. (1999) Science 286, 735-741

Vassar, R. (2004) J. Mol. Neurosci. 23, 105-114

von Rotz, R. C., Kohli, B. M., Bosset, J., Meier, M., Suzuki, T., Nitsch, R. M., and Konietzko, U. (2004) J. Cell Sci. 117, 4435-4448

Voorhees, P., Deignan, E., van, D. E., Humphrey, J., Marks, M. S., Peters, P. J., and Bonifacino, J. S. (1995) EMBO J. 14, 4961-4975

Waldemar, G., Dubois, B., Emre, M., Georges, J., McKeith, I. G., Rossor, M., Scheltens, P., Tariska, P., and Winblad, B. (2007) Eur. J. Neurol. 14, e1-26

Walsh, D. M., Klyubin, I., Fadeeva, J. V., Cullen, W. K., Anwyl, R., Wolfe, M. S., Rowan, M. J., and Selkoe, D. J. (2002) Nature 416, 535-539

Walsh, D. M., Klyubin, I., Fadeeva, J. V., Cullen, W. K., Anwyl, R., Wolfe, M. S., Rowan, M. J., and Selkoe, D. J. (2002) Nature 416, 535-539

Wan, L., Molloy, S. S., Thomas, L., Liu, G., Xiang, Y., Rybak, S. L., and Thomas, G. (1998) Cell 94, 205-216

Wang, Y. and Ha, Y. (2004) Mol. Cell 15, 343-353

Wasco, W., Bupp, K., Magendantz, M., Gusella, J. F., Tanzi, R. E., and Solomon, F. (1992) Proc. Natl. Acad. Sci. U. S. A 89, 10758-10762

Wasco, W., Brook, J. D., and Tanzi, R. E. (1993) Genomics 15, 237-239

Weidemann, A., Konig, G., Bunke, D., Fischer, P., Salbaum, J. M., Masters, C. L., and Beyreuther, K. (1989) Cell 57, 115-126

Wenk, G. L. (2003) J. Clin. Psychiatry 64 Suppl 9, 7-10

Westmeyer, G. G., Willem, M., Lichtenthaler, S. F., Lurman, G., Multhaup, G., Assfalg-Machleidt, I., Reiss, K., Saftig, P., and Haass, C. (2004) J. Biol. Chem. 279, 53205-53212

Westphal, V., Marcusson, E. G., Winther, J. R., Emr, S. D., and van den Hazel, H. B. (1996) J. Biol. Chem. 271, 11865-11870

White, A. R., Reyes, R., Mercer, J. F., Camakaris, J., Zheng, H., Bush, A. I., Multhaup, G., Beyreuther, K., Masters, C. L., and Cappai, R. (1999) Brain Res. 842, 439-444

Worby, C. A. and Dixon, J. E. (2002) Nat. Rev. Mol. Cell Biol. 3, 919-931

Xiang, Y., Molloy, S. S., Thomas, L., and Thomas, G. (2000) Mol. Biol. Cell 11, 1257-1273

Yaar, M., Zhai, S., Pilch, P. F., Doyle, S. M., Eisenhauer, P. B., Fine, R. E., and Gilchrest, B. A. (1997) J. Clin. Invest 100, 2333-2340

Yamazaki, H., Bujo, H., Kusunoki, J., Seimiya, K., Kanaki, T., Morisaki, N., Schneider, W. J., and Saito, Y. (1996) J. Biol. Chem. 271, 24761-24768

Yamazaki, T., Koo, E. H., and Selkoe, D. J. (1997) J. Neurosci. 17, 1004-1010

Yan, Z. and Feng, J. (2004) Curr. Alzheimer Res. 1, 241-248

Zambrano, N., Bruni, P., Minopoli, G., Mosca, R., Molino, D., Russo, C., Schettini, G., Sudol, M., and Russo, T. (2001) J. Biol. Chem. 276, 19787-19792

Zhai, P., He, X., Liu, J., Wakeham, N., Zhu, G., Li, G., Tang, J., and Zhang, X. C. (2003) Biochemistry 42, 13901-13908

Zheng, H., Jiang, M., Trumbauer, M. E., Sirinathsinghji, D. J., Hopkins, R., Smith, D. W., Heavens, R. P., Dawson, G. R., Boyce, S., Conner, M. W., Stevens, K. A., Slunt, H. H., Sisoda, S. S., Chen, H. Y., and Van der Ploeg, L. H. (1995) Cell 81, 525-531

Zhu, G., Zhai, P., He, X., Terzyan, S., Zhang, R., Joachimiak, A., Tang, J., and Zhang, X. C. (2003) Biochemistry 42, 6392-6399

Zhu, Y., Doray, B., Poussu, A., Lehto, V. P., and Kornfeld, S. (2001) Science 292, 1716-1718

Zhu, Y., Bujo, H., Yamazaki, H., Hirayama, S., Kanaki, T., Takahashi, K., Shibasaki, M., Schneider, W. J., and Saito, Y. (2002) Circulation 105, 1830-1836

Zhu, Y., Bujo, H., Yamazaki, H., Ohwaki, K., Jiang, M., Hirayama, S., Kanaki, T., Shibasaki, M., Takahashi, K., Schneider, W. J., and Saito, Y. (2004) Circ. Res. 94, 752-758

7. Appendix

Mein Lebenslauf wird aus Gründen des Datenschutzes nicht veröffentlicht.

Publikationen

2008   M. Rohe, AS. Carlo, H. Breyhan, A. Sporbert, D. Militz, **V. Schmidt**, C. Wozny, A. Harmeier, B. Erdmann, K.R. Bales, S. Wolf, G. Kemper mann, S.M. Paul, D. Schmitz, T.A. Bayer, T.E. Willnow, and O. M. Andersen (2008) SORLA affects APP-dependent stimulation of ERK signaling and adult neurogenesis. *JBC*.

2007   **V.Schmidt**, A.Sporbert, M.Rohe, T.Reimer, A.Rehm, O.M.Andersen and T.E.Willnow (2007) SorLA/LR11 regulates processing of amyloid precursor protein via interaction with adaptors GGA1 and PACS1. *JBC*.

2006   O.M.Andersen, **V.Schmidt**, R.Spoelgen, J.Gliemann, J.Behlke, D.Galatis, B.T. Hyman, R.Cappai, T.E. Willnow (2006) Molecular dissection of the interaction between amyloid precursor protein and its neuronal trafficking receptor SorLA/LR11. *Biochemistry*.

2005   M.Anderson, J.Reiche, **V.Schmidt**, M.Gotthardt and Thomas E. Willnow (2005). Neuronal sorting protein-related receptor sorLA/LR11 regulates processing of the amyloid precursor protein. *PNAS*.

2003   S.Hertwig, I.Klein, **V.Schmidt**, S.Beck, J.Hammerl and Bernd Appel (2003). Sequence Analysis of the Genome of the Temperate Yersinia enterocolitica Phage PY54. *J.Mol.Biol*.

Posterpresentation at the International Conference of Alzheimer Disease 2008 in Chicago, U.S.A.: SorLA/LR11 regulates processing of amyloid precursor protein via interaction with adaptors GGA1 and PACS1.

Presentation at the Euron and ISAO workshop Current aspects in the field of Alzheimer Research 2007 in Bad Honnef: Role of SORLA in processing of APP and the development of Alzheimer's Disease

Presentation at the PhD Retreat 2006 in Motzen, Germany: Role of SORLA in processing of APP and the development of Alzheimer's Disease

Posterpresentation at the PhD Retreat 2005 in Straussberg, Germany: Functional characterization of the lipoproteinreceptor SORLA

Berlin, den 15.08.2008

Vanessa Schmidt

7.2 Selbstständigkeitserklärung

Hiermit erkläre ich, dass ich die vorliegende Arbeit mit dem Titel "SORLA regulates processing of amyloid precursor protein via interaction with adaptors GGA1 and PACS1" selbstständig und ohne Hilfe Dritter angefertigt habe. Sämtliche Hilfsmittel, Hilfen sowie Literaturquellen sind als solche kenntlich gemacht.

Ausserdem erkläre ich hiermit, dass ich mich nicht anderweitig um einen entsprechenden Doktorgrad beworben habe. Die Promotionsordnung des Fachbereichs Biologie, Chemie, Pharmazie der Freien Universität Berlin habe ich gelesen und akzeptiert.

Vanessa Schmidt

Berlin, August 2008

7.3 Danksagung

Ich bedanke mich herzlichst bei Prof. Dr. Thomas E. Willnow. Er hat mir nicht nur dieses interessante Projekt ermöglicht, sondern auch für eine ausgezeichnete Betreuung meiner Arbeit und den erstklassigen Arbeitsbedingungen in seinem Labor gesorgt.

Mein besonderer Dank gilt Prof. Dr. Wolfgang Schuster von der Freien Universität Berlin für die Betreuung und Gutachtung meiner Arbeit.

Ein großes Dankeschön gilt meinen Arbeitskollegen der AG Willnow, insbesondere für das gute Arbeitsklima während meiner Doktorandenzeit. Besonders möchte ich mich bei meinem Kollegen Dr. Olav Andersen bedanken. Er brachte mir immer sehr viel Geduld entgegen und sorgte mit wertvollen Ratschlägen für das Gelingen meiner Arbeit. Danke sage ich auch Dr. Tilman Breiderhoff, der mir bei technischen Fragestellungen immer zur Seite stand. Meinen Dank gilt auch Dr. Juliane Reiche, die besonders in der Anfangsphase meiner Doktorarbeit eine grosse Hilfe war.

Bei der technischen Assistentin Christine Kruse bedanke ich mich für die Unterstützung bezüglich der Kultivierung meiner Zellen.

Meinem Freund möchte ich für die aufmunternde Unterstützung und Geduld während meines Studiums und meiner Doktorandenzeit danken. Er hat mir auch in schwierigen Phasen immer wieder den nötigen Anschwung gegeben.